

OXIDATIVE AND NON-OXIDATIVE APPROACHES TO HIGH  
MOLECULAR WEIGHT ETHER-SUBSTITUTED  
POLYTHIOPHENES

by

David D. Hebert, B.S.

A thesis submitted to the Graduate Council of  
Texas State University in partial fulfillment  
of the requirements for the degree of  
Master of Science  
with a Major in Chemistry  
August 2020

Committee Members:

Jennifer A. Irvin, Chair

Todd W. Hudnall

Tania Betancourt

**COPYRIGHT**

by

David D. Hebert

2020

## **FAIR USE AND AUTHOR'S PERMISSION STATEMENT**

### **Fair Use**

This work is protected by the Copyright Laws of the United States (Public Law 94-553, section 107). Consistent with fair use as defined in the Copyright Laws, brief quotations from this material are allowed with proper acknowledgement. Use of this material for financial gain without the author's express written permission is not allowed.

### **Duplication Permission**

As the copyright holder of this work I, David D. Hebert, authorize duplication of this work, in whole or in part, for educational or scholarly purposes only.

## **DEDICATION**

I dedicate this thesis to my family and to my partner. Your unending support is what keeps me going.

## **ACKNOWLEDGEMENTS**

First of all, I must acknowledge Dr. Jennifer Irvin for her endless guidance, support, and patience throughout my time in her group. I am deeply grateful for her help in my growth as a chemist and for the many hours we have spent deliberating synthetic pathways, new experiments, or whatever chemistry rabbit-hole I had fallen down at the time.

I would also like to thank my other committee members Dr. Tania Betancourt and Dr. Todd Hudnall for their time and support. Dr. Betancourt trained me on the gel-permeation chromatograph and graciously shared her lab and instruments with me. If it were not for Dr. Hudnall and his organometallics class, I would be far less comfortable with organometallic chemistry than I am today. He and his research group were a valuable resource for tips regarding tricky reactions, and generously shared their reagents with me.

I extend my gratitude to Dr. William Hoffmann and Michael Godwin for their help acquiring the mass spectra in this thesis. I am also grateful to Dr. William Brittain, who generously donated one of the GPC columns used in this work. A special shoutout to Al Martinez for saving the day on several occasions, as well as the rest of the Department of Chemistry & Biochemistry staff who we would not last a day without.

To the many wonderful members of the Irvin group, past and present, you have a bigger role in this work than you may think. Michael Naley, Venus

Stanton, David Sharp, and Tim Carrum a huge thank you for all your help and for pulling many long hours with me in the lab. Thank you to Emma Murphy and Danial Morales for helping me with more polymerizations than I care to count. A big shoutout to Steven Gralinski for being an awesome friend and for showing me the ropes of organic synthesis, an experience which has had a huge impact on my path as a synthetic chemist. To Kelli Burke, Mariana Ocampo, Marissa Snapp-Leo, and Xu Wang, thank you for welcoming me into the group from day one and for always being there to talk to. Last but not least, a big thank you to Damilola Runsewe for having the best conversations with me and for always offering a new perspective on whatever problem I might have.

I am a firm believer that passion inspires passion, and there are a few such instances I would like to acknowledge that have contributed in some shape or form to me being where I am today. Thank you to Dr. Benjamin Martin for being an excellent teacher and for inspiring me to strive for not just knowledge but for understanding. A special thank you to grandmaster NMR spectroscopist Dr. Ben Shoulders for sharing his seemingly unending wisdom, and whose kindness and skill is an inspiration.

## TABLE OF CONTENTS

	Page
ACKNOWLEDGEMENTS.....	v
LIST OF TABLES .....	x
LIST OF FIGURES .....	xi
LIST OF SCHEMES .....	xiv
 1. INTRODUCTION TO CONJUGATED POLYMERS.....	 1
1.1 History of Conjugated Polymers.....	1
1.2 Properties of Conjugated Polymers.....	2
1.2.1 Background .....	2
1.2.2 Conductivity .....	3
1.2.3 Charge Transport Properties .....	4
1.2.4 Hierarchical Structures .....	6
1.3 Polyheterocycles .....	7
1.4 Polythiophenes.....	8
1.4.1 Soluble Polythiophenes .....	8
1.4.2 Poly(3,4-alkylenedioxythiophene)s .....	9
1.5 Regioregularity – Heads and Tails .....	11
1.5.1 Background .....	11
1.5.2 Determination of Regioregularity .....	13
1.6 Molecular Weight .....	14
1.6.1 Background .....	14
1.6.2 Impact on Polythiophene Properties.....	17
1.7 Gel Permeation Chromatography.....	20
1.8 Polymerization of Thiophenes .....	22
1.8.1 Chemical Oxidative Polymerization .....	22
1.8.1.1 Background.....	23
1.8.1.2 Mechanistic Insights .....	27
1.8.1.3 Order of Addition.....	32
1.8.2 Grignard Metathesis Polymerization.....	33
1.8.2.1 Background.....	33
1.8.2.2 Mechanism .....	35
1.9 Motivation for Research .....	37
1.10 Thesis of This Work .....	38

2. MONOMER SYNTHESIS .....	39
2.1 Introduction .....	39
2.2 Experimental .....	40
2.2.1 Materials .....	40
2.2.2 Methods .....	41
2.2.3 Synthesis .....	41
2.2.3.1 2-Dodecyl-2H,3H-thieno[3,4-b][1,4]dioxine (EDOT-C <sub>12</sub> ) (Scheme 5) .....	41
2.2.3.2 3,4-Bis(hexyloxy)thiophene (3,4-DHOT) (Scheme 6) .....	43
2.2.3.3 5,7-Dibromo-2-dodecyl-2H,3H-thieno[3,4- b][1,4]dioxine (Br <sub>2</sub> EDOT-C <sub>12</sub> ) (Scheme 7) ...	44
2.3 Results and Discussion .....	45
2.3.1 Transesterification Reaction .....	45
2.3.2 Bromination of EDOT-C <sub>12</sub> .....	50
2.4 Attempted Syntheses .....	54
2.4.1 Synthesis of a Polyether-substituted ProDOT .....	54
2.4.2 Symmetrical $\alpha$ -Diketones as Precursors to Vicinal Diols .....	55
3. POLYMERIZATIONS .....	58
3.1 Introduction .....	58
3.2 Experimental .....	58
3.2.1 Materials .....	58
3.2.2 Methods .....	59
3.2.3 Polymerizations .....	60
3.2.3.1 Chemical Oxidative Polymerization .....	60
3.2.3.2 Grignard Metathesis Polymerization .....	66
3.3 Results and Discussion .....	67
3.3.1 Chemical Oxidative Polymerization .....	67
3.3.2 Grignard Metathesis .....	73
3.3.3 Comparison of Methods .....	75
4. CONCLUDING REMARKS .....	77
4.1 Monomer Synthesis .....	77
4.2 Polymerizations .....	77
5. FUTURE WORK .....	79



5.1 Standard Addition Oxidative Polymerization .....	79
5.2 Synthesis of Symmetrical Vicinal Diols for Novel EDOT Monomers .....	79
5.3 Determination of Regioregularity of PEDOTs.....	80
5.4 Dehydrobrominative Polycondensation .....	82
5.5 Direct Arylation Polycondensation.....	86
APPENDIX SECTION .....	88
REFERENCES .....	91

## LIST OF TABLES

Table	Page
1. Effects of molecular weight on the properties of polythiophenes. ....	18
2. Previously reported molecular weights of relevant polythiophene derivatives.....	25
3. Chemical oxidative polymerization reaction parameters and their effects. ....	29
4. Weight-average molecular weight $M_w$ , weight-average degree of polymerization $X_w$ for polymers synthesized by $FeCl_3$ -initiated chemical oxidative polymerization under different conditions. ....	68
5. Comparison of the yields of polymers synthesized by COP under various standard and reverse addition conditions. ....	72

## LIST OF FIGURES

Figure	Page
1. The structure of aniline and the first conjugated polymer. ....	1
2. The conductivities achievable by conjugated polymers, with other materials listed for reference. ....	2
3. Reversible reduction and oxidation (redox) switching of polythiophene between neutral, radical cation, and dicationic states. ....	3
4. Decreasing energy gap ( $E_g < E_3 < E_2 < E_1$ ) with increasing conjugated length. ....	4
5. Nondegenerate (polythiophene and polyphenylene) ground-states. ....	5
6. The structures of aromatic (neutral), polaronic (radical cation), and bipolaronic (dication) polythiophene. ....	6
7. The hierarchical structures of conjugated polymers and some examples of each. ....	7
8. General structure of substituted polyheterocycles. ....	8
9. Structures of soluble polythiophene derivatives. ....	9
10. General monomer and polymer structures of 3,4-ethylenedioxythiophene (EDOT) and 3,4-propylenedioxythiophene (ProDOT) and their functionalized derivatives. ....	9
11. Alpha and beta couplings. ....	10
12. Different couplings in asymmetric monomers like 3-alkylthiophene. ....	11
13. The four possible triads formed by two consecutive monomer couplings. ....	12
14. Twisting of the conjugated backbone due to steric interactions of side groups in regiorregular polymers containing HH and TT couplings. ....	13
15. Chemical shifts of alpha-methylene protons in HT and HH couplings. ....	14

16. Example of how polymer molecular weight ( $M_w$ ) alone is insufficient for comparing the polymerization of two different monomers.....	17
17. Comparison of high and low $M_w$ P3HT film morphology. ....	19
18. 'Edge-on' and 'face-on' orientations of P3HT in thin films.....	20
19. Generic box diagram for GPC. ....	21
20. Depiction of the operating principle of GPC separation. ....	21
21. Oxidative polymerization of 3-alkylsulfanylthiophenes.....	28
22. Extended COP mechanism illustrating the impact of reaction conditions on polymer regioregularity .....	31
23. Differences between standard and reverse addition in chemical oxidative polymerization.....	32
24. Grignard metathesis mechanism. ....	36
25. Living chain terminations. ....	37
26. Structures, names, and abbreviations of the monomers synthesized.....	40
27. $^1\text{H}$ NMR spectrum of EDOT-C12 in $\text{CDCl}_3$ . ....	46
28. Mass spectrum of EDOT-C12.....	47
29. $^1\text{H}$ NMR spectrum of 3,4-DHOT in $\text{CDCl}_3$ . ....	48
30. Proposed transesterification mechanism.....	49
31. Reaction mechanism for the NBS bromination of thiophenes.....	51
32. $^1\text{H}$ NMR spectrum for $\text{Br}_2\text{EDOT-C12}$ in $\text{CDCl}_3$ . ....	52
33. $^{13}\text{C}$ NMR spectrum for $\text{Br}_2\text{EDOT-C12}$ in $\text{CDCl}_3$ . ....	53
34. Mass spectrum for $\text{Br}_2\text{EDOT-C12}$ .....	54
35. Attempted syntheses of $\alpha$ -diketones inspired from previously published methods. ....	57

36. Structures of the polymers synthesized.....	58
37. GPC chromatograms for ether-substituted polymers synthesized by FeCl <sub>3</sub> -initiated chemical oxidative polymerization (right-angle light scattering detector).....	69
38. GPC chromatogram for P3HT synthesized by chemical oxidative polymerization under different conditions (right-angle light scattering detector).....	71
39. GPC Chromatogram for P3HT and PEDOT-C12 prepared by the GRIM method (right-angle light scattering detector).....	74
40. Comparison of GPC chromatograms of PEDOT-C12 prepared by COP (best case: standard addition with 4 equivalents FeCl <sub>3</sub> in C <sub>6</sub> H <sub>5</sub> Cl) and GRIM methods.....	76
41. Derivatization of asymmetric vs. symmetric EDOT monomers.....	80
42. Four possible conformational triads in substituted PEDOTs.....	81
43. Structure of [CpNiCl(SiPr)] catalyst and SiPr ligand. ....	83
44. Tentative DHPB Mechanism.....	85
45. Examples of homocoupling and cross-coupling polymerizations possible through DArP. ....	87

## LIST OF SCHEMES

Scheme	Page
1. Chemical oxidative polymerization equation.....	23
2. Chemical oxidative polymerization. ....	24
3. Grignard metathesis (GRIM) polymerization.....	34
4. General Kumada cross-coupling reaction.....	34
5. Synthesis of EDOT-C12. ....	41
6. Synthesis of 3,4-DHOT.....	43
7. Synthesis of Br <sub>2</sub> EDOT-C12. ....	44
8. General transesterification reaction.....	45
9. General bromination reaction. ....	50
10. Attempted synthesis of ProDOT-OG <sub>2</sub> , a polyether-substituted thiophene monomer.....	55
11. Vanadium-catalyzed pinacol coupling of aliphatic aldehydes to vicinal diols. ....	80
12. Dehydrobrominative polycondensation reaction. ....	82
13. Generalized direct arylation polycondensation (DArP) reaction.....	86

# 1. INTRODUCTION TO CONJUGATED POLYMERS

## 1.1 History of Conjugated Polymers

The first synthesis of a conjugated polymer dates back to the early 1830s with Friedlieb Runge's work on the oxidative polymerization of aniline (Figure 1a).<sup>1</sup> Later in 1862, Henry Letheby described the first electrochemical polymerization of aniline, where he found that oxidizing sulfuric acid solutions of aniline via a Pt electrode gave a deeply colored material (Figure 1a) which was only soluble in concentrated sulfuric acid.<sup>1</sup> Reducing the material with ammonia caused it to take on a brilliant blue color (Figure 1b), though it remained insoluble.<sup>1</sup> At the time, the chemical nature of the resulting material was not well understood, though it was noted for its vibrant colors and insolubility. These observations would foreshadow the things to come with the birth of the field of conjugated polymers over a hundred years later.

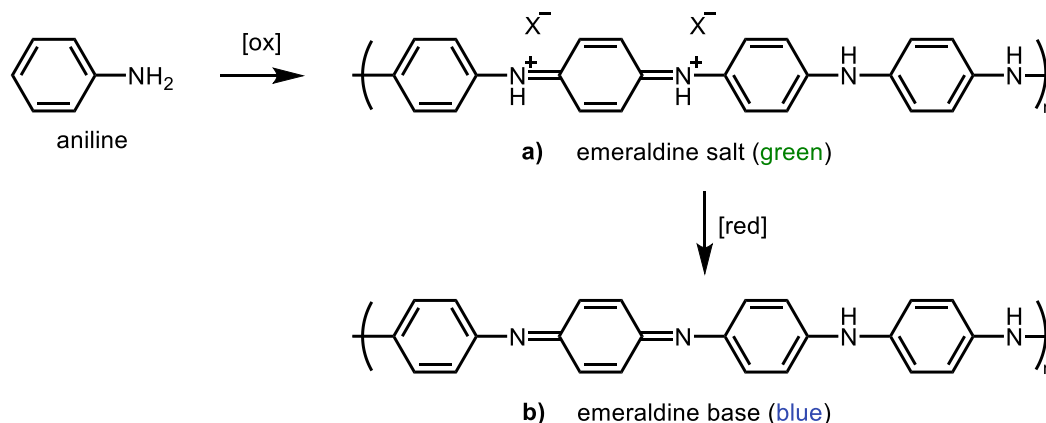


Figure 1. The structure of aniline and the first conjugated polymer ( $[\text{ox}]$  = oxidize,  $[\text{red}]$  = reduce).

In 1971, the first free-standing semiconducting polyacetylene film was synthesized by Shirakawa and Ikeda.<sup>2</sup> Six years later in 1977, Shirakawa *et al.*

showed that by doping these films with iodine vapor their conductivity could be increased by up to seven orders of magnitude (Figure 2).<sup>3</sup> In 2000, the Nobel Prize in chemistry was awarded to Heeger, MacDiarmid, and Shirakawa “for the discovery and development of conductive polymers.”

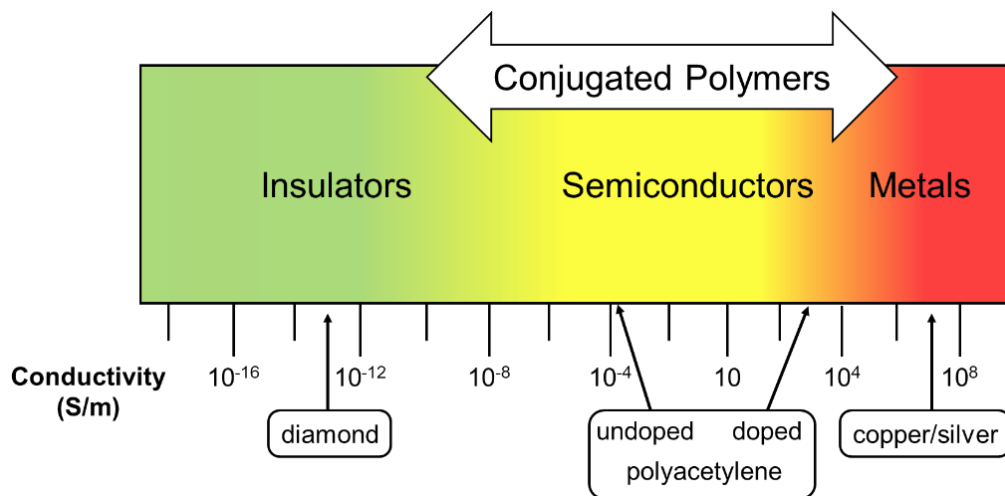


Figure 2. The conductivities achievable by conjugated polymers, with other materials listed for reference.

## **1.2 Properties of Conjugated Polymers**

### **1.2.1 Background**

Conjugated polymers are organic materials with unique electronic and optical properties. All conjugated polymers possess a  $sp^2$  hybridized backbone with a continuous  $\pi$ -system, which is responsible for their ability to conduct charge as well as their unique optical properties. The utility of conjugated polymers arises from their ability to switch reversibly between oxidized and reduced (redox) states (Figure 3). This redox switching can be accompanied by a change in color, conductivity, solubility, volume, and reactivity. These properties make conjugated polymers attractive materials for applications such as



electrochromic devices, flexible photovoltaics, flexible OLED displays, biochemical sensors, energy storage, and actuators to name a few.<sup>4-9</sup>

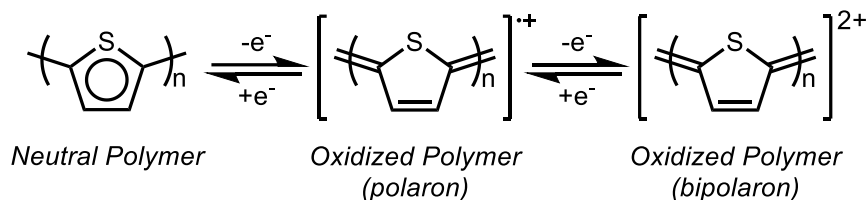


Figure 3. Reversible reduction and oxidation (redox) switching of polythiophene between neutral, radical cation, and dicationic states.

### 1.2.2 Conductivity

Materials become conductive when sufficient energy is input to promote electrons in the highest occupied molecular orbital (HOMO) to the lowest unoccupied molecular orbital (LUMO). In many atom systems (e.g. polymers, crystals), discrete molecular orbitals converge into valence (HOMO) and conduction (LUMO) bands. Most organic materials are insulators, meaning there is a substantial energy gap ( $E_g$ ) between the HOMO and LUMO. For semiconductors, this energy gap is small, and in metals, is absent entirely. In conjugated systems band gap decreases with increasing conjugation (Figure 4), meaning less energy is required to promote an electron in the HOMO to the LUMO. This is because as conjugation increases, charges can be delocalized over a physically larger space. This effect is responsible for the semiconducting behavior exhibited by many conjugated polymers.

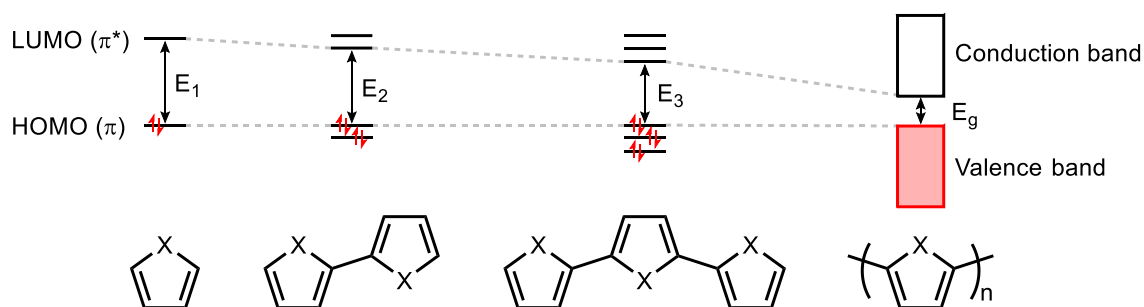


Figure 4. Decreasing energy gap ( $E_g < E_3 < E_2 < E_1$ ) with increasing conjugated length ( $X = \text{NH}, \text{O}, \text{S}, \text{Se}, \text{Te}$ ).

### 1.2.3 Charge Transport Properties

The majority of conjugated polymers researched are p-type semiconductors, meaning positive charges (holes) are the dominant carriers.<sup>10</sup> Conjugated polymers exhibit highly anisotropic electronic structure, with the greatest conductivity in the direction of the conjugated backbone.<sup>4,11,12</sup> This is because  $\pi$ - $\pi$  overlap is largest among neighboring monomers along a chain. Whereas traditional semiconductors are three-dimensional rigid structures, conjugated polymers are essentially one-dimensional and thus much more susceptible to structural distortion upon electronic excitation or charge transport, meaning electronic excitations and charge transport are intrinsically coupled to chain distortions.<sup>12,13</sup> In other words, removing (or adding) an electron from the conjugated backbone induces a topological 'kink' in the polymer chain. These topological defects give rise to the unique conduction mechanisms found in conjugated polymers.

Conjugated polymers can be broadly categorized into two types, those with a degenerate ground-state, and those without. In the scope of this work, we

will concern ourselves with only the latter, to which the vast majority of conjugated polymers belong. Examples include polythiophene and poly(*p*-phenylene), shown in Figure 5. The ground-state resonance structures of these two polymers are energetically nonequivalent (nondegenerate). In the case of polythiophene and poly(*p*-phenylene), the quinoid form has higher energy than the aromatic form such that the aromatic form is favored.<sup>12,14</sup> Besides the different locations of double and single bonds, these two resonance structures also have slightly differing C-C bond lengths along the conjugated backbone.<sup>15</sup>

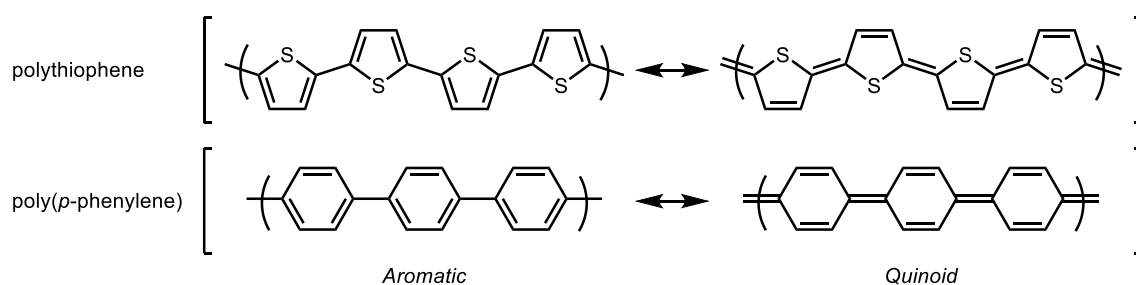


Figure 5. Nondegenerate (polythiophene and polyphenylene) ground-states.

When an electron is removed from the conjugated backbone, the resulting positive charge is delocalized over several adjacent rings. This delocalization results in a small, charged segment of polymer with quinoidal geometry. The slight differences in the bond lengths of the conjugated backbone between these quinoidal and aromatic regions creates the topological ‘kink’ that accompanies charge transport.<sup>15</sup> Conjugated polymers with this property exhibit polarons (radical cation, electron/hole pair) and bipolarons (dication, hole/hole pair) as the dominant charge carriers (Figure 6).

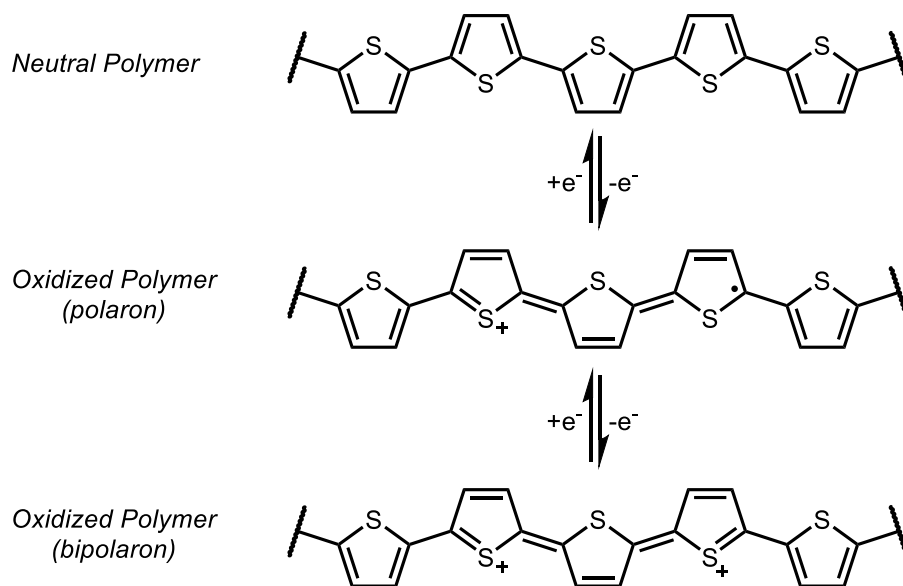


Figure 6. The structures of aromatic (neutral), polaronic (radical cation), and bipolaronic (dication) polythiophene.

#### 1.2.4 Hierarchical Structures

Without the aid of added solubilizing or stabilizing substituents, almost all conjugated polymers suffer from some common issues. Their rigid structure makes them highly insoluble and thus difficult to characterize and process. Additionally, most suffer from sensitivities to oxygen and moisture, thereby limiting their practical application. The design of functional conjugated polymers requires consideration of their primary (repeat unit), secondary (conformational), and tertiary (morphological) hierarchical structures (Figure 7), as they can greatly impact their thermal, optical, and electronic properties.<sup>16</sup>

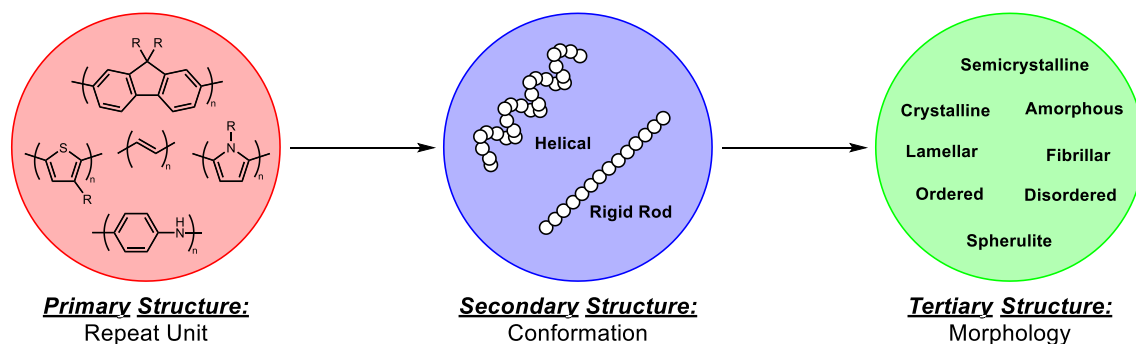


Figure 7. The hierarchical structures of conjugated polymers and some examples of each.

The hierarchical structures of conjugated polymers are altered by the choice of monomer, polymerization conditions, and processing conditions.<sup>16</sup> Optimization of each of these factors is key to the large-scale commercial application of conjugated polymers. In this work, we will focus primarily on how different polymerization conditions affect the secondary structures of some conjugated polythiophenes.

### 1.3 Polyheterocycles

Polyheterocycles (Figure 8) are of much interest as they provide a highly tunable scaffold to construct conjugated polymers with tailored electronic and optical properties. Modifying the heteroatom and adding functional groups allows the solubility, stability, band gap ( $E_g$ ), and oxidation potential of the polymers to be tuned.<sup>13</sup> The methods developed by Sugimoto *et al.* in the mid-1980s remain a staple in synthesis of polyheterocycles, including but not limited to polypyrrole ( $X = NH$ ), polyfuran ( $X = O$ ), polythiophene ( $X = S$ ), polyselenophene ( $X = Se$ ), and polytellurophene ( $X = Te$ ).<sup>17–19</sup> Much of the early research on conjugated polyheterocycles was dedicated to those containing the lighter main group

elements (N, O, S). However, recently there has been considerable interest in exploring the chemistries of those containing the heavier chalcogens (Se and Te).<sup>20–23</sup>

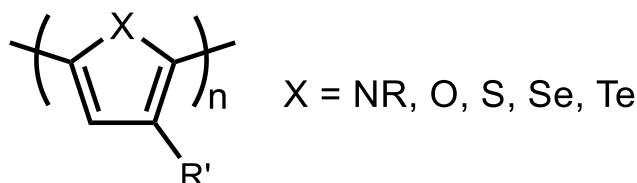


Figure 8. General structure of substituted polyheterocycles. R' = alkyl, alkoxy. R = alkyl, H.

## **1.4 Polythiophenes**

### **1.4.1 Soluble Polythiophenes**

Polythiophenes are one of the most widely researched conducting polymers, owing to their remarkable stability towards oxygen and moisture.<sup>24,25,26</sup> Because unfunctionalized polythiophene is an insoluble material, an early goal of polythiophene research was the development of soluble derivatives that could be characterized in greater detail. It was quickly discovered that polymerization of alkyl-substituted thiophenes with alkyl chains longer than three carbons (butyl and greater) rendered poly(alkylthiophene)s (PATs) (Figure 9a) that were soluble in organic solvents and melt processable.<sup>19,27,28</sup> Long-chain alkoxy groups (Figure 9b) were found to have several advantages over alkyl substituents, such as increased solubility and a significant reduction in polymer band gap.<sup>29</sup> To date, PATs are one of the most extensively researched classes of polythiophenes, of which poly(3-hexylthiophene) (P3HT) is the most notable example (Figure 9c).

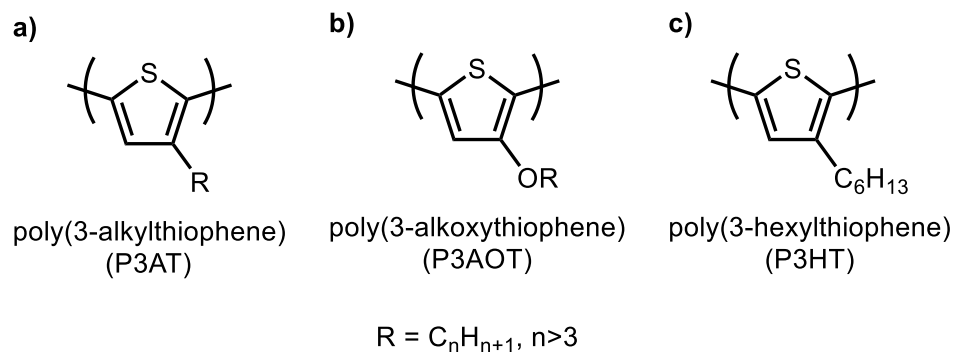


Figure 9. Structures of soluble polythiophene derivatives.

#### 1.4.2 Poly(3,4-alkylenedioxythiophene)s

The development of 3,4-alkylenedioxythiophenes 3,4-ethylenedioxythiophene (EDOT) and 3,4-propylenedioxythiophene (ProDOT) (Figure 10), by BAYER AG in the late 1980s presented a new platform for highly conductive and stable polythiophenes.<sup>30,31</sup> Similar to polythiophene, unfunctionalized poly(3,4-ethylenedioxythiophene) (PEDOT) is an insoluble material, which necessitated the development of soluble alkyl<sup>32–34</sup> and alkoxy<sup>34–36</sup> substituted derivatives. The general structures of functionalized EDOTs and ProDOTs are shown in Figure 10.

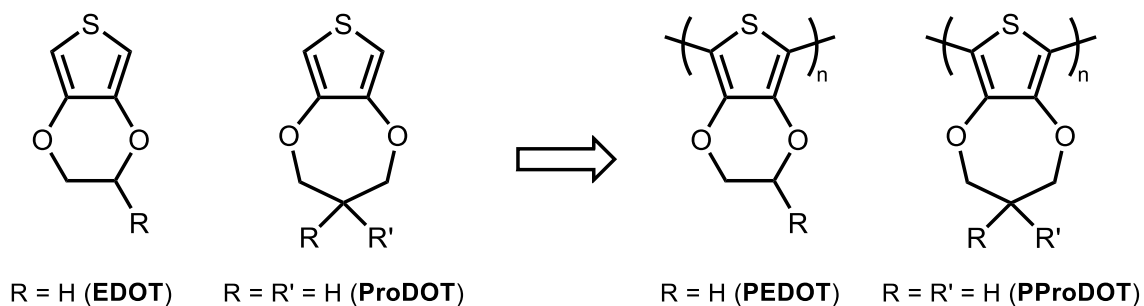


Figure 10. General monomer and polymer structures of 3,4-ethylenedioxythiophene (EDOT) and 3,4-propylenedioxythiophene (ProDOT) and their functionalized derivatives.

3,4-Alkylenedioxythiophenes present many advantages over 3-hexylthiophene. Namely, the electron-donating ether substituents decrease the polymer's oxidation potential and increase its stability in the doped state.<sup>31,37</sup> Additionally, unlike 3-hexylthiophene, EDOT and ProDOT benefit from substitution at both the 3 and 4 positions, thereby eliminating the possibility of  $\beta$ -couplings (Figure 11) during polymerization which lead to poorly defined, insoluble materials.<sup>31</sup>

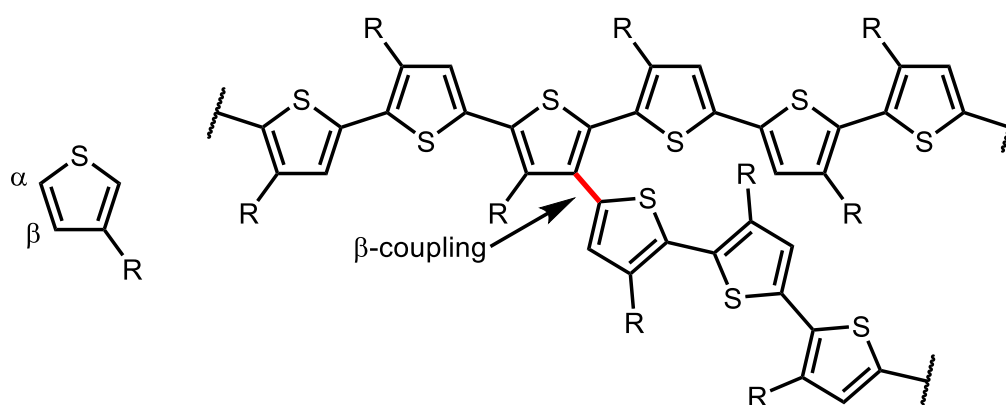


Figure 11. Alpha and beta couplings.

3,4-Alkylenedioxythiophene monomers such as EDOT and ProDOT have proven to be highly versatile platforms for functional conductive polymers.<sup>33,38–42</sup> To date, 3,4-alkylenedioxythiophenes and their derivatives have received much attention and have been extensively researched for numerous applications.<sup>7,9,31,32,43</sup>



## 1.5 Regioregularity – Heads and Tails

### 1.5.1 Background

Once soluble polythiophenes such as P3HT were characterized in greater detail, it became obvious that the methods and conditions employed to prepare such polymers had a large impact on the polymer's secondary structure, which in turn affected its electronic properties. For asymmetric monomers like 3-alkylthiophenes, monomers can couple in three different ways, in either a 2,2'-, 2,5'-, or 5,5'-fashion (Figure 12). The relative number of different couplings present in a polymer is referred to as its regioregularity, which is a measure of its structural homogeneity.

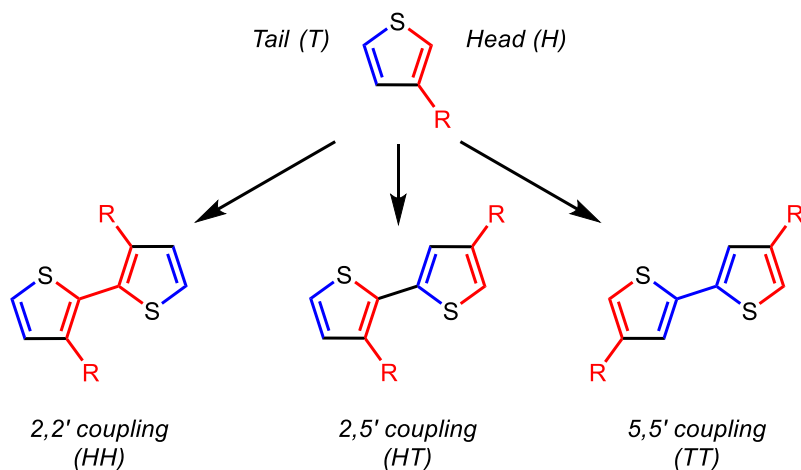


Figure 12. Different couplings in asymmetric monomers like 3-alkylthiophene (where R=alkyl).

Combining two of these couplings yields four spectroscopically distinct triads (Figure 13). In 3-substituted thiophenes, the 2 position is often referred to as the “head” and the 5 position the “tail”. Head-to-tail (HT) couplings are the

most desirable as they inflict the smallest steric demand on the polymer's conjugated backbone, allowing for maximal orbital overlap and effective conjugation length.<sup>44,45</sup>

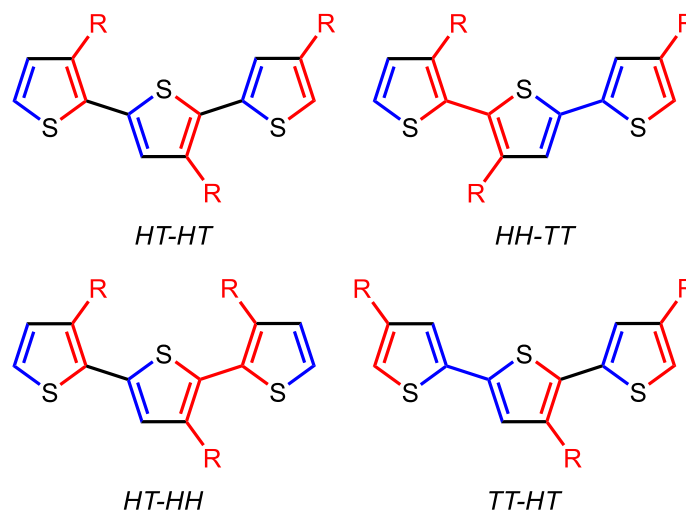


Figure 13. The four possible triads formed by two consecutive monomer couplings ( $R \neq H$ ).

Erroneous head-to-head (HH) couplings induce twisting of the conjugated backbone (Figure 14) due to steric interactions of the side groups, thereby reducing the effective conjugation length. A torsion angle of  $\geq 30^\circ$  between  $\pi$  orbitals has a significant impact on the polymer band gap and conductivity.<sup>46</sup> As a result, much research has gone into developing synthetic methodologies which maximize HT couplings in order to produce structurally homogenous polythiophenes with improved properties over regiorandom ones.<sup>47–52</sup> The twisting effect is prominent in 3,4-disubstituted polythiophenes, which demonstrate remarkable solubility and stability albeit poorer conductivity, higher band gaps, and lower molecular weights.<sup>53,54</sup> EDOT and ProDOT derivatives, however, do not suffer from these issues as their fused ring structure effectively

“pins back” side groups in such a way that steric interactions between neighboring substituents are reduced.<sup>28,31</sup>

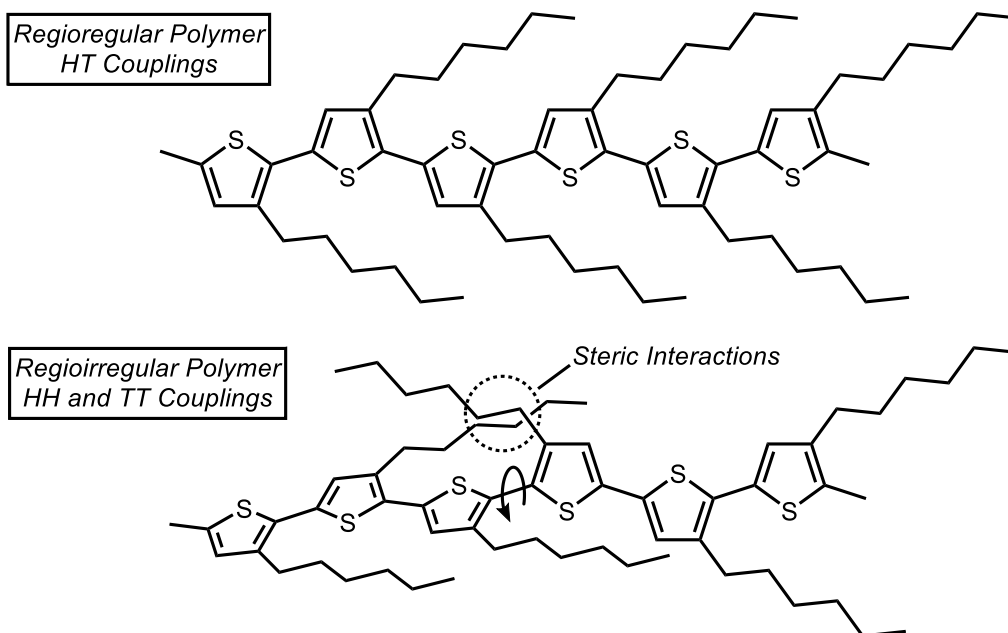


Figure 14. Twisting of the conjugated backbone due to steric interactions of side groups in regiorregular polymers containing HH and TT couplings.

### 1.5.2 Determination of Regioregularity

Methods for determining the regioregularity of P3HT using  $^1\text{H}$  NMR spectroscopy are well-described. The relative areas of the peaks at 2.80 ppm and 2.56 ppm are proportional to the relative amounts of HT and HH couplings, respectively.<sup>55</sup> These resonances correspond to the methylene protons  $\alpha$  to the thiophene ring (Figure 15).<sup>55</sup>

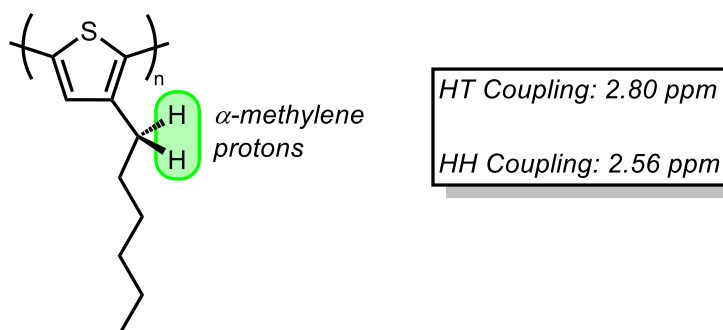


Figure 15. Chemical shifts of alpha-methylene protons in HT and HH couplings.

Methods for determining the regioregularity of PEDOT polymers are much less established. Side groups on EDOT-based polymers are significantly further away from the main chain, and thus their chemical shifts are affected by the polymer's regiochemistry to a much lower degree.<sup>34</sup> Because of this increased distance from the main chain, it is unclear whether or not regiorregularity due to side-groups in EDOT based polymers significantly impacts polymer properties.

## **1.6 Molecular Weight**

### **1.6.1 Background**

When polymers are synthesized, rarely does every polymer chain contain the same number of monomer units. Instead, a polymer sample typically contains a distribution of varying chain lengths. This is in contrast with small molecules and biopolymers, which have well-defined structures and molecular weights (e.g. benzene, C<sub>6</sub>H<sub>6</sub>, 78.11 g/mol). The molecular weight of a polymer is typically described through statistical averaging of the molecular weight distribution of a polymer sample. There are four quantities used to describe the molecular weight of a polymer sample: number-average molecular weight ( $M_n$ ), weight-average

molecular weight ( $M_w$ ), z-average molecular weight ( $M_z$ ), and viscosity-average molecular weight ( $M_v$ ). In the context of this work (linear homopolymers), we will focus primarily on  $M_n$  and  $M_w$ .

Number-average molecular weight  $M_n$  is the arithmetic mean of the molecular weight of each polymer chain, and is equal to the sum of the molecular weight of each polymer chain divided by the total number of polymer chains<sup>56</sup> ( $N_i$ ):

$$M_n = \frac{\text{total weight of sample}}{\text{number of molecules } N_i} = \frac{\sum M_i N_i}{\sum N_i} \quad \text{Equation 1}$$

$M_n$  is a measure of average molecular weight where every molecule is considered equally regardless of its weight or size.  $M_n$  is most influenced by the number of molecules present and thus is most relevant to properties that depend on the number of particles present (i.e. colligative properties: freezing-point depression, boiling-point elevation).<sup>56</sup>

Weight-average molecular weight  $M_w$  is equal to the weighted arithmetic mean, and is described mathematically as:

$$M_w = \frac{\sum M_i^2 N_i}{\sum M_i N_i} \quad \text{Equation 2}$$

$M_w$  accounts for the fact that polymer molecules with higher molecular weight are physically larger, and thus represent a greater portion of bulk sample.  $M_w$  is most influenced by the number of larger molecules present and for this reason is

relevant to properties which depend on molecule size such as viscosity and toughness.<sup>56</sup>

The method by which the molecular weight distribution of a polymer sample is measured ultimately determines which quantity,  $M_n$  or  $M_w$ , is found. Methods which measure the number of molecules in a sample, such as ebulliometry, cryometry, osmometry, and end-group analysis allow for the determination of  $M_n$ .<sup>56</sup> On the other hand, experiments where molecules contribute to the measured results relative to their size, such as light-scattering photometry, allow for the determination of  $M_w$ .<sup>56,57</sup>

The polydispersity index, denoted as  $\bar{D}$  (or PDI in older literature), is equal to the ratio of the weight-average molecular weight to the number-average molecular weight:

$$\bar{D} = \frac{M_w}{M_n} \quad \text{Equation 3}$$

The polydispersity index is a measure of the width of the molecular weight distribution of a polymer sample. Higher polydispersity values indicate of a wider distribution, signifying there is a larger breadth of polymer chain lengths in the sample. A polydispersity index of 1 ( $M_w=M_n$ ) would indicate a sample is monodisperse, meaning all polymer chains are of uniform length.

If the molecular weights of polymers with different primary structure (monomer structures) are to be compared, it is useful to describe the molecular weight in terms of degree of polymerization. The weight-average degree of polymerization  $X_w$  is calculated by the equation:

$$X_w = \frac{M_w}{M_0} \quad \text{Equation 4}$$

Where  $M_w$  is the weight-average molecular weight and  $M_0$  is the molecular weight of the repeating unit.  $X_w$  is a unitless quantity that describes the number of monomer repeat units in a polymer. Consider for example poly(3-methylthiophene) ( $M_0$  96.147 g/mol) and poly(3-dodecylthiophene) ( $M_0$  250.444 g/mol). The molecular weight of the repeat unit of the latter is over two times higher, meaning that at the same polymer molecular weight  $M_w$ , poly(3-dodecylthiophene) contains less than half the repeat units of the poly(3-methylthiophene) (Figure 16).

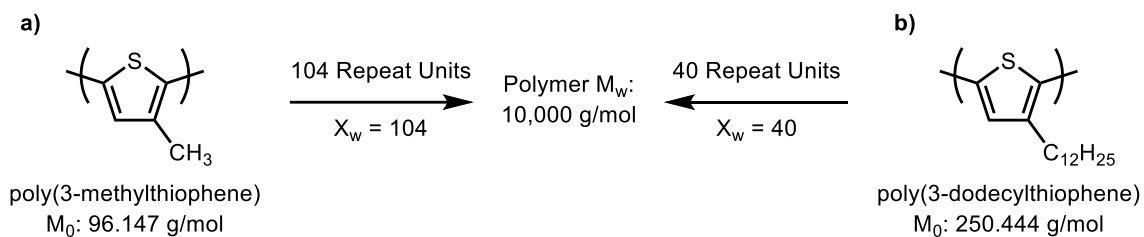


Figure 16. Example of how polymer molecular weight ( $M_w$ ) alone is insufficient for comparing the polymerization of two different monomers.

### 1.6.2 Impact on Polythiophene Properties

The optoelectronic properties of polythiophenes are greatly impacted by their molecular weight (Table 1). As molecular weight increases, average conjugation length increases, and bandgap decreases. This is evidenced by a

bathochromic shift (shift to lower energy) of  $\lambda_{\text{max}}$  in solution and solid-state optical absorption spectra of polythiophenes with increasing molecular weight.<sup>58–60</sup>

Table 1. Effects of molecular weight on the properties of polythiophenes.

<b>Molecular Weight</b>	<b>Effective Conjugation Length</b>	<b>Charge Carrier Mobility</b>	<b>Crystallinity</b>	<b>Grain Boundaries</b>	<b>Bulk Morphology</b>
<b>High</b>	Longer	Higher	Lower	Less Defined	Isotropic Nodular
<b>Low</b>	Shorter	Lower	Higher	Well-defined	Rod-shaped Crystallites

Charge carrier mobility is a measure of how quickly charge carriers (electrons, holes, polarons, bipolarons) move through a conductor or semiconductor in the presence of an electric field. In conjugated polymer thin films, molecular weight has a significant impact on charge carrier mobility. For P3HT, mobility increases with molecular weight.<sup>59–62</sup>

Perhaps the most important factor influencing the mobility of P3HT films is the nature of the polymer chain packing and crystallinity.<sup>60–62</sup> Molecular weight affects chain packing in P3HT thin films to such a degree that it can vary charge carrier mobility by at least four orders of magnitude.<sup>62</sup> Atomic force microscopy (AFM) studies reveal that as molecular weight increases, the morphology (tertiary structure) of P3HT films shifts from regularly stacked rod-shaped crystallites to an isotropic nodular structure (Figure 17).<sup>59,62</sup> X-ray diffraction (XRD) experiments also show for high molecular weight films that although they exhibit lower overall crystallinity, a much larger fraction of the bulk resides within semi-



ordered domains.<sup>59</sup> The general structure of high molecular weight P3HT films thus consists of long polymer chains connecting small, ordered domains.<sup>11,59,62,63</sup>

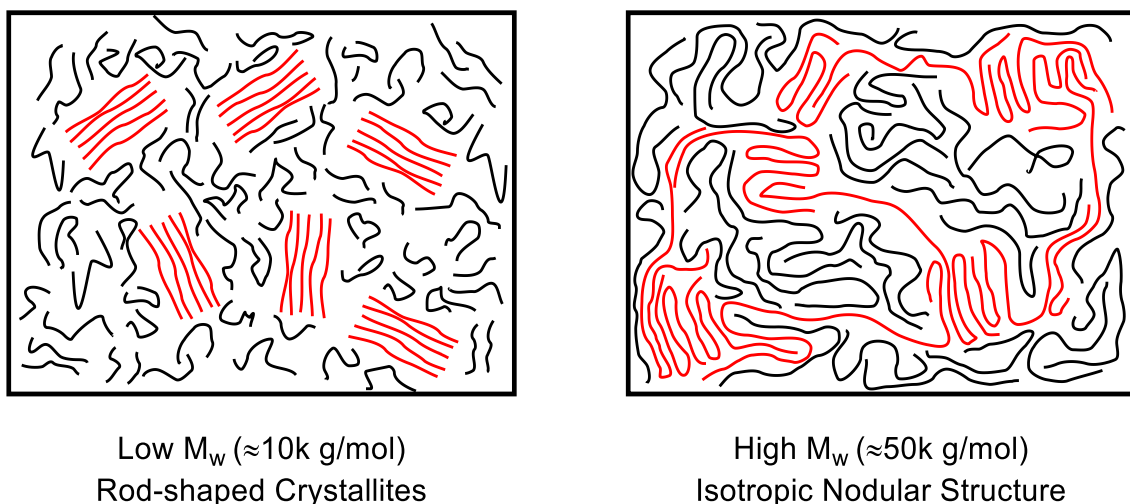


Figure 17. Comparison of high and low  $M_w$  P3HT film morphology. Ordered regions highlighted in red. Adapted from ref.<sup>64</sup>

For P3HT it is hypothesized that mobility is limited by trapping at crystalline boundaries.<sup>59,62</sup> The less well-defined grain boundaries in high molecular weight films are likely responsible for their enhanced mobility compared to low molecular weight films.<sup>59,60,62</sup> Additionally, because longer chain lengths allow charge carriers to travel farther before having to possibly hop to an adjacent chain, it is plausible that a net decrease in hopping events is also partly responsible for the increase in mobility observed with increasing molecular weight.<sup>62</sup> Studies on very high molecular weight (up to 828,000 g/mol) P3HT films show that as molecular weight increases, the orientation of P3HT chains relative to the substrate gradually shifts from 'edge-on' to 'face-on' (Figure 18).<sup>61</sup> Because polythiophenes have highly anisotropic charge transport<sup>4,11</sup>, tuning the molecular weight of the polymer allows the axis of  $\pi$ -stacking to be changed from

parallel to the substrate to perpendicular to the substrate. This is important because the organization of polymer chains at the substrate interface critically impacts charge transport at those interfaces.<sup>65</sup>

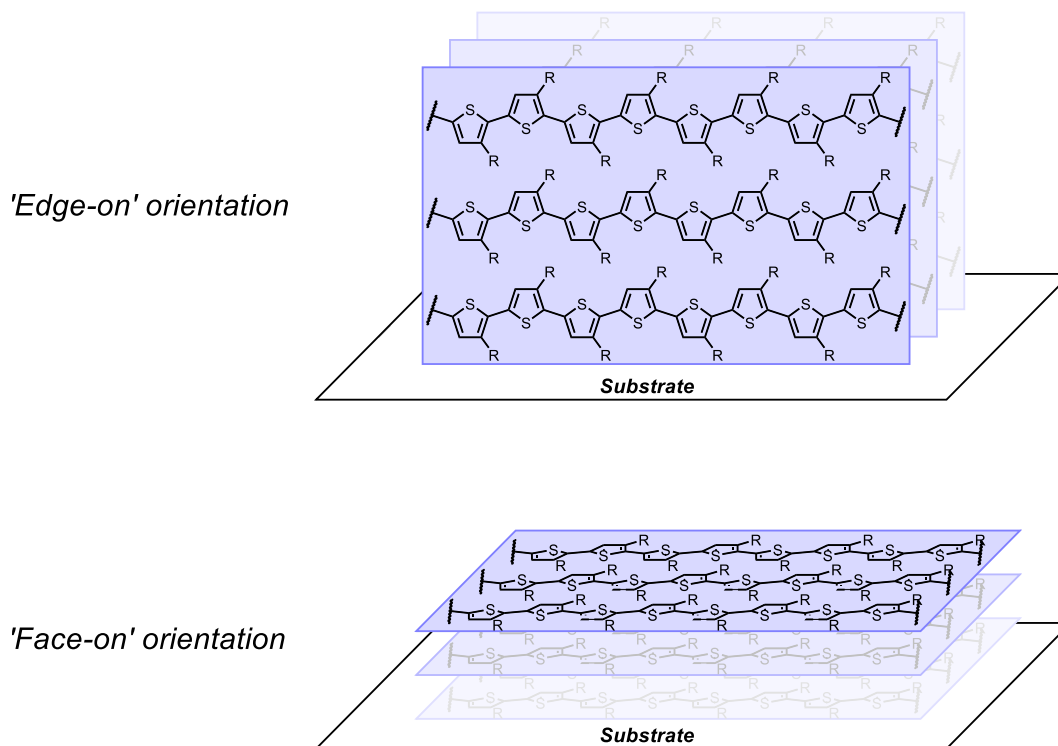


Figure 18. 'Edge-on' and 'face-on' orientations of P3HT in thin films.  $R = C_6H_{13}$ .

### **1.7 Gel Permeation Chromatography**

Gel permeation chromatography (GPC) is a chromatographic technique that separates the components of a sample based on their physical size. A generic box diagram for a typical GPC instrument setup is shown in Figure 19. The injected sample is pumped through a column containing a porous cross-linked gel stationary phase with specific pore sizes. As the sample travels through the column, analytes are separated by their ability to fit into the pores in the stationary phase. Analytes that are too large to fit into the pores are not

retained by the column and elute first, while smaller analytes get trapped in the pores and elute later (Figure 20). Because a constant flow rate is used, elution volume is directly proportional to time.

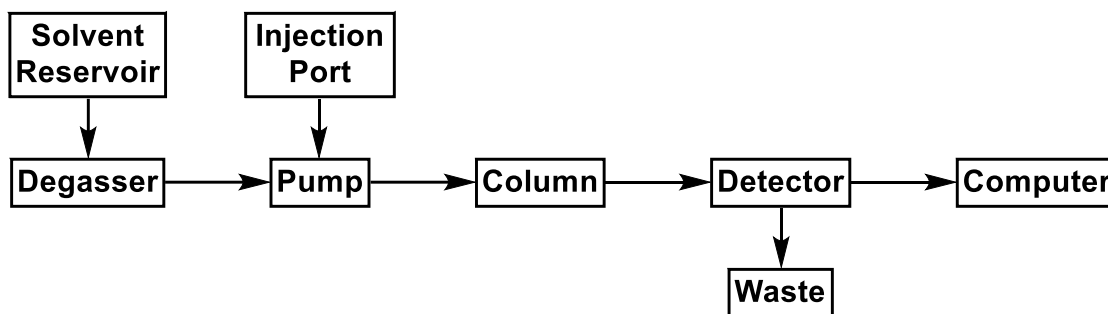


Figure 19. Generic box diagram for GPC.

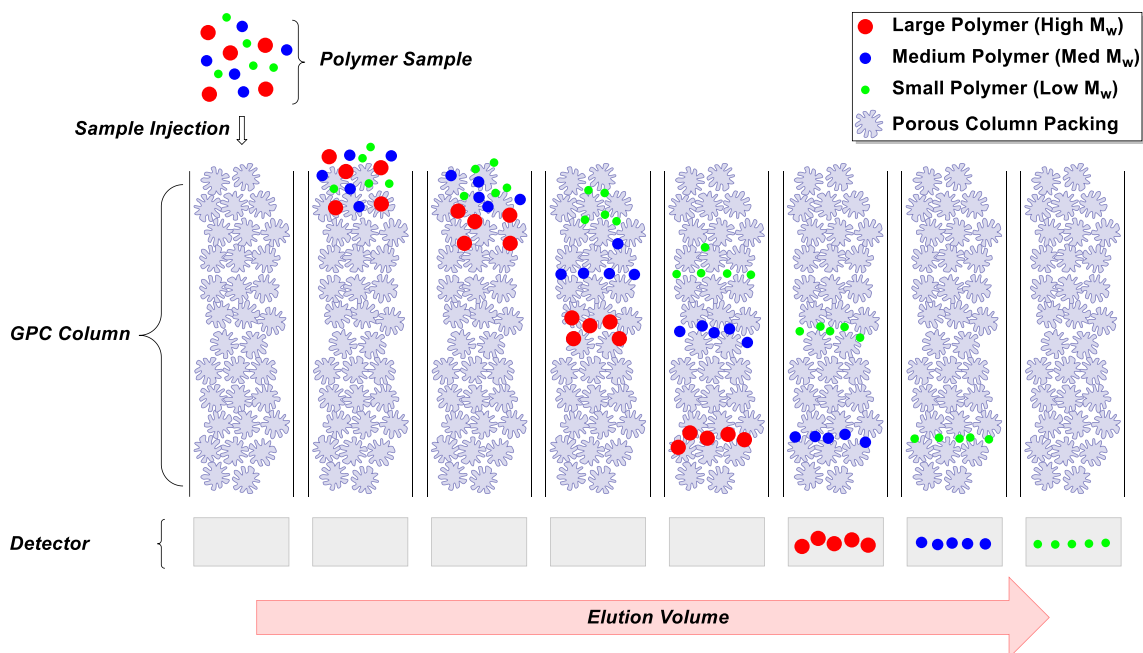


Figure 20. Depiction of the operating principle of GPC separation. High  $M_w$  polymers (red spheres) are too large to fit into the pores of the column packing, and thus pass through the column first. Medium and low  $M_w$  polymers (blue and green spheres, respectively) are small enough to fit into the pores and get trapped, increasing the volume of solvent needed to elute them from the column. The smaller the polymer is, more time it spends within the pores, thereby requiring a greater volume to be eluted from the column.

A calibration curve can be built by measuring the volume of eluent required to elute different polymer samples of known molecular weight. Ideally, plotting elution volume versus the logarithm of the molecular weight of the samples produces a straight line. A simple linear regression of this plot produces the calibration curve. The elution volume of an unknown sample is related to the logarithm of its (weight average) molecular weight by the relation:<sup>66</sup>

$$\log_{10} M_w = mx + b \quad \text{Equation 5}$$

Where  $x$  is the sample's elution volume, and  $m$  and  $b$  are the slope and intercept of the calibration curve, respectively. Polystyrene is typically the calibration standard of choice for the molecular weight characterization of polythiophenes and other conjugated polymers.<sup>67</sup> However, because the structure of polystyrene differs significantly from most conjugated polymers, their behavior in solution is significantly different. The relatively rigid structure of conjugated polymers hinders them from adopting the same coiled conformation as polystyrene in solution. This means that for a given molecular weight, conjugated polymers tend to occupy a larger hydrodynamic volume than polystyrene, and thus their molecular weight is typically overestimated.<sup>68–71</sup> Molecular weights determined this way are not absolute; instead they are described relative to the polymer used for calibration (in this case, polystyrene).

## **1.8 Polymerization of Thiophenes**

### **1.8.1 Chemical Oxidative Polymerization**

To date, numerous synthetic approaches to polythiophenes have been described including electrochemical,<sup>4</sup> chemical oxidative,<sup>19</sup> and transition metal-

mediated polymerization.<sup>72–74</sup> Despite this abundance of possibilities, chemical oxidative polymerization remains a valuable tool for the synthesis of polythiophenes since it was initially described by Sugimoto *et al.* in the mid-1980s.<sup>19</sup> Compared to electrochemical and organometallic approaches, the method is convenient, low cost, and can be performed on large scales.<sup>75</sup> The reaction is well-described for P3HT but remains to be optimized for ether-substituted monomers like PEDOT derivatives.

#### 1.8.1.1 Background

Chemical oxidative polymerization (COP) is the earliest known method to produce conjugated polymers. The general methodology has not changed much since Fritzsche described the oxidation of aniline salts with potassium chlorate in 1843.<sup>1</sup> The modern method, applied to polyheterocycles including polythiophenes was developed in the mid-1980s by Sugimoto *et al.*<sup>18,19</sup> In its most general form, COP simply requires treating a monomer with an oxidant. For polythiophenes, the oxidant of choice is typically FeCl<sub>3</sub> or another Fe<sup>3+</sup> salt.<sup>19</sup> The reaction is most commonly performed in solution, though it can also be performed in the solid or gas<sup>76</sup> phase. The equation for the COP with FeCl<sub>3</sub> is generally given as (Scheme 1):<sup>77–79</sup>

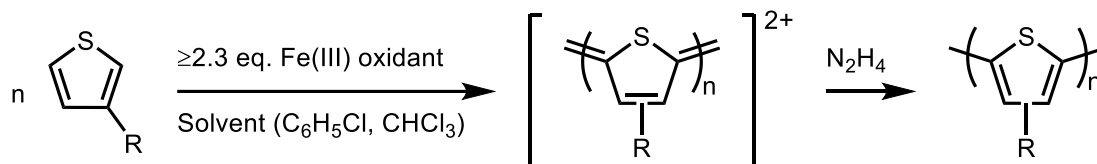


Scheme 1. Chemical oxidative polymerization equation.

However it is commonly observed that high yields and molecular weights are obtained only if a 2.3:1 molar ratio or greater (Scheme 2) of oxidant to monomer

is employed, with 4 equivalents being used frequently in the literature.<sup>19,55,77,78,80–</sup>

<sup>82</sup> This is thought to be partly due to consumption of the FeCl<sub>3</sub> oxidant to FeCl<sub>4</sub><sup>–</sup> by the generated HCl.<sup>77</sup>



Scheme 2. Chemical oxidative polymerization.

Poly(3-hexylthiophene) (P3HT) was one of the first polymers reported to be synthesized by the modern chemical oxidative polymerization method, and since has become one of the most extensively researched polythiophenes. Chemical oxidative polymerization methodologies for P3HT are well-established, and in such context, it may be classified as a model system. For example, in the case of the chemical oxidative method, high molecular weight ( $X_w \geq 420$ ,  $M_w \geq 70,000$  g/mol) P3HT with regioregularity of 70-90% is readily obtainable in good yields.<sup>28,41,55,80,83,84</sup> However, outside of 3-hexylthiophene and other closely related alkylthiophenes, polymerization conditions often require significant optimization to achieve similar yields and molecular weights. Given the wide scope of conjugated polymer applications, P3HT alone is insufficient in meeting the needs of every application.

A survey of the literature reveals that chemical oxidatively polymerized ether-substituted polythiophenes (3,4-alkylenedioxy and 3,4-dialkoxy derivatives) rarely achieve the degree of polymerization reported for P3HT and related 3-alkylthiophenes (Table 2).<sup>85,86</sup> Methods to improve these polymers' molecular

weights and regioregularities are of interest because polymers with higher molecular weight and regioregularity exhibit improved thermal properties,<sup>64</sup> optical properties,<sup>58</sup> and carrier mobilities.<sup>62</sup>

Table 2. Previously reported molecular weights of relevant polythiophene derivatives. Polymerizations were performed under reverse addition conditions (monomer added to oxidant) in  $\text{CHCl}_3$ . The structure and abbreviation of each polymer is given, along with weight-average molecular weight  $M_w$ , polydispersity index  $\mathcal{D}$ , weight-average degree of polymerization  $X_w$ .

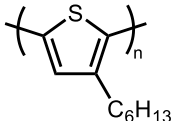
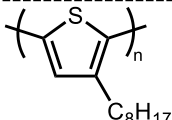
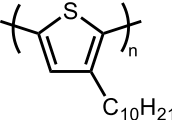
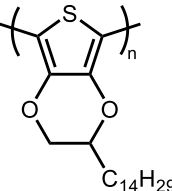
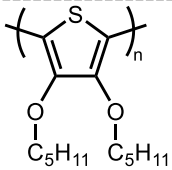
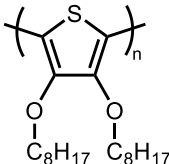
Structure	Abbreviation	Entry	Equivalents	$M_w$	$\mathcal{D}$	$X_w$	ref
			$\text{FeCl}_3$				
	P3HT	1	2	140,000	3.5	842	41
		2	4	110,700	2.7	666	55
		3	4	411,000	3.5	2472	80
	P3OT	7	4	181,440	4.8	933	87
	P3DT	9	4	303,050	5.5	1362	87
	PEDOT-C14	11	2	11,200	2	33	32
		12	4	22,500	2.74	67	32
	PDPOT	13	4	11,528	1.83	34	88

Table 2. Continued

	PDOOT	14	4	9,743	1.8	38	88
---	-------	----	---	-------	-----	----	----

It is important to note that there is a considerable variability<sup>28</sup> in the molecular weights reported for polymers prepared under similar conditions, for example P3HT synthesized in chloroform with 4 equivalents of FeCl<sub>3</sub> (entries 2 and 3 in Table 2). Some of this variability is due to discrepancies between the amounts of solvent used and whether the solvent contains a radical inhibitor (for example ethanol in chloroform).

Though COP remains an attractive method for the quick preparation of conjugated polymers, the harsh (highly oxidizing) reaction conditions make this method inappropriate for monomers bearing sensitive functional groups. Polymers prepared by COP are often contaminated with significant amounts of oxidant, which can make them inappropriate for some sensitive applications without extensive purification.<sup>89</sup> Polymerization of asymmetric monomers like 3-hexylthiophene produces polymers with poor regioregularity compared to other polymerization methods. Additionally, monomers with unsubstituted 4-position are also susceptible to  $\beta$  couplings (Figure 11), leading to poorly defined cross-linked materials with decreased solubility.



### 1.8.1.2 Mechanistic Insights

There have been many mechanisms proposed for the oxidative polymerization of polythiophenes to date.<sup>41,55,77–79</sup> The reaction has been proposed to proceed through either a radical mechanism<sup>77,90</sup> or radical cation mechanism.<sup>41,77–79,91</sup> Work by Barbarella *et al.* on the oxidative polymerization of 3-(alkylsulfanyl)thiophenes gives interesting insight into the COP reaction mechanism, as it relates to 3-substituted thiophenes (Figure 21).<sup>79</sup> The authors found that when polymerization conditions which normally produce high molecular weight poly(3-alkylthiophene)s were applied to 3-(methylsulfanyl)thiophene and 3-(dodecylsulfanyl)thiophene, only short oligomers were produced.<sup>79</sup> The oligomers were separated and characterized individually. Interestingly, the oligomers displayed consistent regiochemistry; each oligomer contained 1 HH coupling, the rest being HT.<sup>79</sup> The authors suggest that first, two radical cation monomers couple at the 2 position to give a 2,2' (HH) dication dimer, as it is known for thiophenes that electron donating substituents (alkyl, alkoxy, alkylsulfanyl, etc.) at the 3 position make the 2 position more reactive to oxidative coupling.<sup>77,79</sup> The dication loses two protons, regaining aromaticity. The dimer, which has an oxidation potential lower than the monomer, is quickly oxidized to a radical cation. Further couplings must occur at the 5 or 5' position, resulting in a 2,5' (HT) coupling. These findings support a radical cation mechanism similar to the one proposed by Niemi *et al.*<sup>77,79</sup> It is expected that 3-alkylthiophenes and other thiophenes follow a similar mechanism.

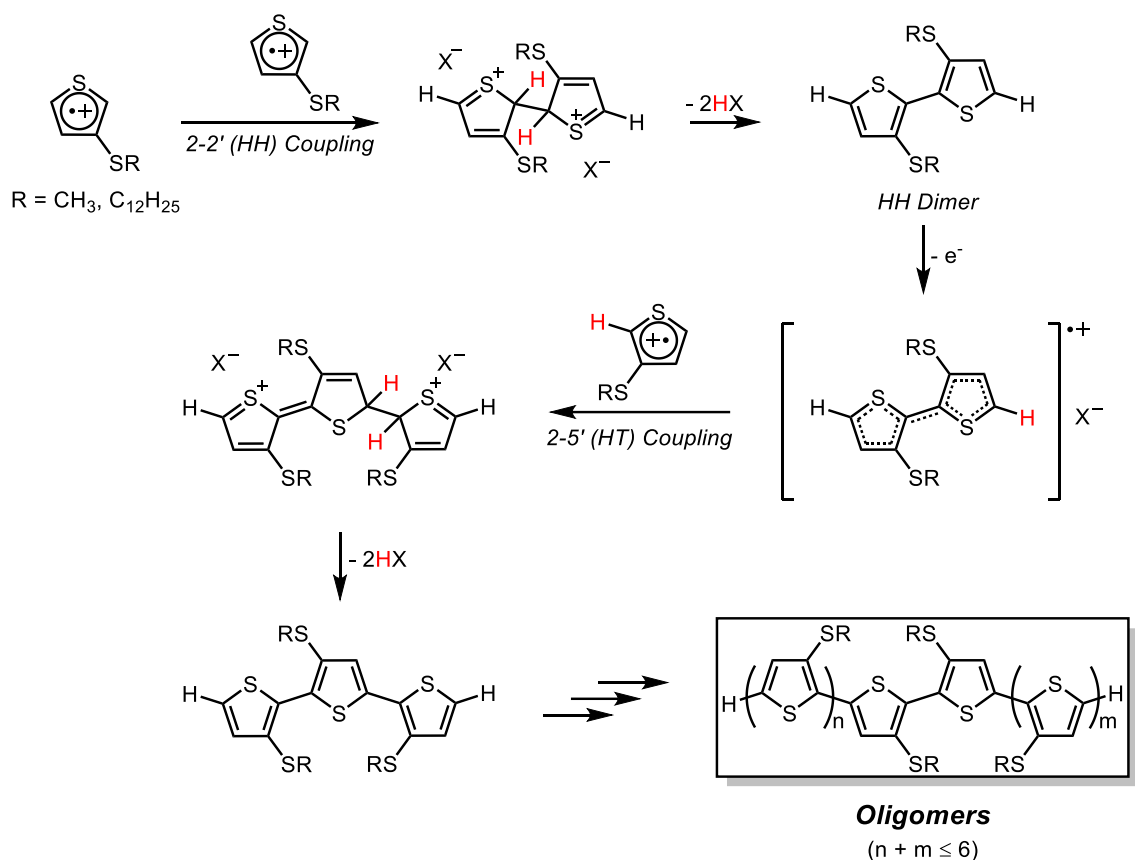


Figure 21. Oxidative polymerization of 3-alkylsulfanyltiophenes.<sup>79</sup>

From these findings we can gather that regioregular polymers are formed predominantly from monomer-oligomer couplings, as these result in HT linkages.<sup>55</sup> Irregularities are increased as oligomers couple, as this introduces TT linkages.<sup>55</sup> To support this, Amou *et al.* found that by decreasing the monomer concentration and reaction temperature, the regioregularity of P3HT could be increased up to 91% HT.<sup>55</sup> Lowering the reaction temperature suppresses the amount of active (oxidized) monomer in solution, limiting the amount of HH dimer produced.<sup>55</sup> At dilute concentrations, dimer-dimer (TT) couplings can be

effectively minimized.<sup>55</sup> These conditions promote monomer-oligomer HT couplings, thereby producing a more regular polymer.

Several studies have been conducted to examine the effects of varying different reaction parameters. Varying the reaction temperature, solvent, monomer concentration, and monomer/oxidant ratio can affect reaction yields as well as polymer regioregularity, molecular weight, and polydispersity index (summarized in Table 3).<sup>41,55,77,78,80,83,92,93</sup> Lower reaction temperatures improves the polydispersity index at the cost of a slight reduction in yield.<sup>78</sup> Polymers prepared in better solvents tend to have higher molecular weight and improved regioregularity.<sup>78</sup> Reducing the ratio of oxidant to monomer sharply decreases yields, and at sub-stoichiometric amounts molecular weight is severely impacted.<sup>41</sup>

Table 3. Chemical oxidative polymerization reaction parameters and their effects.

<b>Reaction Parameter:</b>	<b>Effect:</b>	<b>Mechanism:</b>	<b>Reference:</b>
<b>Reduced Temperature</b>	Improvement of Đ and regioregularity with slight decrease in yield.	Suppression of active (oxidized) monomers in favor of dimers/oligomers.	55,78
<b>Improved Solvent</b>	Increased molecular weight and improved regioregularity.	Improved solvation of polymer.	78
<b>Reduced Monomer Concentration</b>	Increased molecular weight and improved regioregularity.	Suppression of dimer/oligomer couplings and improved solvation of polymer.	55
<b>Decreased Oxidant/Monomer Ratio</b>	Yields are severely decreased, molecular weight sharply decreases (sub-stoichiometric ratio).	Overall reduction in amount of oxidized species present.	41

With this information, we propose the more thorough oxidative polymerization mechanism shown in Figure 22. The first step involves oxidation of monomer to give a radical cation. This radical cation can couple with either neutral monomer or another monomer radical cation (Figure 22 **a** and **b**, respectively). In the case of the former, the resulting radical cation dimer gets oxidized to give a dicationic dimer; in the case of the latter a dicationic dimer is formed directly. The dicationic dimer loses two protons and regains aromaticity.<sup>4,41,75,78</sup> The dimer is oxidized, then depending on reaction conditions, grows through monomer-chain, or chain-chain couplings to give an oxidized polymer of varying regioregularity.<sup>55</sup> The oxidized polymer can then be reduced to yield the neutral polymer. The idealized regiochemistry depicted in the extended COP mechanism (Figure 22) is based on the calculated coefficients of the highest occupied molecular orbital (HOMO) of the 2 and 5 position.<sup>77,79</sup> The figure serves to illustrate how the reaction conditions influence the prevalence of different possible couplings which ultimately affect the polymer's regioregularity (secondary structure) though it is not an exhaustive representation of every possibility.

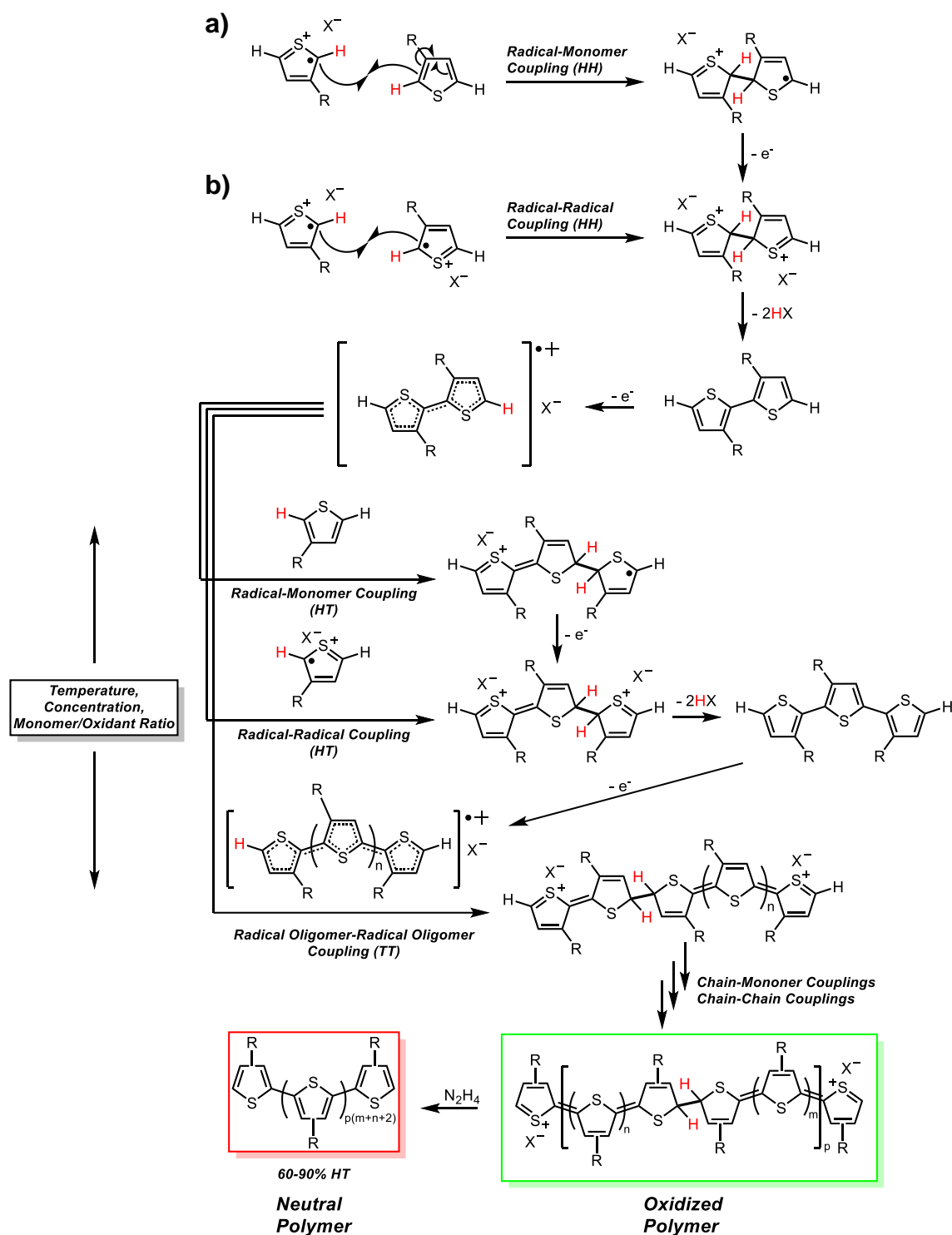


Figure 22. Extended COP mechanism illustrating the impact of reaction conditions on polymer regioregularity. The idealized regiochemistry shown is based on calculated coefficients of the HOMO at the 2 and 5 positions.

### 1.8.1.3 Order of Addition

Among the many studies on the oxidative polymerization reaction, the order of addition of reagents is rarely considered. The reaction can be performed under what we term “standard addition” or “reverse addition” conditions (Figure 23). Under standard conditions, the oxidant is added to the monomer. Under reverse conditions, the opposite occurs. The original publication by Sugimoto *et al.*<sup>19</sup> describes polymerization of 3-hexylthiophene under reverse addition conditions, and the bulk of other studies are carried out in this fashion.<sup>26,32,87,88,94,41,55,78–81,83,85</sup>

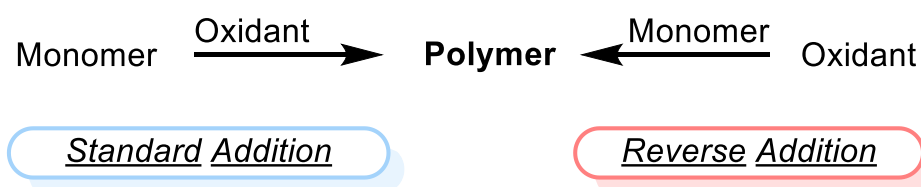


Figure 23. Differences between standard and reverse addition in chemical oxidative polymerization.

There are relatively few papers describing the reaction under standard addition conditions.<sup>75,84,95</sup> This could be due in part to the poor solubility of  $\text{FeCl}_3$  in chloroform, which typically makes it more convenient to add a monomer solution to a flask containing a catalyst suspension than *vice versa*. Creating a oxidant suspension that is suitable for use over an extended period (e.g. slow addition over several minutes) typically requires extensive sonication.<sup>41,83</sup> An alternative is to simply perform the reaction in a good solvent for the oxidant. However, the polar solvents which  $\text{FeCl}_3$  is soluble in are typically poor solvents for alkyl-substituted polythiophenes, which can lead to significantly decreased

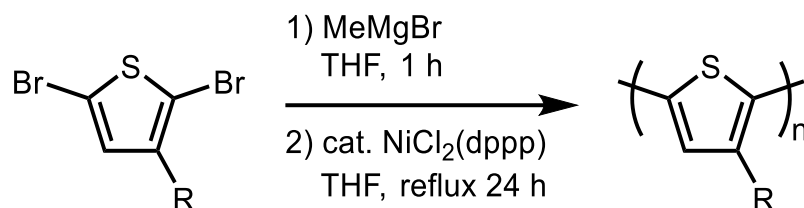
molecular weights.<sup>26,80</sup> This guided us to explore other approaches that kept the convenience of working with an oxidant solution without significantly impacting the solubility and thus the molecular weight of the polymer. The standard addition approach described herein involves the use of a minimal amount of acetonitrile to dissolve the  $\text{FeCl}_3$  to give a solution which is then added to a solution of monomer in a good solvent ( $\text{CHCl}_3$  or chlorobenzene).

### **1.8.2 Grignard Metathesis Polymerization**

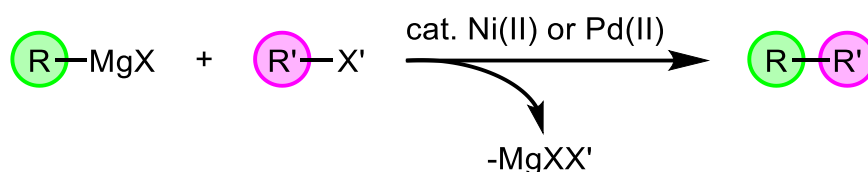
Transition metal-mediated polymerization methods such as Grignard Metathesis (GRIM) provide a degree of synthetic control<sup>96</sup> and regiochemical purity<sup>47,73</sup> that is not easily attained through electrochemical and chemical oxidative polymerization methods. These qualities make GRIM an invaluable tool for the synthesis of conjugated polymers with well-defined structures. In the context of polythiophene synthesis, GRIM polymerization is a flexible and well-established method.

#### **1.8.2.1 Background**

GRIM polymerization (Scheme 3), also known as Kumada catalyst transfer polymerization, was first reported in 1999 by Loewe, Khersonsky, and McCullough.<sup>49</sup> The method was developed with the goal of creating a more industrially relevant alternative to previous Kumada type cross-coupling (Scheme 4) polymerizations of alkylthiophenes like those developed by McCullough and Lowe.<sup>47,48</sup>



Scheme 3. Grignard metathesis (GRIM) polymerization.



Scheme 4. General Kumada cross-coupling reaction.

The GRIM method is advantageous in that it can be done at ambient temperatures or at reflux, in contrast to the cryogenic temperatures required by earlier Grignard-type methods. Generally, GRIM polymerization involves treating a dihalogenated monomer with 1 equivalent of alkyl or vinyl Grignard reagent (typically methylmagnesium bromide) at ambient temperature or at reflux. The resulting monometalated monomer is polymerized by addition of a nickel catalyst, typically  $\text{NiCl}_2(\text{dppp})$  ( $\text{dppp}$  = 1,3-bis(diphenylphosphino)propane).

With the GRIM method, polymer molecular weight can be controlled by altering reaction time and catalyst loading.<sup>97</sup> The method is scalable to large scales and, in the case of P3HT, produces polymers with high regioregularity.<sup>49</sup> Because it is a transition metal-mediated reaction, highly purified monomers are needed to attain high molecular weights as impurities introduce chain-terminating groups. It is also notable that there is significant mass loss through the reaction



because the two bromine atoms in the monomer account for a significant portion of its mass.

#### 1.8.2.2 Mechanism

After the initial formation of a tail-to-tail (TT) dimer, the reaction follows a classic oxidative addition, transmetalation, reductive elimination catalytic mechanism (Figure 24). When applied to thiophene monomers or other small electron-rich heterocycles, the reaction displays “quasi-living” chain-growth polymerization kinetics.<sup>97–99</sup> Chain-growth refers to polymerization that occurs by consecutive addition of monomers to the end of an active chain, as opposed to homogenous polymer growth throughout the reaction matrix (step-growth polymerization). Living polymerizations are those which continue indefinitely as long as monomer is supplied, or in other words, the polymer chain ends remain active until the reaction is terminated.

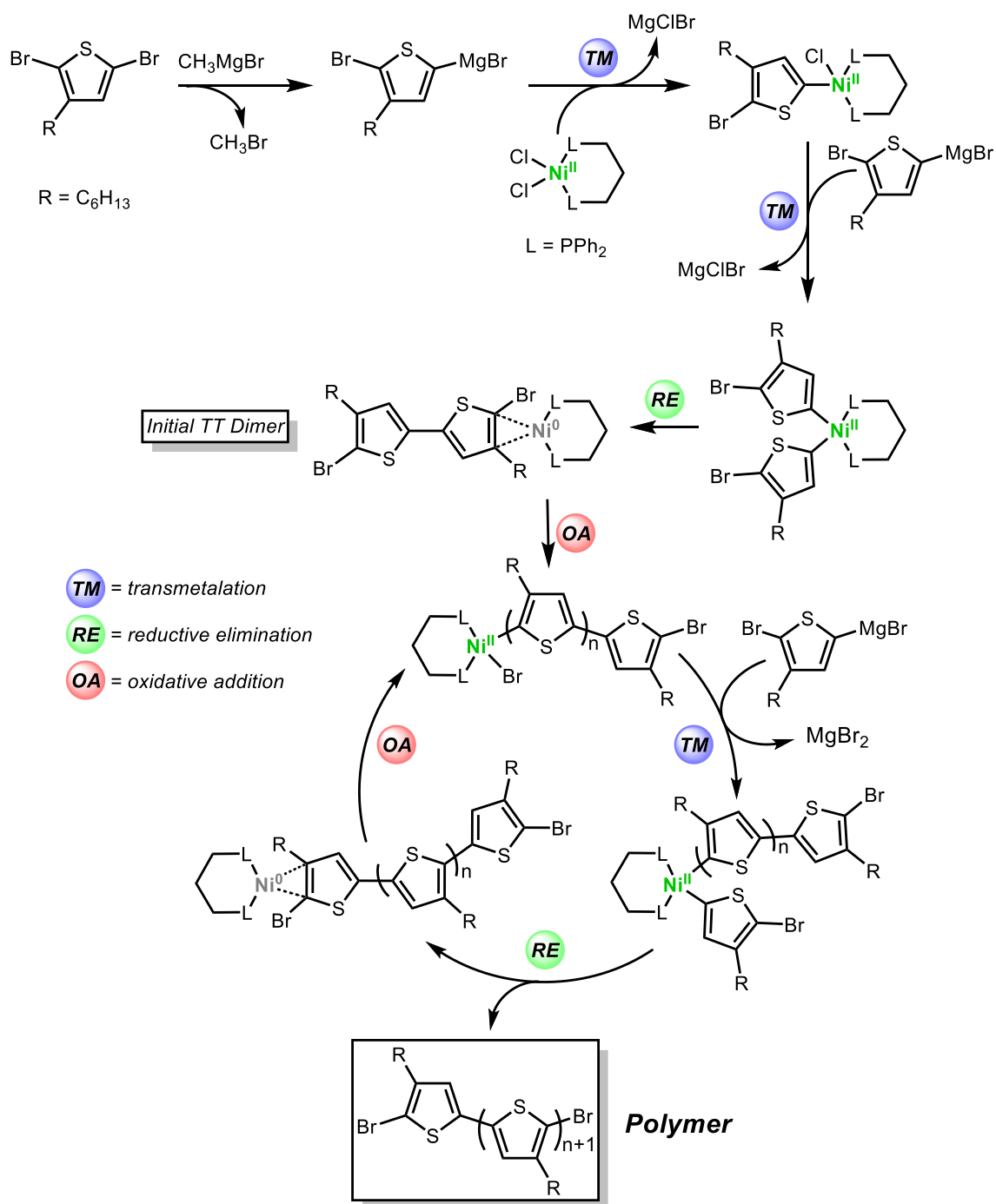


Figure 24. Grignard metathesis mechanism.

During GRIM polymerization, the growing polymer chains and catalyst remain closely associated throughout the reaction due to the strongly stabilizing

effect of the monomer  $\pi$  bonds on the  $\text{Ni}^0$  intermediate.<sup>100</sup> Chains terminated with  $\text{NiBr}(\text{dppp})$  moieties (Figure 25) are subject to further polymerization if additional metalated monomer is added.<sup>97</sup> Other monomers such as phenylene derivatives which are unable to facilitate such strong chain-catalyst interactions instead display step-growth polymerization kinetics due to dissociation of the catalyst from the growing chain.<sup>100</sup>

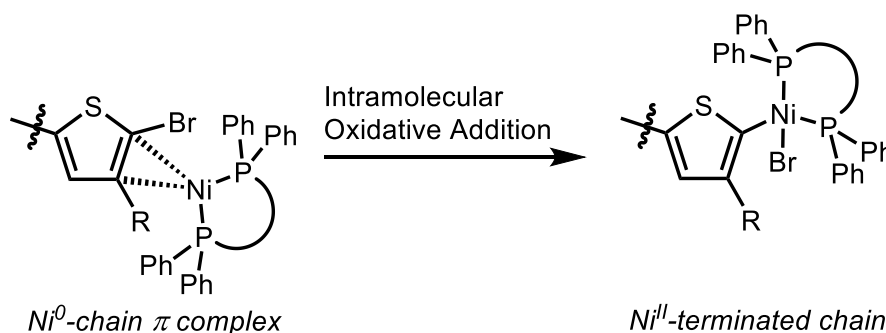


Figure 25. Living chain terminations.

### 1.9 Motivation for Research

Polythiophenes and other conjugated polymers are promising materials for new generations of flexible organic electronic devices. For the applications of conjugated polymers to be fully realized, we must possess a detailed and broad understanding of the interconnection between monomer design, polymerization conditions, and polymer properties. An important endeavor in conjugated polymer research is to develop synthetic methodologies that produce high molecular weight polymers, as their properties are often enhanced over shorter chains and oligomers. Though many methods to produce polythiophenes have been described, research to expand the scope of their synthetic utility is still of

much interest. This is particularly pertinent in the context of the large scale and commercial application of polythiophenes and other conjugated polymers.

### **1.10 Thesis of This Work**

Ether-substituted thiophene monomers were synthesized and polymerized under various reaction conditions via oxidative and non-oxidative approaches. For comparison, the prototypical soluble polythiophene poly(3-hexylthiophene) was also synthesized under various conditions. The polymers were characterized by gel permeation chromatography in order to determine the impact of the different synthetic approaches on the polymer's molecular weight and degree of polymerization.

## 2. MONOMER SYNTHESIS

### 2.1 Introduction

To explore the effects of various synthetic approaches on the molecular weight of ether-substituted polythiophenes, monomers 2-dodecyl-2H,3H-thieno[3,4-b][1,4]dioxine (EDOT-C12), 3,4-bis(hexyloxy)thiophene (3,4-DHOT), and 5,7-dibromo-2-dodecyl-2H,3H-thieno[3,4-b][1,4]dioxine (Br<sub>2</sub>EDOT-C12) were synthesized (Figure 26). As discussed in section 1.4.2, ether-substituted thiophenes present many advantages over 3-hexylthiophene, a prototypical thiophene monomer. The dodecyl (EDOT-C12 and Br<sub>2</sub>EDOT-C12) and hexyl (3,4-DHOT) alkyl substituents were chosen as they allow the corresponding polymers to be soluble in common organic solvents. Monomers EDOT-C12 and 3,4-DHOT were prepared for use in chemical oxidative polymerization, and Br<sub>2</sub>EDOT-C12 was prepared for use in transition metal-mediated Grignard Metathesis polymerization.

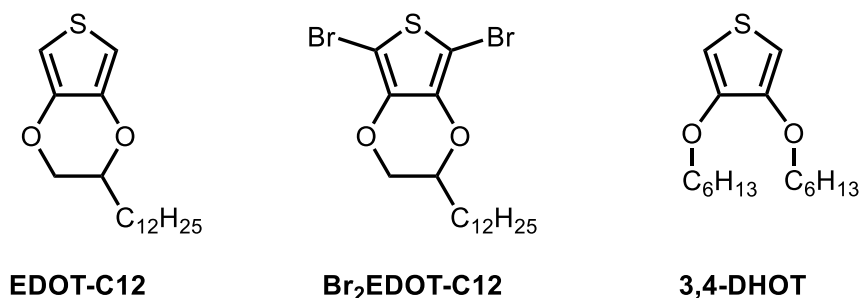


Figure 26. Structures, names, and abbreviations of the monomers synthesized.

## **2.2 Experimental**

### **2.2.1 Materials**

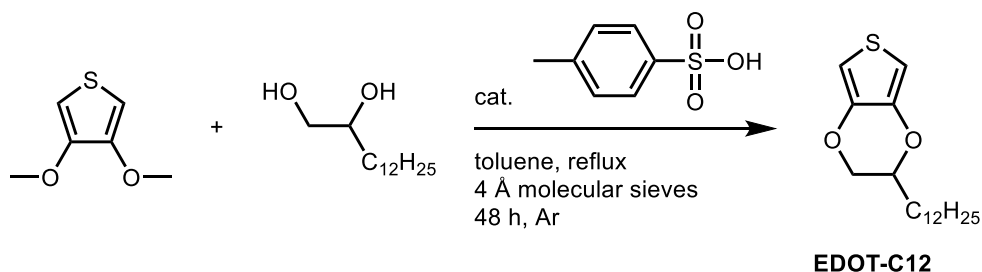
NBS (99%, Alfa Aesar) was recrystallized from water according to a literature procedure.<sup>101</sup> *p*-Toluenesulfonic acid monohydrate (99%) was purchased from Acros and used as received, provided it was sufficiently dry (the material is very hygroscopic). In some instances, ‘wet’ *p*-toluenesulfonic acid was dried by heating it to its melting point under rotary evaporator vacuum for 30-45 min. Molecular sieves (4 Å) were activated by first drying at 200 °C under vacuum in a vacuum-oven for 24 h, then quickly transferred to a Schlenk flask and flame-dried under high vacuum several times. The sieves were kept under high vacuum for 6 h before use. The following chemicals were all used as received: 1,2-tetradecanediol (90% technical grade), toluene (99.8%, anhydrous), and 1-hexanol (≥99%, anhydrous) purchased from Sigma, 3,4-dimethoxythiophene (97%) purchased from Ark Pharm Inc, acetic acid (99.7% ACS) purchased from EMD, chloroform (ACS grade) purchased from Avantor.

### 2.2.2 Methods

Structural characterization of the monomers was performed using nuclear magnetic resonance (NMR) spectroscopy and mass spectrometry.  $^1\text{H}$  and  $^{13}\text{C}$  NMR spectra were collected using a Bruker Avance 400 MHz NMR spectrometer with deuteriochloroform as the solvent.  $^1\text{H}$  spectra were collected over 32 scans, and  $^{13}\text{C}$  spectra were collected over 128 scans. Atmospheric-pressure chemical ionization mass spectra were collected using a Thermo-Scientific Velos Pro mass spectrometer equipped with a dual linear ion trap operating in positive mode. Monomer solutions for mass analysis were prepared in 1:1 v/v methanol/dichloromethane and diluted with additional 1:1 v/v methanol/dichloromethane to a concentration of  $\sim 20\ \mu\text{M}$  by serial dilution.

### 2.2.3 Synthesis

#### 2.2.3.1 2-Dodecyl-2H,3H-thieno[3,4-b][1,4]dioxine (EDOT-C<sub>12</sub>) (Scheme 5)



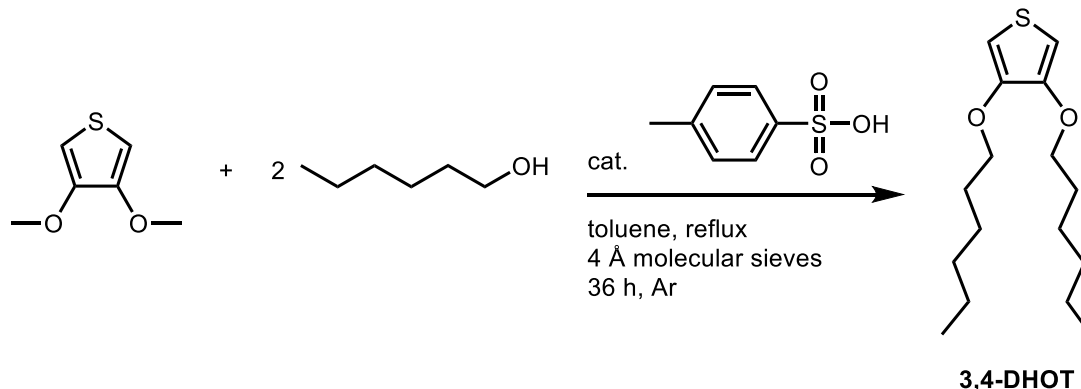
Scheme 5. Synthesis of EDOT-C12.

All glassware was dried in an oven overnight prior to use. A 1 L three-necked round bottom flask was outfitted with magnetic stir bar, Soxhlet extractor charged with activated 4 Å molecular sieves, and high efficiency condenser. 1,2-Tetradecanediol (17.594 g, 76.37 mmol) and *p*-toluenesulfonic acid (1.334 g,

7.01 mmol) were added against a positive pressure of argon. Toluene (400 mL) was added, and the flask was sealed with a rubber septum. Stirring was initiated, and the flask was heated to 60 °C. After approximately 15 min when all solids had dissolved, the septum was removed and 3,4-dimethoxythiophene (9.998 g, 69.27 mmol) (DMT) was added against a positive pressure of argon. The flask was resealed, and the mixture was refluxed at 120 °C for 48 h under argon. The colorless reaction mixture slowly darkened to dark brown over several hours after addition of the DMT. After this period, the mixture was cooled to room temperature, poured into a 1 L separatory funnel, and washed four times with deionized water (ca. 200 mL each). The organic fraction was collected, dried over anhydrous MgSO<sub>4</sub>, and filtered. The filtrate was concentrated under reduced pressure to give the crude product as a dark brown oil. The crude product was purified by filtration through silica gel with hexanes followed by removing the solvent under reduced pressure. The resultant yellow solid was recrystallized from diethyl ether at -78 °C to give 6.02 g (28%) product as a slightly yellow powder. <sup>1</sup>H NMR (400 MHz, CDCl<sub>3</sub>) δ: 6.30 (s, 2H), 4.14 (dd, J = 2.1 Hz, 1H), 4.10 (m, 1H), 3.86 (dd, J = 7.9 Hz, 1H), 1.27 (m, 22H), 0.89 (t, 3H). [Lit.: 6.30 (s, 2H), 4.12 (m, 2H), 3.86 (m, 1H), 1.40 (m, 22H), 0.88 (t, 3H)]<sup>33</sup>



### 2.2.3.2 3,4-Bis(hexyloxy)thiophene (3,4-DHOT) (Scheme 6)



Scheme 6. Synthesis of 3,4-DHOT.

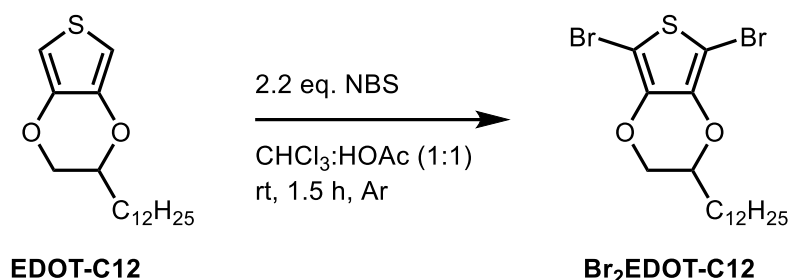
To a three-necked round bottom flask outfitted with Soxhlet extractor charged with activated 4 Å molecular sieves, high efficiency condenser, and magnetic stir bar was added toluene (100 mL). *p*-Toluenesulfonic acid (0.396 g, 20.81 mmol) was added to the flask, and stirring was initiated. The flask was sealed and heated to 60 °C under argon. After stirring for 5-10 min at that temperature, *n*-hexanol (5.78 mL, 46.39 mmol) was added via syringe. After an additional 5 min, 3,4-dimethoxythiophene (2.998 g, 20.80 mmol) in 5 mL toluene was added slowly via syringe. The mixture was heated to 130 °C and stirred for 36 h under argon. The mixture was cooled to room temperature and transferred to a 500 mL separatory funnel. The crude reaction mixture was washed three times with water (60 mL each), once with saturated aqueous NaHCO<sub>3</sub> (60 mL), and once again with water (60 mL). The organic layer was dried over anhydrous MgSO<sub>4</sub>, filtered, and the solvents removed under reduced pressure to give the crude product as a brown oil. The crude product was purified by short-path distillation. Yield 4.51 g (76.2%) as light-yellow oil. <sup>1</sup>H NMR (400 MHz, CDCl<sub>3</sub>) δ:

6.16 (s, 2H), 3.98 (t, 2H), 1.81 (p, 2H), 1.44 (p, 2H), 1.33 (sx, 2H), 0.90 (t, 3H).

[Lit.: 6.15 (s, 2H), 3.98 (t, 4H), 1.81 (m, 4H), 1.35 - 1.43 (m, 12H), 0.97 (t, 6H)]<sup>102</sup>

### 2.2.3.3 5,7-Dibromo-2-dodecyl-2H,3H-thieno[3,4-b][1,4]dioxine (Br<sub>2</sub>EDOT-C12)

(Scheme 7)



Scheme 7. Synthesis of Br<sub>2</sub>EDOT-C12.

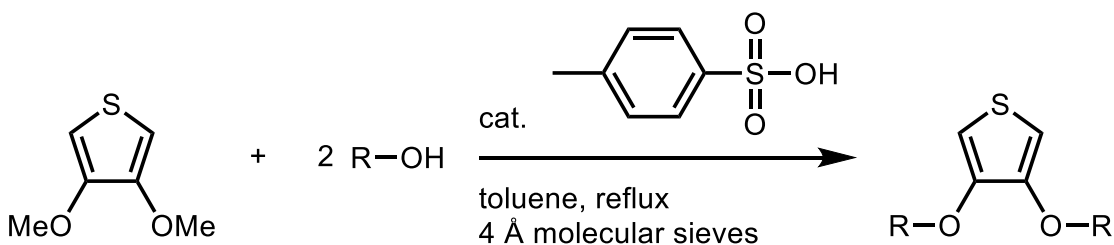
EDOT-C12 (0.9924 g, 3.2 mmol) was added to a three-necked round bottom flask containing chloroform (25 mL) and glacial acetic acid (HOAc, 25 mL) under argon. NBS (1.263 g, 7.1 mmol) was added slowly in portions over 10 min against a positive pressure of argon. The reaction mixture quickly changed to a vivid blue color, which deepened in color with further addition of NBS. The reaction mixture was protected from light and stirred for 1.5 h at room temperature. The reaction mixture was transferred to a separatory funnel and washed with portions of saturated aqueous NaHCO<sub>3</sub> (ca. 50 mL) until neutral, then with water (ca. 50 mL). The organic fraction was collected, dried over anhydrous MgSO<sub>4</sub>, and filtered. The solvent was removed under reduced pressure to give the crude product as a greenish oil. The crude product was purified by filtration through a silica gel plug using pentane:toluene (95:5) as the eluent. The solvent was removed under reduced pressure to give 0.944 g

(62.5%) product as a colorless oil.  $^1\text{H}$  NMR (400 MHz,  $\text{CDCl}_3$ )  $\delta$ : 4.23 (dd,  $J$  = 2.2 Hz, 1H), 4.14 (m, 1H), 3.90 (dd,  $J$  = 7.8 Hz, 1H), 1.27 (m, 22H), 0.88 (t, 3H).  $^{13}\text{C}$  NMR (400 MHz,  $\text{CDCl}_3$ )  $\delta$ : 139.83, 85.28, 77.16, 74.68, 68.76, 32.07, 30.46, 29.80, 29.75, 29.68, 29.55, 29.51, 29.49, 25.09, 22.84, 14.26.

## 2.3 Results and Discussion

### 2.3.1 Transesterification Reaction

Ether-substituted thiophene monomers EDOT-C12 and 3,4-DHOT were synthesized via an acid-catalyzed transesterification reaction between 3,4-dimethoxythiophene and the corresponding alcohol (Scheme 8).<sup>103–106</sup> A Soxhlet extractor containing activated 4 Å molecular sieves was used to capture the methanol generated, driving the equilibrium toward formation of products.



Scheme 8. General transesterification reaction.

EDOT-C12 was synthesized in 28% yield and was characterized using  $^1\text{H}$  NMR spectroscopy and mass spectrometry. The proton spectrum for EDOT-C12 is shown in Figure 27 and corroborates previously published data.<sup>33</sup> EDOT-C12 contains one chiral center located at the carbon bound to the dodecyl chain. The chiral center gives rise to the characteristic splitting of the peaks labelled **b**, **c**, and **d**, that are common to singly-substituted EDOTs. Protons **b** and **c** are

diastereotopic, meaning that substituting either hydrogen with a different group not already contained in the molecule would create a pair of diastereomers (non-mirror image stereoisomers). For this reason, protons **b** and **c** are chemically nonequivalent, which is evidenced by the presence of two separate resonances in the proton spectrum. The presence of the characteristic peaks **b**, **c**, and **d**, and the resonance corresponding to thienyl protons **a** give strong support that the product was synthesized successfully.

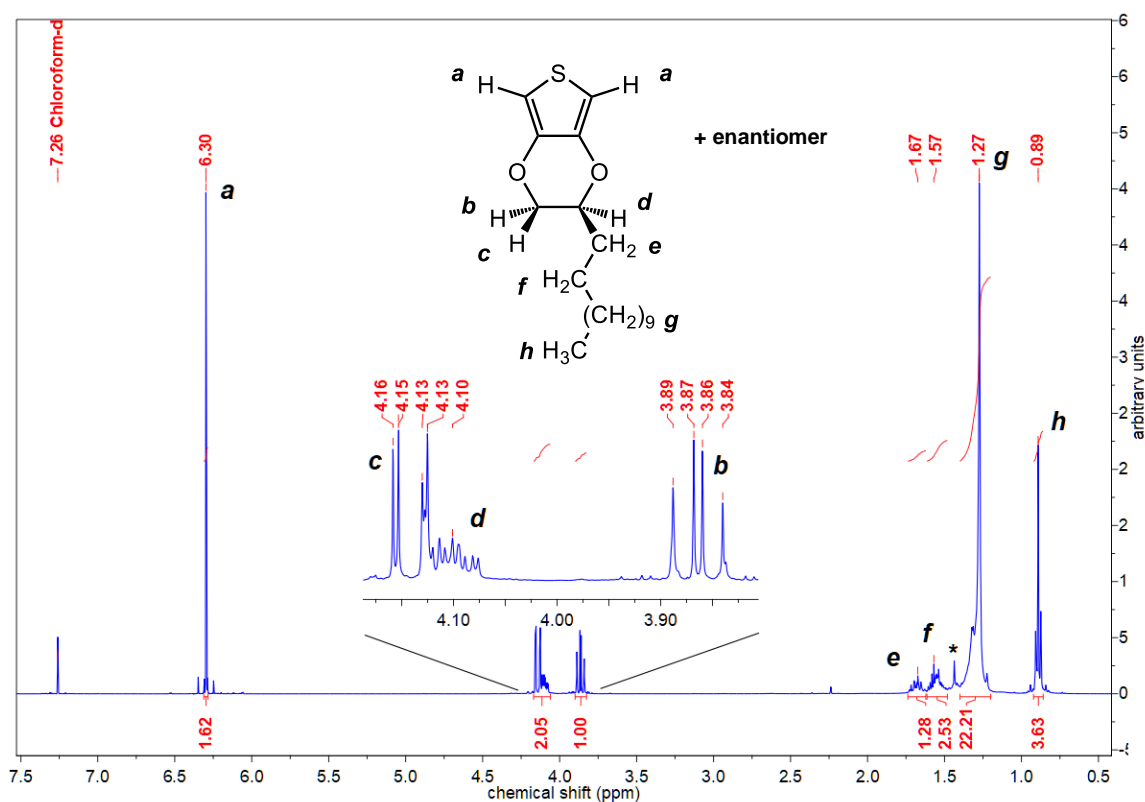


Figure 27. <sup>1</sup>H NMR spectrum of EDOT-C12 in CDCl<sub>3</sub>. The peak labelled '\*' corresponds to cyclohexane.

The mass spectrum for EDOT-C12 is shown in Figure 28. The base peak at *m/z* 311.167 corresponds to the protonated molecular ion [M+H]<sup>+</sup>. The isotopic

distribution agrees with expected values and gives strong support that the desired product was synthesized.

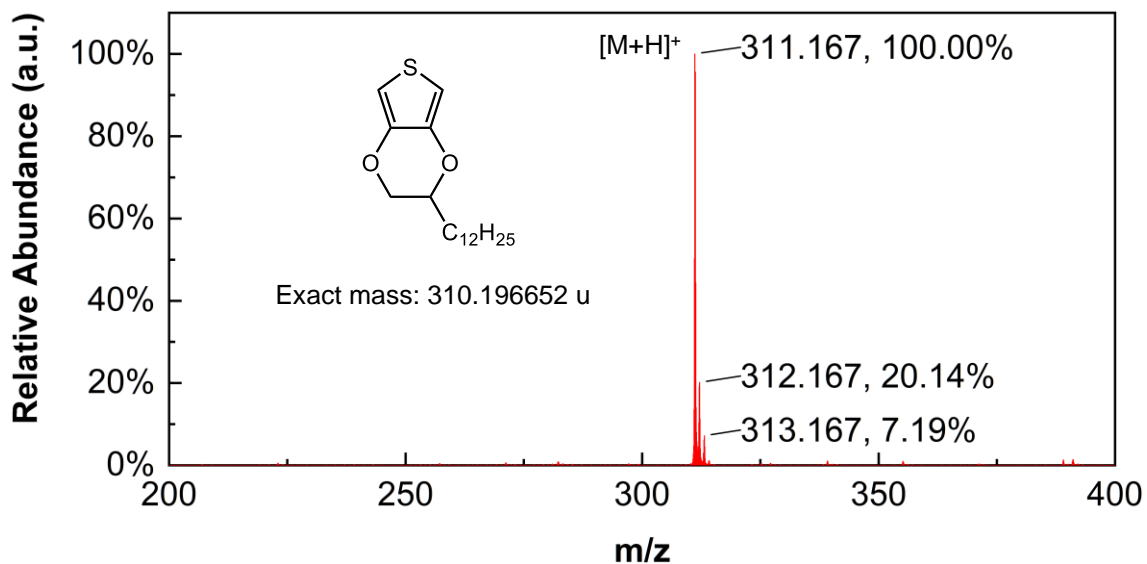


Figure 28. Mass spectrum of EDOT-C12.

3,4-DHOT was synthesized in 76% yield and characterized using  $^1\text{H}$  NMR spectroscopy (Figure 29). The proton spectrum is in agreement with previously published spectra.<sup>102</sup> Successful synthesis of the desired product is indicated by the presence of the singlet at 6.16 ppm, corresponding to the thienyl protons labelled **a**, and the lack of a peak at 3.86 ppm belonging to the protons in the methoxy groups in the 3,4-dimethoxythiophene starting material.

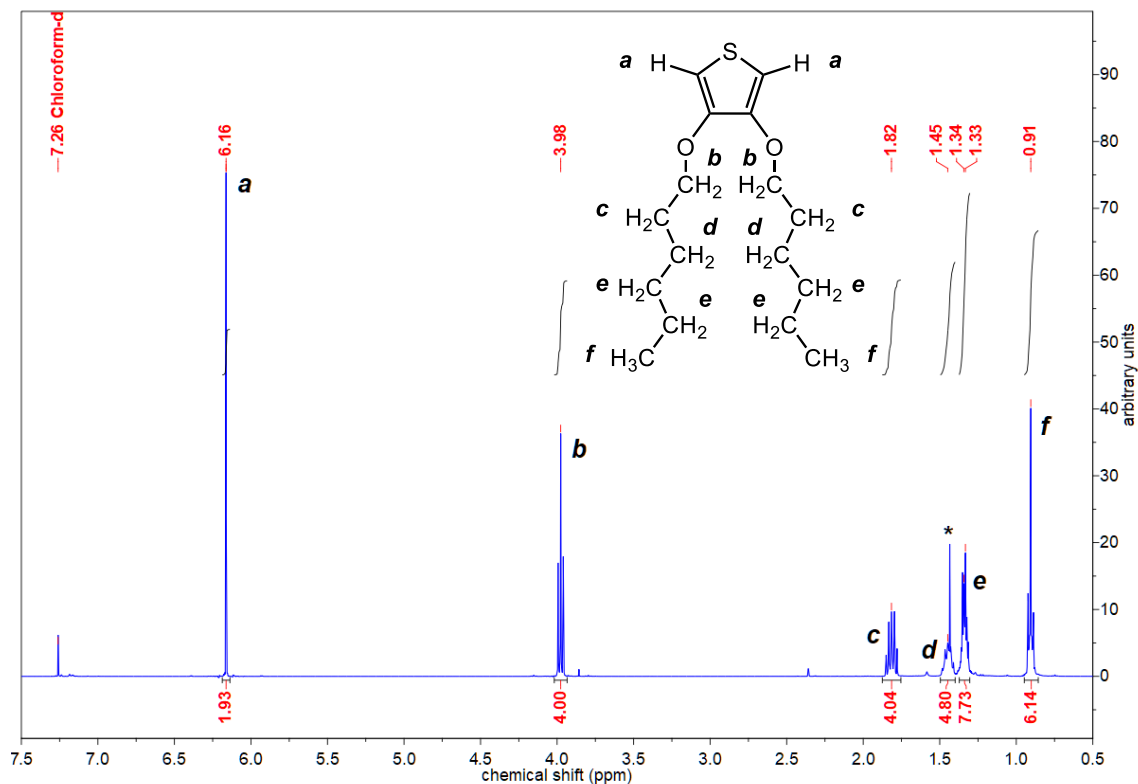


Figure 29. <sup>1</sup>H NMR spectrum of 3,4-DHOT in CDCl<sub>3</sub>. The peak labelled '\*' corresponds to cyclohexane.

Overall, there is a surprising lack of literature examining the transesterification reaction in depth. The reaction is presumed to occur through an equilibrium S<sub>N</sub>2 mechanism (Figure 30), with the committing steps being the loss of methanol and its subsequent removal from the reaction mixture. Reported yields of this reaction vary widely, though low yields (sub-50%) are commonly reported.<sup>105–109</sup> We suggest this is due partly to toluene being a poor solvent for polar (cationic) reaction mechanisms of this type, and due to the equilibrium nature of the reaction. Additionally, a number of undesirable side-reactions are possible under the conditions employed (acid, heat) which may also contribute too, for example: etherification of alcohol precursors, dehydration of alcohol

precursors to alkenes, and acid-catalyzed oligomerization of thiophenes.<sup>110</sup> To support this, it was observed experimentally that the reaction mixture is highly fluorescent under long-wave UV irradiation, indicating the presence of highly conjugated species (e.g. thiophene oligomers).

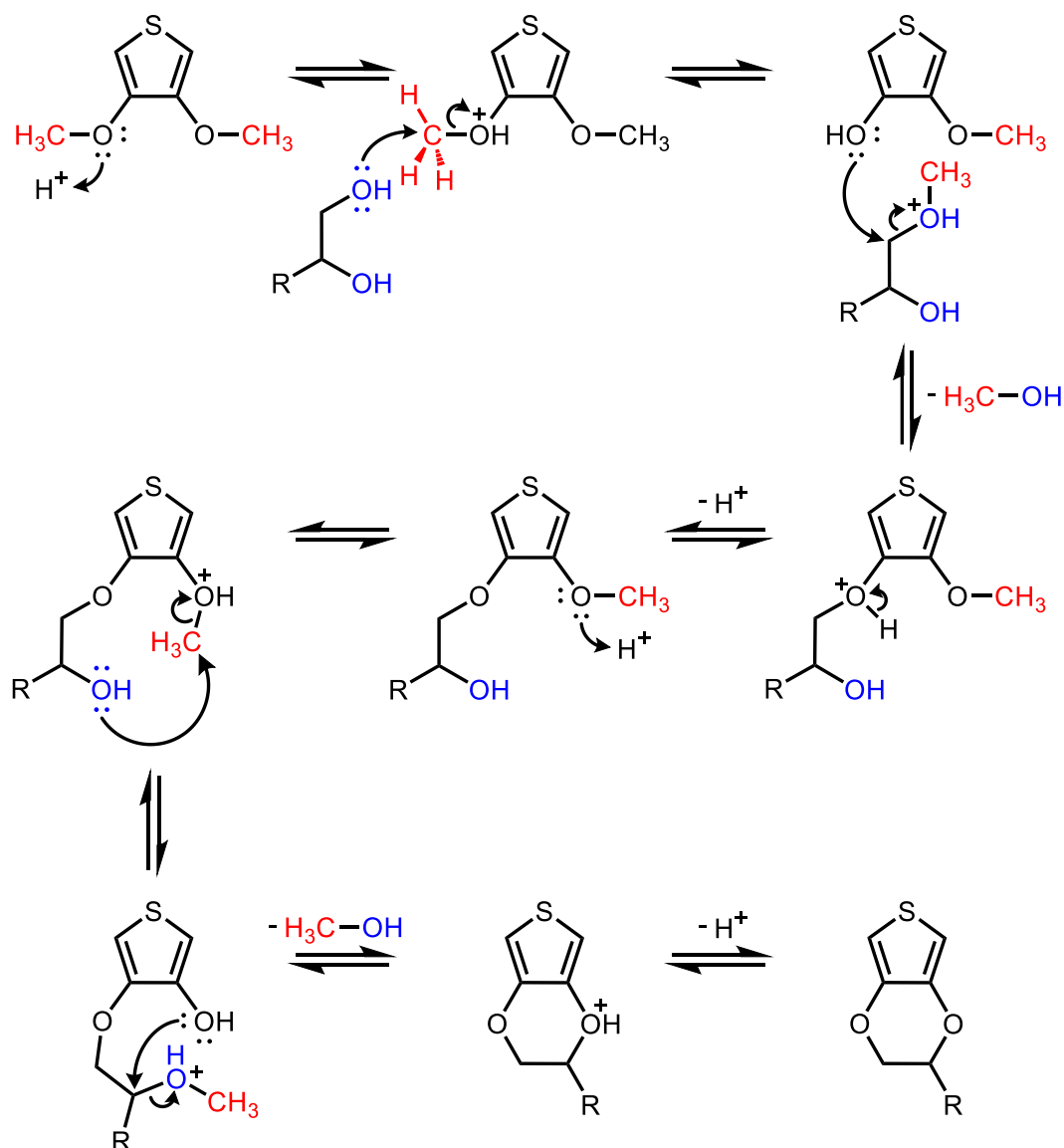
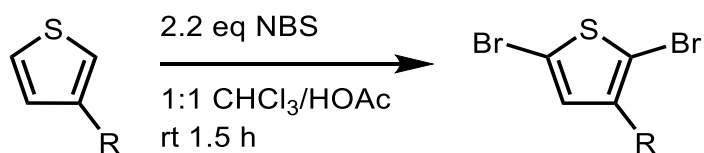


Figure 30. Proposed transesterification mechanism.

Beyond the initial patent, there has been little innovation or optimization of the reaction conditions. Through multiple syntheses of EDOT-C12 and 3,4-DHOT, we determined two parameters that were key to a successful synthesis. Firstly, if a Soxhlet extractor with sieves is used to sequester methanol, it is important to choose a size that is appropriate for the scale of the reaction. We found that it was more beneficial to yield and purity to use a smaller Soxhlet extractor that can siphon rapidly (every 10-15 minutes) as opposed to a larger one that siphons more slowly. This helps to ensure methanol is removed quickly and prevents the volume of solvent in the reaction flask from becoming too low such that the solubility of the reagents is significantly affected.

### 2.3.2 Bromination of EDOT-C12

The doubly brominated derivative of EDOT-C12 was synthesized according to the procedure described by McCullough *et al.* (Scheme 9).<sup>73</sup> EDOT-C12 was reacted with a slight excess (2.2 molar equivalents) of N-bromosuccinimide (NBS) in  $\text{CHCl}_3$ /acetic acid (HOAc) (1:1 v/v) at room temperature under argon.



Scheme 9. General bromination reaction.

The bromination reaction is an example of an electrophilic aromatic substitution (EAS) reaction, where an aromatic ring attacks an electrophile leading to substitution of a group on the aromatic ring. In the bromination reaction



employed for this thesis, NBS provides the electrophilic species, and the thiophene ring is the aromatic substrate. Heterolytic cleavage of the N-Br bond in NBS gives the resonance stabilized succinimide anion and the electrophilic bromonium ( $\text{Br}^+$ ) ion (Figure 31). The thiophene  $\pi$ -bonds attack the bromonium ion, resulting in a thiophenium intermediate. Loss of a proton reestablishes aromaticity and gives the brominated product. If one equivalent of NBS is used, the reaction stops here, otherwise if two equivalents are used the same process repeats on the other side of the thiophene ring.

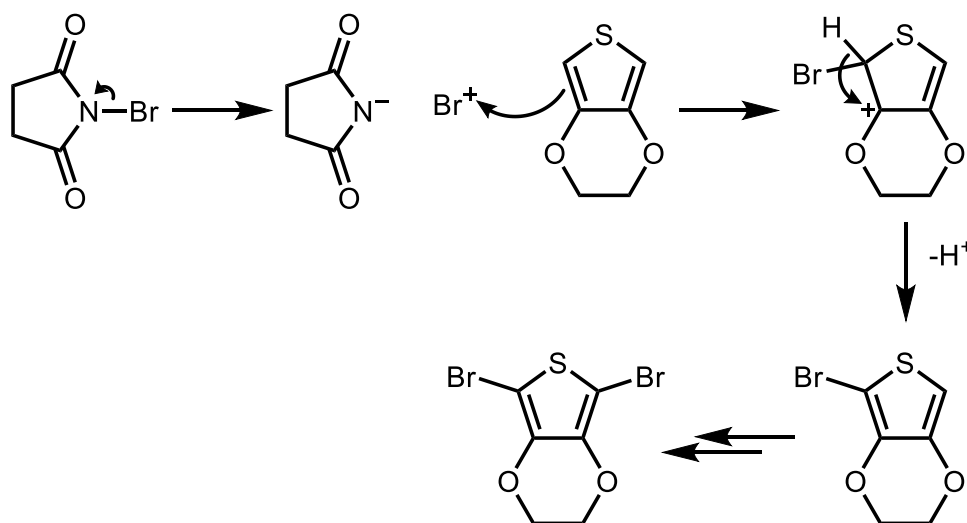


Figure 31. Reaction mechanism for the NBS bromination of thiophenes.

The dibromo derivative of EDOT-C12,  $\text{Br}_2\text{EDOT-C12}$ , was synthesized in 63% yield. The structure was characterized using  $^1\text{H}$  and  $^{13}\text{C}$  NMR spectroscopy and mass spectrometry. The proton spectrum for the monomer is shown in Figure 32. The absence of thienyl proton resonances (6.16 ppm in EDOT-C12) indicates substitution at those positions was successful.

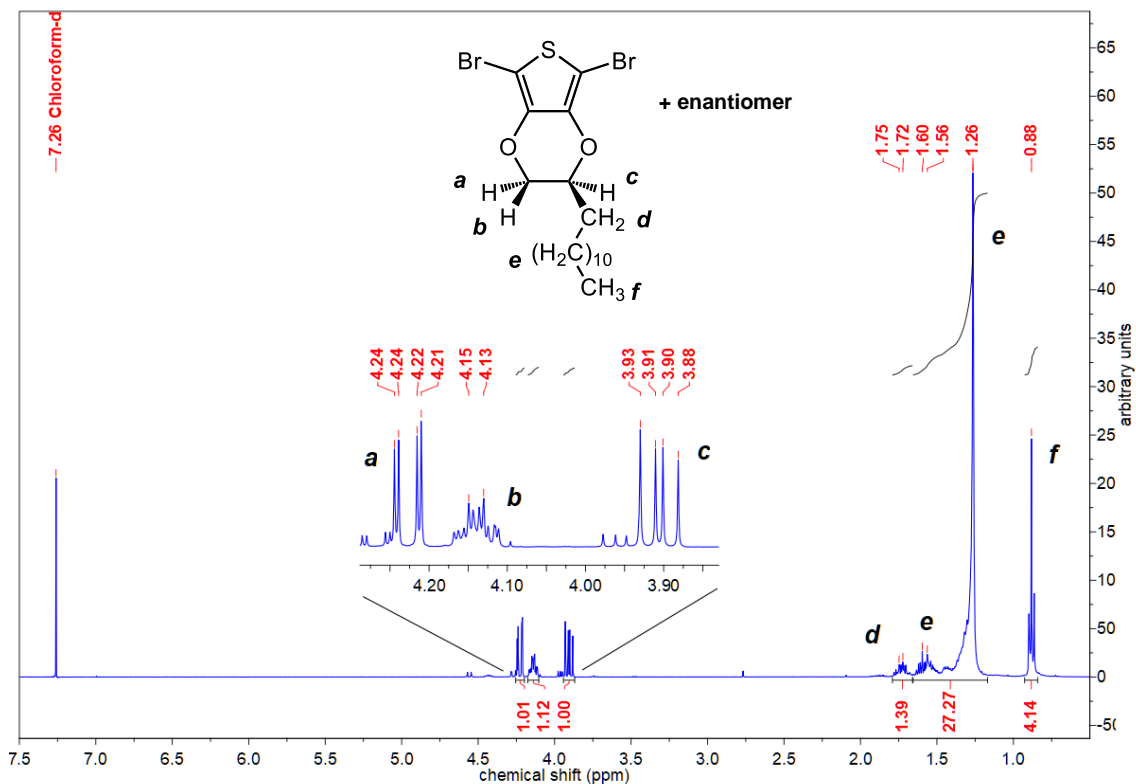


Figure 32. <sup>1</sup>H NMR spectrum for Br<sub>2</sub>EDOT-C12 in CDCl<sub>3</sub>.

The <sup>13</sup>C NMR spectrum for Br<sub>2</sub>EDOT-C12 is shown in Figure 33. The spectrum resembles that of the precursor compound EDOT-C12,<sup>33,111</sup> however the resonances corresponding to the thienyl carbons have shifted upfield slightly. In the precursor compound, the carbon atoms labelled **a** adjacent to sulfur atom resonate at 142 ppm,<sup>33,111</sup> in Br<sub>2</sub>EDOT-C12 these peaks are shifted upfield by 3 ppm to 139 ppm. The resonances corresponding to the peaks labelled **b** appear at 99 ppm in the precursor compound and are shifted upfield by 14 ppm to 85 ppm in the spectrum for Br<sub>2</sub>EDOT-C12. The upfield shift of these resonances is due to an increase in magnetic shielding at these carbons as a result of spin-orbit coupling interactions between the carbon and bromine atoms.<sup>112,113</sup>

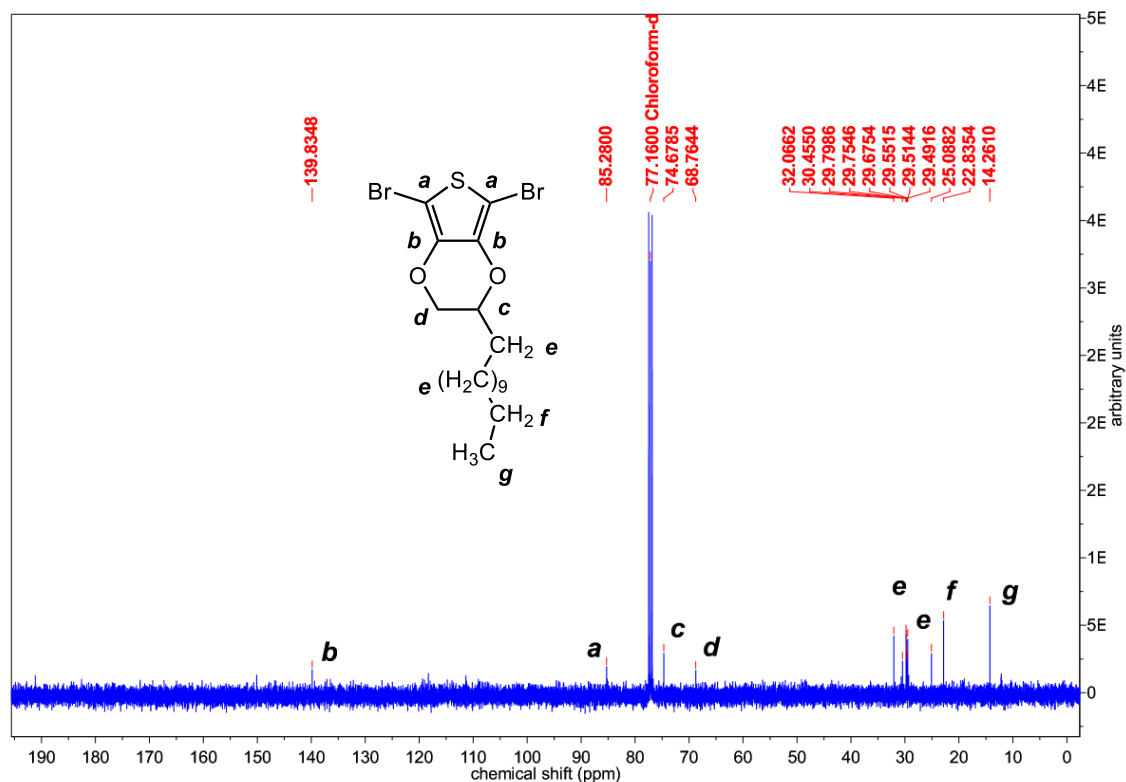


Figure 33. <sup>13</sup>C NMR spectrum for Br<sub>2</sub>EDOT-C12 in CDCl<sub>3</sub>.

The mass spectrum for Br<sub>2</sub>EDOT-C12 is shown in Figure 34. The peak at  $m/z$  467.084 corresponds to the protonated molecular ion  $[M+H]^+$ . The 1:2:1 relationship between the peaks at  $m/z$  467, 469, and 471 are characteristic of a molecule containing two bromine atoms, giving strong evidence the product was successfully synthesized. It is unclear if the peak at  $m/z$  403.084 is a singly brominated impurity or the result of fragmentation of Br<sub>2</sub>EDOT-C12 inside the mass spectrometer.

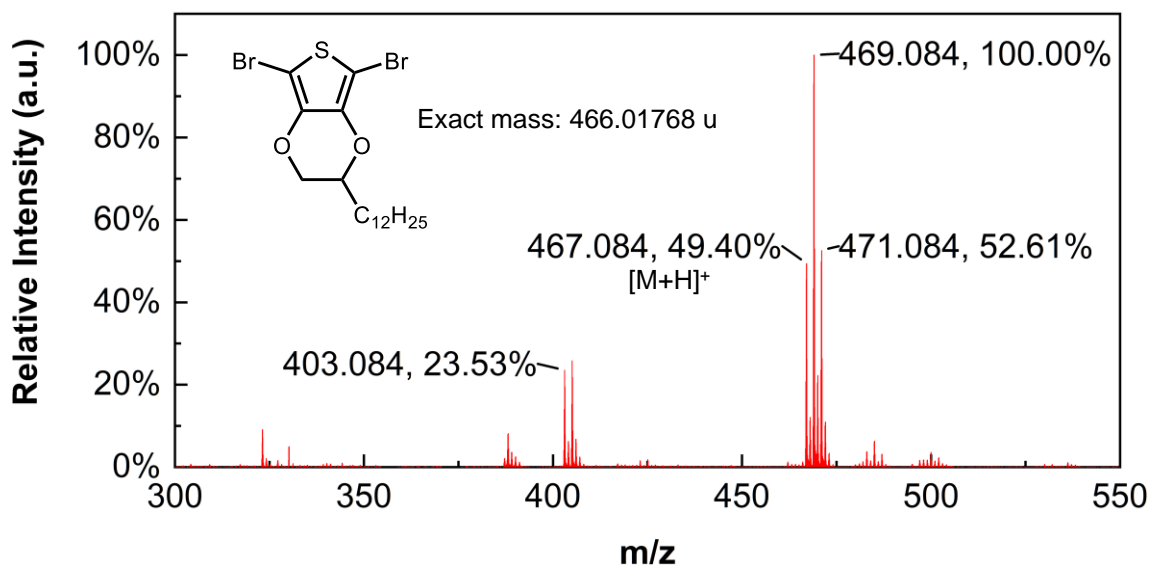
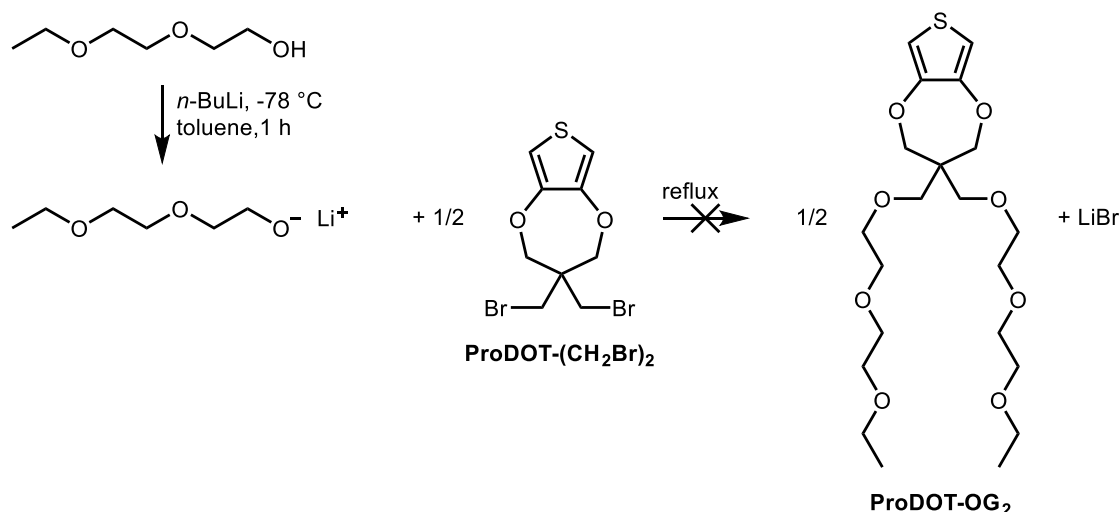


Figure 34. Mass spectrum for Br<sub>2</sub>EDOT-C12.

## 2.4 Attempted Syntheses

### 2.4.1 Synthesis of a Polyether-substituted ProDOT

In addition to the monomers described above, the synthesis of a polyether-substituted ProDOT monomer, ProDOT-OG<sub>2</sub> (Scheme 10) was attempted. A nucleophilic S<sub>N</sub>2 substitution of the bromine atoms in ProDOT-(CH<sub>2</sub>Br)<sub>2</sub> (Scheme 10) by lithium 2-(2-ethoxyethoxy)ethanolate was attempted, although unsuccessfully. In all cases, negligible substitution was observed according to <sup>1</sup>H NMR spectroscopy. Failure to synthesize the desired product was likely due to failure to maintain anhydrous conditions.

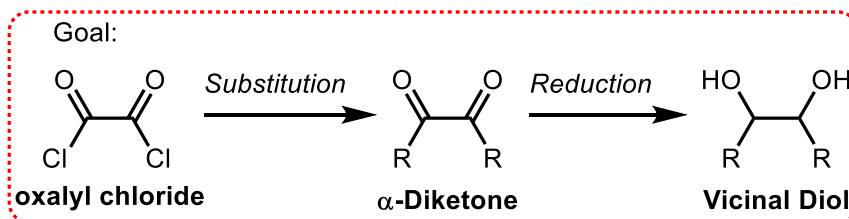


Scheme 10. Attempted synthesis of ProDOT-OG<sub>2</sub>, a polyether-substituted thiophene monomer.

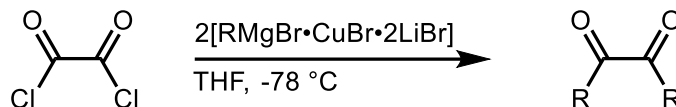
#### 2.4.2 Symmetrical $\alpha$ -Diketones as Precursors to Vicinal Diols

Many efforts were made to prepare commercially unavailable symmetrical vicinal diols for use in the transesterification reaction with the intention of synthesizing novel di-substituted EDOT monomers. Retrosynthetic analysis of the desired compounds prompted us to consider a route involving the analogous  $\alpha$ -diketones, which can be reduced in one step<sup>114</sup> to the corresponding vicinal diol. Two approaches were attempted, based on the methods described by Babudri *et al.*<sup>115</sup> and Scheiper *et al.*<sup>116</sup> (Figure 35). The method described by Babudri *et al.*, which details the coupling of aliphatic Grignard reagents with oxalyl chloride in the presence of copper(I) bromide and lithium bromide was attempted first. Our attempts to prepare 13,14-hexacoseanedione (Figure 35a) via the coupling of oxalyl chloride and two equivalents of *n*-dodecylmagnesium bromide using this method were unsuccessful, possibly due to a failure to sufficiently purify the

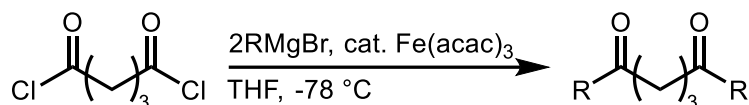
starting materials. A procedure adapted from Scheiper *et al.* was attempted next. The mentioned authors' work describes the coupling of diacyl chlorides with aliphatic Grignard reagents in the presence of an organometallic iron catalyst,  $\text{Fe}(\text{acac})_3$  (acac = acetylacetonato). While the authors did not report the use of oxalyl chloride as a substrate, we attempted to couple oxalyl chloride with two equivalents of n-hexylmagnesium bromide in the presence of  $\text{Fe}(\text{acac})_3$  (Figure 35b). Synthesis of the desired compound, 7,8-tetradecanedione was unsuccessful. The reason for the failure of this reaction is unclear, however oxalyl chloride often exhibits different reactivity than other acyl chlorides which may make it an unsuitable substrate for this reaction.<sup>117</sup>



Babudri *et al. Tetrahedron Lett.*, **1995**, 36, 7305–7308.



Scheiper *et al. J. Org. Chem.*, **2004**, 69, 3943–3949.



Attempted Methods:

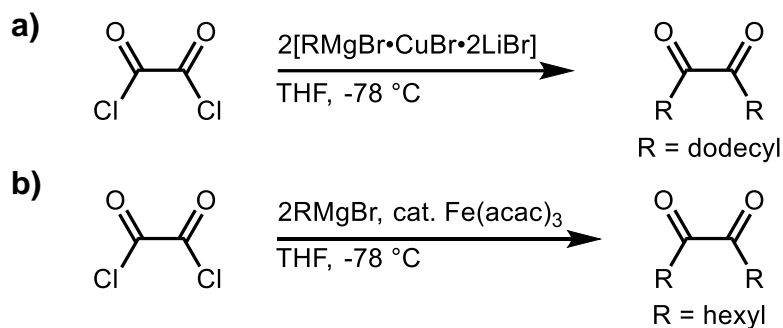


Figure 35. Attempted syntheses of  $\alpha$ -diketones inspired from previously published methods.

### 3. POLYMERIZATIONS

#### 3.1 Introduction

In this chapter, we examine the chemical oxidative polymerization method and the impact of order of addition of reagents and other parameters on the degree of polymerization of ether-substituted polythiophene derivatives PEDOT-C12 and PDHOT (Figure 36). To compare the utility of the GRIM polymerization method to that of the chemical oxidative polymerization method for producing high molecular weight ether-substituted polythiophenes, the dibromo derivative of EDOT-C12 was polymerized via GRIM. In addition, P3HT was polymerized under analogous oxidative and non-oxidative methods to serve as a model case. The molecular weights of the polymers were characterized by GPC.

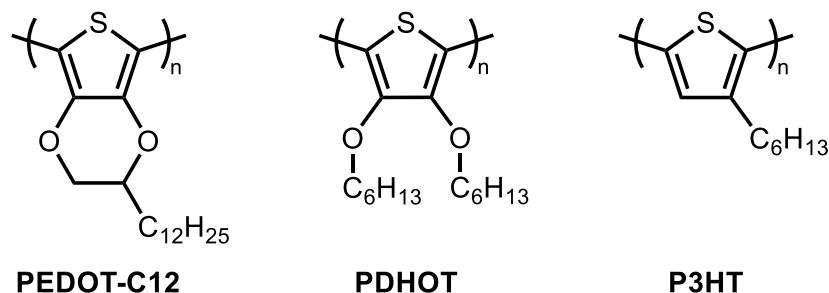


Figure 36. Structures of the polymers synthesized. All three polymers were synthesized using chemical oxidative polymerization. PEDOT-C12 and P3HT were also synthesized using Grignard Metathesis polymerization.

#### 3.2 Experimental

##### 3.2.1 Materials

Glassware was dried in an oven prior to use unless noted otherwise. Molecular sieves (4 Å) were activated by first drying at 200 °C under vacuum in a vacuum-oven for 24 h, then quickly transferred to a Schlenk flask and flame-dried



under high vacuum several times. The sieves were kept under high vacuum for 6 h before use. Chloroform (ACS grade) purchased from Avantor and chlorobenzene (99%) purchased from Alfa Aesar were protected from light and dried over activated 4 Å molecular sieves and used rapidly. Basified chloroform was prepared by shaking repeatedly with portions of saturated aqueous  $\text{NaHCO}_3$  solution until the washings were basic to pH paper. The chloroform was dried over anhydrous  $\text{MgSO}_4$  and filtered, then used immediately for GPC sample preparation. The following chemicals were used as received: anhydrous  $\text{FeCl}_3$  (98%) purchased from Alfa Aesar, anhydrous hydrazine (98%) purchased from Sigma, methanol (HPLC grade) purchased from JT Baker, acetonitrile (99.9%+) purchased from Acros, 3-hexylthiophene (>98%) and 2,5-dibromo-3-hexylthiophene ( $\geq 97\%$ ) purchased from TCI, methylmagnesium bromide (3.0 M in diethyl ether) purchased from Sigma, tetrahydrofuran (anhydrous,  $\geq 99.9\%$ ) purchased from Millipore,  $\text{NiCl}_2(\text{dppp})$  (99%) purchased from Acros, iron(III) perchlorate hydrate (reagent grade) purchased from Alfa Aesar.

### 3.2.2 Methods

**GPC Sample Preparation:** A small sample of polymer was weighed into a 50 mL scintillation vial and diluted to a concentration between 0.1-0.25 mg/mL with freshly basified chloroform under argon. Chloroform readily decomposes on exposure to air<sup>118</sup> and light<sup>119</sup> to form phosgene and HCl. Care must be taken to eliminate these as they can dope the neutral polymers to the oxidized (quinoidal) state, reducing their solubility. The sample was left undisturbed for 24 h at room temperature in the dark (stirring causes much of the polymer to adhere to the

walls of the vial). After this period, the sample were gently shaken for a few minutes. Immediately before analysis, a small aliquot (~1 mL) of the sample was filtered through a 0.2  $\mu\text{m}$  PTFE syringe filter into a clean and dry vial. The filtered aliquot was then used for analysis.

**GPC Molecular Weight Characterization:** Molecular weight characterization was performed using a Viscotek gel-permeation chromatographic system with dual light-scattering detector (Viscotek 270 Dual Detector). Samples (100  $\mu\text{L}$ ) were injected through a VE 1122 solvent delivery system and separated with a porous styrene divinylbenzene copolymer column (Viscotek T3000 or LT4000L) using chloroform as an eluent at a flow rate of 1 mL/min. Molecular weights were determined relative to polystyrene standards. The LT4000L column was calibrated with polystyrene standards with molecular weight 1,055, 5,200, 13,000, 25,000, 50,000, 65,000, and 235,000 g/mol (exclusion limit 400,000 g/mol). The molecular weights of the polystyrene standards used for calibration of the T3000 column were 5,200, 13,000, 25,000, 30,000, 50,000, and 65,000 g/mol (exclusion limit 70,000 g/mol). The polydispersity of all polymer standards used was 1.06. The calibration curves for the GPC columns can be found in the appendix.

### 3.2.3 Polymerizations

#### 3.2.3.1 Chemical Oxidative Polymerization

**General Procedure – COP Reverse Addition:** A typical reverse addition polymerization procedure is as follows: anhydrous  $\text{FeCl}_3$  (2.3 molar equivalents) was weighed and quickly transferred to a Schlenk flask. The flask was flushed

with argon, and 25 mL of dry solvent ( $\text{CHCl}_3$ , chlorobenzene) was added via syringe. The oxidant suspension was stirred rapidly for 3-5 min under argon. Monomer (0.7-1.0 mmol) was dissolved in 5 mL of dry solvent and added dropwise to the stirred oxidant suspension via syringe. The mixture was stirred for 24 h at room temperature, after which the polymer was precipitated by dropwise addition of the reaction mixture into an excess (250 mL) of rapidly stirred methanol. The polymer was collected by vacuum filtration and washed thoroughly with methanol. The polymer was resuspended in 30 mL solvent under argon and reduced by the addition of anhydrous hydrazine (1 molar equivalent) via syringe. The mixture was stirred for 20-24 h at room temperature, after which the polymer was precipitated into excess methanol and collected by filtration and washed as above. The polymer was dried under high vacuum and stored under argon in the dark.

**PEDOT-C12 – Reverse Addition, 2.3 eq.  $\text{FeCl}_3/\text{C}_6\text{H}_5\text{Cl}$ :** A solution of EDOT-C12 (0.251 g, 0.81 mmol) in chlorobenzene (5 mL) was added dropwise to a well-stirred suspension of anhydrous  $\text{FeCl}_3$  (0.314 g, 1.9 mmol) in chlorobenzene (25 mL). The reaction mixture quickly turned a dark blue color. After precipitation and filtration, the polymer was resuspended in chlorobenzene (25 mL) under argon and reduced by the addition of anhydrous hydrazine (0.03 mL, 0.96 mmol) via syringe. The addition of hydrazine caused a gradual color change of the solution from blue to violet. The polymer was purified and isolated as described above. Yield 0.1825 g (73.1%) product as a dark violet powder.

**PEDOT-C12 – Reverse Addition, 2.3 eq.  $\text{Fe}(\text{ClO}_4)_3/\text{C}_6\text{H}_5\text{Cl}$ :** A solution of PEDOT-C12 (0.308 g, 1.0 mmol) in chlorobenzene (5 mL) was added dropwise to a well-stirred suspension of  $\text{Fe}(\text{ClO}_4)_3$  monohydrate (0.862 g, 2.3 mmol) in chlorobenzene (25 mL). The reaction mixture gradually turned a dark blue color. After precipitation and filtration, the polymer was resuspended in chlorobenzene (25 mL) under argon and reduced by the addition of anhydrous hydrazine (0.03 mL, 0.96 mmol) via syringe. The addition of hydrazine caused a gradual color change of the solution from blue to violet. The polymer was purified and isolated as described above. Yield 0.117 g (38.2%) product as a dark violet powder.

**PEDOT-C12 – Reverse Addition, 2.3 eq.  $\text{FeCl}_3/\text{CHCl}_3$ :** A solution of PEDOT-C12 (0.252 g, 0.81 mmol) in chloroform (5 mL) was added dropwise to a well-stirred suspension of anhydrous  $\text{FeCl}_3$  (0.326 g, 2 mmol) in chloroform (25 mL). The reaction mixture quickly turned a dark blue color. After precipitation and filtration, the polymer was resuspended in chloroform (25 mL) under argon and reduced by the addition of anhydrous hydrazine (0.03 mL, 0.96 mmol) via syringe. The addition of hydrazine caused a gradual color change of the solution from blue to violet. The polymer was purified and isolated as described above. Yield 0.200 g (79.8%) product as a dark violet powder.

**P3HT – Reverse Addition, 2.3 eq.  $\text{FeCl}_3/\text{C}_6\text{H}_5\text{Cl}$ :** A solution of 3-hexylthiophene (0.25 mL, 1.4 mmol) in chlorobenzene (6 mL) was added dropwise to a well-stirred suspension of anhydrous  $\text{FeCl}_3$  (0.525 g, 3.2 mmol) in chlorobenzene (30 mL). After addition of the monomer solution, the reaction

mixture took on a dark green color. The polymer was purified and isolated as described above. Yield 0.893 g (64.4%) product as a dark red powder.

**PDHOT – Reverse Addition, 2.3 eq.  $\text{FeCl}_3/\text{C}_6\text{H}_5\text{Cl}$ :** A solution of 3,4-DHOT (0.21989 g, 0.25 mL, 0.77 mmol) in chlorobenzene (6 mL) was added dropwise to a well-stirred suspension of anhydrous  $\text{FeCl}_3$  (0.295 g, 1.8 mmol) in chlorobenzene (30 mL). After addition of the monomer solution, the reaction mixture took on a dark greenish/blue color. The polymer was purified and isolated as described above. Yield 0.0924 g (42.3%) product as a blood red powder.

**General Procedure – COP Standard Addition:** A typical standard addition procedure is as follows: anhydrous  $\text{FeCl}_3$  (2.3 molar equivalents) was quickly weighed into a dry 20 mL scintillation vial and sealed with a septum cap. The vial was purged with argon and 5 mL ACN was added via syringe to give a dark red solution. The  $\text{FeCl}_3$ :ACN solution was added dropwise to a well-stirred solution of monomer (0.7-1.0 mmol) dissolved in 30 mL dry solvent ( $\text{CHCl}_3$ ,  $\text{C}_6\text{H}_5\text{Cl}$ ) under argon. The mixture was stirred for 24 h at room temperature. The polymer was precipitated, reduced, and isolated as described in the reverse addition procedure.

**PEDOT-C12 – Standard Addition, 2.3 eq.  $\text{FeCl}_3$ :** A solution of anhydrous  $\text{FeCl}_3$  (0.31176 g, 1.9 mmol) in acetonitrile (5 mL) was added dropwise to a well-stirred solution of EDOT-C12 (0.2527 g, 0.81 mmol) in chlorobenzene (30 mL) under argon. Over the course of the addition, the mixture slowly darkened to a deep green color. After precipitation and filtration, the polymer was resuspended

in 24 mL chlorobenzene and anhydrous hydrazine 0.04 mL, 1.3 mmol) was added, which induced a color change from dark blue to violet. The mixture was stirred for 24 h and purified and isolated as described above. Yield 0.0647 g (25.8%) product as dark purple powder.

**PEDOT-C12 – Standard Addition, 4 eq. FeCl<sub>3</sub>:** A solution of anhydrous FeCl<sub>3</sub> (0.4345 g, 2.7 mmol) in acetonitrile (5 mL) was added dropwise to a well-stirred solution of EDOT-C12 (0.2023 g, 0.65 mmol) in chlorobenzene (30 mL) under argon. Over the course of the addition, the mixture slowly darkened to a deep green color. After precipitation and filtration, the polymer was resuspended in 40 mL chlorobenzene and anhydrous hydrazine (0.04 mL) was added, which induced a color change from dark blue to violet. The mixture was stirred for 24 h and purified and isolated as described above. Yield 0.1163 g (26.9%) product as dark purple powder.

**P3HT – Standard Addition, 2.3 eq. FeCl<sub>3</sub>:** A solution of anhydrous FeCl<sub>3</sub> (0.521 g, 3.2 mmol) in acetonitrile (5 mL) was added dropwise to a well-stirred solution of P3HT (0.25 mL, 1.4 mmol) in chlorobenzene (30 mL) under argon. Over the course of the addition, the mixture slowly darkened to a dark green color. After precipitation and filtration, the polymer was resuspended in 40 mL chlorobenzene and anhydrous hydrazine (0.04 mL) was added, which induced a color change from dark blue to violet. The mixture was stirred for 24 h and purified and isolated as described above. Yield 0.604 g (43.6%) product as a dark red powder.

**PDHOT – Standard Addition, 2.3 eq. FeCl<sub>3</sub>:** A solution of anhydrous FeCl<sub>3</sub> (0.32973 g, 2 mmol) in acetonitrile (5 mL) was added dropwise to a well-stirred solution of 3,4-DHOT (0.251 g, 0.285 mL, 0.88 mmol) in chlorobenzene (30 mL) under argon. The mixture quickly took on a reddish color which darkened to violet before ultimately changing to a deep green. After precipitation and filtration, the polymer was resuspended in 35 mL chlorobenzene and anhydrous hydrazine (0.03 mL) was added (Note: methanol alone was sufficient to reduce this polymer as evidenced by the change to a red color during the precipitation step). The mixture was stirred for 24 h. Attempts to isolate the de-doped polymer by precipitation directly from the reaction mixture failed. Instead, the polymer was isolated by removal of all solvents under reduced pressure. Yield 0.1945 g (78.1%) dark oily product.

**PDHOT – Standard Addition, 4 eq. FeCl<sub>3</sub>:** A solution of anhydrous FeCl<sub>3</sub> (0.4666 g, 2.9 mmol) in acetonitrile (5 mL) was added dropwise to a well-stirred solution of 3,4-DHOT (0.205 g, 0.72 mmol) in chlorobenzene (30 mL) under argon. The mixture quickly took on a reddish color which darkened to a deep green color. The polymer was precipitated by dropwise addition of the reaction mixture into an excess of methanol (250 mL) at -78 °C. After filtration, the polymer was resuspended in 35 mL chlorobenzene and anhydrous hydrazine (0.03 mL) was added (Note: methanol alone was sufficient to reduce this polymer as evidenced by the change to a red color during the precipitation step). The mixture was stirred for 24 h and purified and isolated as described above. Yield 0.0218 g (10.7%) product as a blood red powder.

### 3.2.3.2 Grignard Metathesis Polymerization

**PEDOT-C12:** Br<sub>2</sub>EDOT-C12 (0.8059 g, 1.72 mmol) was added to a dry Schlenk flask. The flask containing the monomer was evacuated under high-vacuum for approximately 1 h to remove moisture. THF (10 mL, freshly distilled from Na/benzophenone ketyl) was added via argon-purged syringe. To the stirred monomer solution was added methylmagnesium bromide (0.58 mL, 3 M in diethyl ether) dropwise via syringe, and the mixture was stirred at room temperature for 1.5 h. The metalated monomer solution was transferred dropwise via canula to a dry flask containing NiCl<sub>2</sub>(dppp) (0.01354 g, 25 µmol). Immediately the solution darkened to a purple color, and polymer began to precipitate. The mixture was refluxed overnight. The polymer was precipitated into methanol (100 mL) and collected by filtration in near quantitative yield (0.58935 g). The metallic purple polymer was dried under high vacuum and stored under argon in the dark.

**P3HT:** 2,5-dibromo-3-hexylthiophene (0.75 mL, 3.5 mmol) followed by THF (10 mL) was transferred to a 250 mL 3-necked round-bottom flask outfitted with magnetic stir bar, reflux condenser, argon inlet/outlet, and rubber septum via syringe. To the stirred monomer solution was added methylmagnesium bromide solution (1.2 mL, 3.0 M in Et<sub>2</sub>O) via argon-purged syringe. The mixture was refluxed for 1 h. NiCl<sub>2</sub>(dppp) (0.0189 mg 34.9 µmol) was added and the reaction mixture refluxed for 2 h, during which the reaction mixture took on a red color. After this period, the reaction mixture was cooled to room temperature and added dropwise to rapidly stirring methanol (100 mL). The polymer was collected by



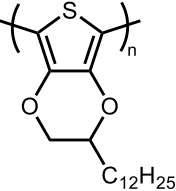
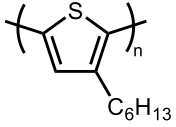
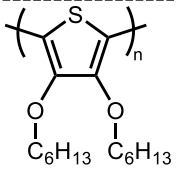
vacuum-filtration and dried in a desiccator under high vacuum. Yield 0.308 g (53%) polymer as a lustrous dark red solid.

### **3.3 Results and Discussion**

#### **3.3.1 Chemical Oxidative Polymerization**

For all monomers tested, order of addition of reagents had a significant effect on the molecular weight of the resulting polymer (Table 4). The GPC chromatograms for the ether-substituted polythiophenes PEDOT-C12 and PDHOT are shown in Figure 37 (chromatograms for entries 4 and 5 can be found in the appendix). In the case of EDOT-C12 (Figure 37a), polymerization under reverse addition conditions led to low molecular weight polymers irrespective of the solvent (chloroform or chlorobenzene) or  $\text{Fe}^{3+}$  oxidant ( $\text{FeCl}_3$ ,  $\text{Fe}(\text{ClO}_4)_3$ ) tested (Table 4, entry 3-5). In the best case (chlorobenzene solvent and  $\text{FeCl}_3$  oxidant), PEDOT-C12 with weight-average molecular weight ( $M_w$ ) 2,200 g/mol was obtained, corresponding to a heptamer. Switching from reverse to standard addition conditions resulted in a sizeable (36-fold) increase in degree of polymerization  $X_w$  to 256 repeat units ( $M_w$  to 79,000 g/mol, Table 4, entry 1) and a broadening of the molecular weight distribution. Using 4 molar equivalents of  $\text{FeCl}_3$  further increased  $X_w$  to 476 ( $M_w$  147,000 g/mol, Table 4, entry 2), which is a 68-fold increase over entry 3, and significantly narrowed the molecular weight distribution.

Table 4. Weight-average molecular weight  $M_w$ , weight-average degree of polymerization  $X_w$  for polymers synthesized by  $\text{FeCl}_3$ -initiated chemical oxidative polymerization under different conditions.  $M_w$  determined from right-angle light scattering detector peak retention volume. \* indicates  $\text{Fe}(\text{ClO}_4)_3$  oxidant was used.

Structure	Acronym	Entry	Addition	Oxidant	Solvent	$M_w$	$X_w$
	PEDOT-C12	1	Standard	2.3 eq.	$\text{C}_6\text{H}_5\text{Cl}$	79,000	256
		2	Standard	4 eq.	$\text{C}_6\text{H}_5\text{Cl}$	147,000	476
		3	Reverse	2.3 eq.	$\text{C}_6\text{H}_5\text{Cl}$	2,200	7
		4	Reverse	2.3 eq.*	$\text{C}_6\text{H}_5\text{Cl}$	1,400	4
		5	Reverse	2.3 eq.	$\text{CHCl}_3$	1,600	5
	P3HT	6	Standard	2.3 eq.	$\text{C}_6\text{H}_5\text{Cl}$	$\geq 70,000$	$\geq 421$
		7	Reverse	2.3 eq.	$\text{C}_6\text{H}_5\text{Cl}$	37,000	222
	PDHOT	8	Standard	4 eq.	$\text{C}_6\text{H}_5\text{Cl}$	25,000	88
		9	Reverse	2.3 eq.	$\text{C}_6\text{H}_5\text{Cl}$	4,500	16

The effect of order of addition was less pronounced for 3,4-dialkoxy monomer 3,4-DHOT (Figure 37b), which increased five-fold to 88 repeat units (25,000 g/mol) from 16 (4,500 g/mol) only after the amount of  $\text{FeCl}_3$  used was increased to 4 molar equivalents (Table 4, entry 8, 9). When 2.3 molar equivalents  $\text{FeCl}_3$  were used, an oily product was obtained which was highly soluble in methanol, a nonsolvent for polymers of this type, indicating the product was of very low molecular weight (oligomer). This oligomer product was not characterized by GPC. For 3,4-disubstituted monomers, steric interactions between side-groups are thought to play a role in limiting the molecular

weight.<sup>28,53,54,88</sup> We attribute this effect to the smaller increase in molecular weight observed for PDHOT compared to PEDOT-C12. GPC characterization also shows for the polymer prepared via standard addition the appearance of a peak corresponding to  $X_w$  205 ( $M_w$  58,000 g/mol). This suggests that molecular weights may be improved further if the reaction time or equivalents of oxidant are increased.

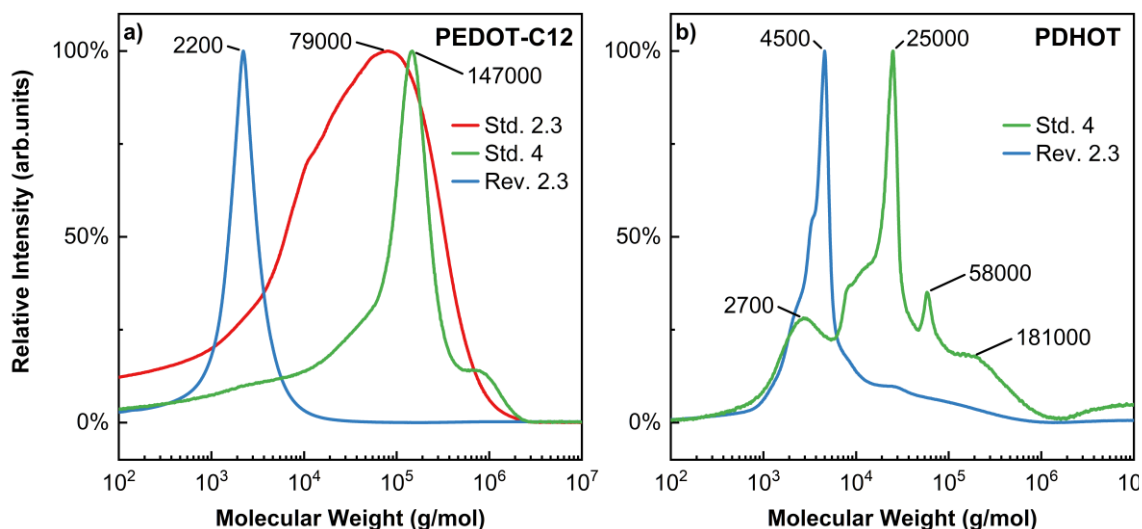


Figure 37. GPC chromatograms for ether-substituted polymers synthesized by  $\text{FeCl}_3$ -initiated chemical oxidative polymerization (right-angle light scattering detector). Red and green traces correspond to polymers synthesized via standard addition conditions with 2.3 and 4 molar equivalents  $\text{FeCl}_3$ , respectively. Blue traces represent polymers synthesized under reverse addition conditions. Exclusion limit: 400,000 g/mol.

Examining the GPC chromatograms for P3HT shows that both reverse addition and standard addition samples contain three common peaks, albeit in different relative abundance (Figure 38).  $\text{FeCl}_3$ -initiated oxidative polymerization of 3-hexylthiophene under reverse addition conditions predominantly yielded P3HT with degree of polymerization  $X_w$  222 ( $M_w$  37,000 g/mol), with additional

peaks at  $M_w$  85,000 g/mol, and  $M_w$  740,000 g/mol, which are both beyond the exclusion limit of the analytical column used for these samples (70,000 g/mol). The very high molecular weight polymers (740,000 g/mol) may be crosslinked ( $\beta$ -coupled) species, which can form under strongly oxidizing (high relative  $Fe^{3+}$ /monomer ratio) conditions, as this leads to decreased regiochemical selectivity polymerization.<sup>75</sup> The GPC trace for the sample prepared under standard addition conditions shows a narrow band at the exclusion limit ( $X_w \geq 420$ ,  $M_w \geq 70,000$  g/mol), with a decrease in intensity of the peak corresponding to  $X_w$  202 ( $M_w$  35,000 g/mol). Additionally, a decrease in abundance of very high molecular weight ( $M_w$  740,000 g/mol) polymer was observed, which could indicate a net-reduction in  $\beta$ -couplings.

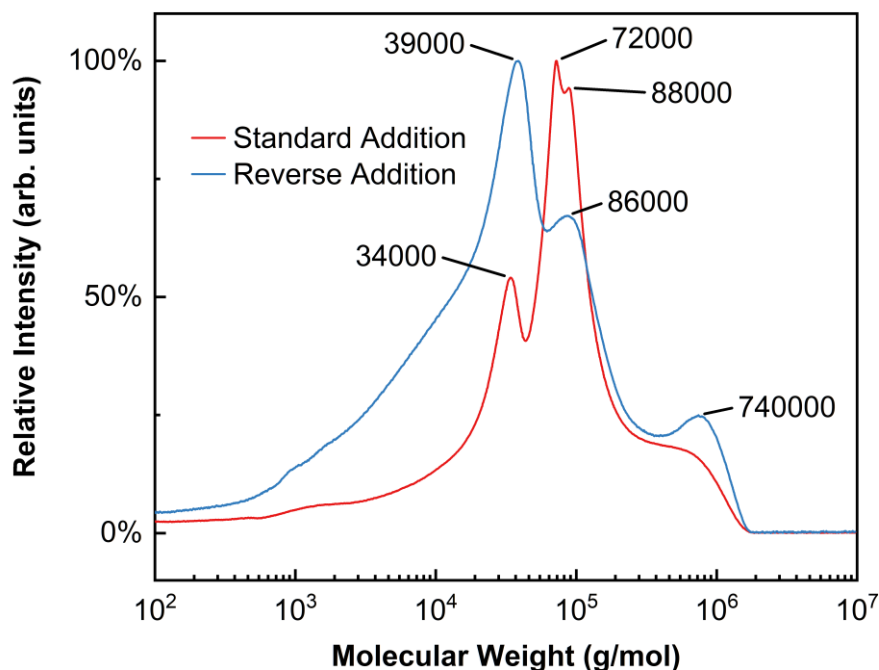


Figure 38. GPC chromatogram for P3HT synthesized by chemical oxidative polymerization under different conditions (right-angle light scattering detector). The red and blue traces correspond to entries 6 and 7 in Table 4, respectively. Exclusion limit: 70,000 g/mol.

A possible explanation for the low molecular weight and degree of polymerization observed for ether-substituted polythiophenes synthesized by reverse addition COP compared to P3HT could be due their lower oxidation potential. When the monomer is added slowly to the oxidant (reverse addition), the relative ratio of oxidant to monomer is extremely high. For example, if a 0.2 M monomer solution is added dropwise (assuming 20 drops/mL) to 4 equivalents of oxidant, the initial oxidant/monomer ratio is nearly 400:1. Under such strongly oxidizing conditions, polythiophenes and thiophene oligomers have been observed to undergo extensive oxidation to polycationic states,<sup>120</sup> and also irreversible overoxidation where electroactivity is destroyed.<sup>121</sup> The lower

oxidation potential of ether-substituted polythiophenes compared to P3HT should make them more easily oxidized to these heavily oxidized states than P3HT. Each consecutive oxidation event lowers the solubility of the polymer as it becomes more cationic. This decrease in solubility could cause the polymers to precipitate from the reaction mixture before they are able to achieve a high degree of polymerization.

A comment should also be made about the yield of these reactions. In most cases, the yields of polymers prepared by COP decreased when order of addition was changed from reverse to standard, although degree of polymerization increased (Table 5). When the polymers were precipitated into methanol after the oxidation step, the filtrates of the polymers prepared under standard addition conditions were observed to contain a larger fraction of methanol-soluble oligomers compared to those prepared under reverse addition conditions. This is one explanation for the decreased isolated yields of the polymers prepared under standard conditions.

Table 5. Comparison of the yields of polymers synthesized by COP under various standard and reverse addition conditions. The weight-average degree of polymerization  $X_w$  is also given for each polymer.

Polymer	Entry	Addition	Oxidant	Solvent	Yield	$X_w$
PEDOT-C12	1	Standard	2.3 eq. $\text{FeCl}_3$	$\text{C}_6\text{H}_5\text{Cl}$	25.8%	256
	2	Standard	4 eq. $\text{FeCl}_3$	$\text{C}_6\text{H}_5\text{Cl}$	26.9%	476
	3	Reverse	2.3 eq. $\text{FeCl}_3$	$\text{C}_6\text{H}_5\text{Cl}$	73.1%	7
	4	Reverse	2.3 eq. $\text{Fe}(\text{ClO}_4)_3$	$\text{C}_6\text{H}_5\text{Cl}$	38.2%	4
	5	Reverse	2.3 eq. $\text{FeCl}_3$	$\text{CHCl}_3$	79.8%	5

Table 5. Continued

<i>P3HT</i>	6	Standard	2.3 eq. $\text{FeCl}_3$	$\text{C}_6\text{H}_5\text{Cl}$	43.6%	$\geq 421$
	7	Reverse	2.3 eq. $\text{FeCl}_3$	$\text{C}_6\text{H}_5\text{Cl}$	64.4%	222
PDHOT	8	Standard	4 eq. $\text{FeCl}_3$	$\text{C}_6\text{H}_5\text{Cl}$	10.7%	88
	9	Reverse	2.3 eq. $\text{FeCl}_3$	$\text{C}_6\text{H}_5\text{Cl}$	42.3%	16

### 3.3.2 Grignard Metathesis

The GPC chromatograms for polymers prepared by GRIM polymerization are shown in Figure 39. The degree of polymerization ( $X_w$ ) of P3HT prepared by GRIM was 210 (35,000 g/mol) which is in good agreement with previously published data.<sup>49,97</sup> PEDOT-C12 synthesized by GRIM achieved a much higher  $X_w$  of 437 (135,000 g/mol), and a significant portion of the sample was over the exclusion limit of the GPC column ( $\geq 400,000$  g/mol).

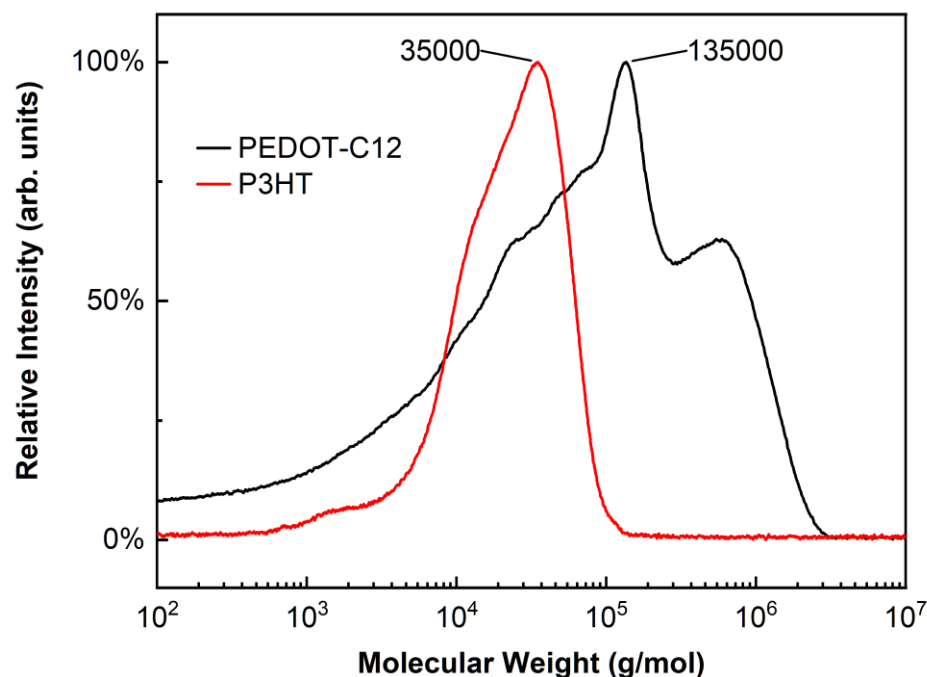


Figure 39. GPC Chromatogram for P3HT and PEDOT-C12 prepared by the GRIM method (right-angle light scattering detector). Exclusion limit: 70,000 g/mol (P3HT, orange line) 400,000 g/mol (PEDOT-C12, black line).

Contrary to the COP method, ether-substituted PEDOT-C12 was synthesized with a high degree of polymerization and in high yields with minimal optimization of the reaction conditions. It is notable to mention that for the GRIM polymerization to be successful, it is crucial to ensure the monomer is highly purified and the solvent is exceptionally dry. Polymerization attempts where these conditions were not met resulted in severely decreased yields and molecular weights.

As discussed in section 1.8.2.2, the more electron-rich a monomer is, the more chain-growth polymerization kinetics are favored over step-growth polymerization kinetics. Compared to P3HT, PEDOT-C12 is more electron-rich



owed to donation of electron density from the ether oxygens into the thiophene ring. This should facilitate strong polymer-catalyst interactions thereby increasing the chain-growth nature of the reaction. This is relevant to the goal of synthesizing high molecular weight polythiophenes because under chain-growth kinetics, polymer molecular weight increases rapidly while monomers are consumed slowly, as opposed to step-growth kinetics where monomers are consumed rapidly and polymer molecular weight increases slowly until almost all monomers are consumed.<sup>56</sup>

### **3.3.3 Comparison of Methods**

Using PEDOT-C12 as an example to compare the COP and GRIM methods, we see that both approaches are capable of producing polymers with a high degree of polymerization (Figure 40). In both GRIM, and the best case of COP (standard addition with 4 equivalents  $\text{FeCl}_3$  in chlorobenzene), PEDOT-C12 with similar molecular weights were produced, both polymers containing over 400 repeat units. Comparing the GPC traces for each polymer shows that the molecular weight distribution of PEDOT-C12 prepared by COP is much narrower compared to the polymer prepared by GRIM. In addition, in the COP prepared polymer there is a substantially smaller fraction of sample with molecular weight above the exclusion limit of the GPC column (400,000 g/mol). The greater fraction of high molecular weight PEDOT-C12 in the GRIM prepared sample could be attributed to the polymer being grown in the neutral state as opposed to the cationic state like in COP. The neutral polymer should have better solubility in the reaction solvent and thus can grow to a larger size before precipitating.

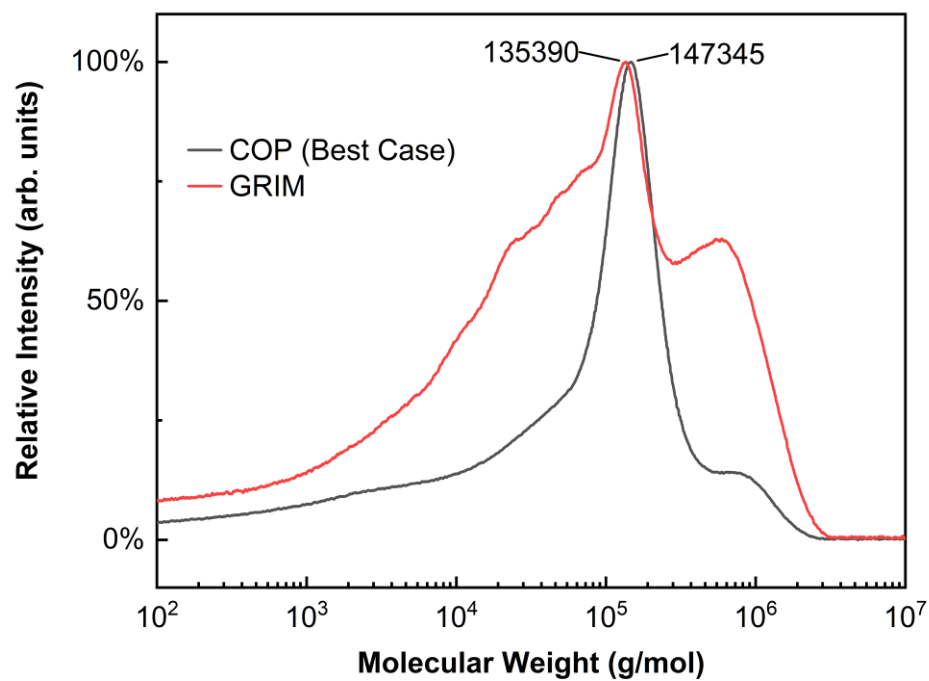


Figure 40. Comparison of GPC chromatograms of PEDOT-C12 prepared by COP (best case: standard addition with 4 equivalents  $\text{FeCl}_3$  in  $\text{C}_6\text{H}_5\text{Cl}$ ) and GRIM methods.

## 4. CONCLUDING REMARKS

### 4.1 Monomer Synthesis

To explore the effects of different reaction conditions on the molecular weight of ether-substituted polythiophenes prepared via an oxidative approach, monomers EDOT-C12 and 3,4-DHOT were synthesized via an acid-catalyzed transesterification reaction. The structures of the monomers were verified by  $^1\text{H}$  NMR spectroscopy and mass spectrometry (EDOT-C12 only).

For comparison of a non-oxidative approach, the dibromo derivative of EDOT-C12,  $\text{Br}_2\text{EDOT-C12}$  was synthesized by electrophilic aromatic substitution with two equivalents of NBS. The structure of this monomer was confirmed by  $^1\text{H}$  and  $^{13}\text{C}$  NMR spectroscopy and mass spectrometry.

### 4.2 Polymerizations

For ether-substituted polythiophenes (PEDOT-C12 and PDHOT) synthesized via an oxidative approach, the common literature procedure (reverse addition) produces polymers with low molecular weight and degree of polymerization compared to the model system, P3HT. Due to the lower oxidation potential of ether-substituted polythiophenes compared to P3HT, these polymers are more susceptible to overoxidation under strongly oxidizing conditions. This effect may be responsible for the low degree of polymerization observed for ether-substituted polythiophene synthesized under reverse addition conditions. Changing the order of addition to standard addition led to a significant increase in the molecular weights and degrees of polymerization of all polythiophenes, albeit at the cost of reduced yields.

PEDOT-C12 synthesized via a non-oxidative GRIM approach had high molecular weight and degree of polymerization compared to P3HT, provided the monomer was highly purified and stringent anhydrous conditions were maintained. The electron-rich nature of ether-substituted thiophenes compared to alkylthiophenes facilitates strong polymer-catalyst interactions which favors chain-growth kinetics over step-growth kinetics.

While the oxidative approach may be regarded as a more convenient alternative to non-oxidative approaches, the sensitivity of the polymer to overoxidation must be considered. For ether-substituted polythiophenes synthesized via COP, significant optimization of reaction conditions was necessary in order for high molecular weights and degrees of polymerization to be achieved. However, minimal optimization of reaction conditions was needed to achieve the same results for ether-substituted polymers synthesized via GRIM. Consideration of these factors is vital for the future synthesis of high molecular weight, electron-rich thiophene monomers.

## 5. FUTURE WORK

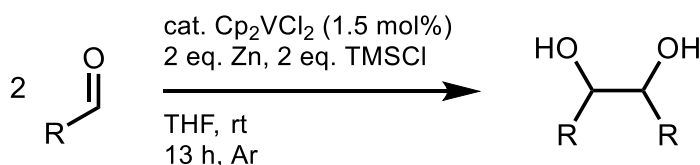
### **5.1 Standard Addition Oxidative Polymerization**

Future work should explore longer reaction times for the chemical oxidative polymerization under standard addition conditions. Reaction times should be increased to 48 hours or longer to see if yields and molecular weights can be improved. Another approach that could yield interesting results would be to add portions of oxidant solution to the reaction mixture multiple times over hours or days. For example, if 4 equivalents of oxidant were to be added, adding 1 equivalent every hour for 4 hours, or adding 2 equivalents once a day for 2 days, etc.

### **5.2 Synthesis of Symmetrical Vicinal Diols for Novel EDOT Monomers**

The transesterification reaction for the synthesis of EDOT monomers is highly versatile, however the number of commercially available vicinal diols is very limited. In particular, symmetrical vicinal diols are few and costly.

A possible route to symmetrical vicinal diols is via the vanadium-catalyzed pinacol coupling of aldehydes (Scheme 11).<sup>122</sup> By this method, inexpensive primary aliphatic aldehydes can be coupled at the carbonyl carbon to form vicinal diols. This route is particularly attractive compared to other di-hydroxylation methods, which employ dangerous reagents (e.g. osmium tetroxide) or require a symmetrical alkene starting material (which presents a problem in and of itself).<sup>123–125</sup>



Scheme 11. Vanadium-catalyzed pinacol coupling of aliphatic aldehydes to vicinal diols.

Exploration of this route could open new possibilities for symmetrical alkyl-substituted monomers. Synthesis of substituted EDOT monomers with symmetrical diols provides the benefit of eliminating the possibility of regiochemical defects during polymerization. Additionally, derivatization of these monomers is simplified by removing the possibility of generating diastereomers when only a single functional group is added (Figure 41).

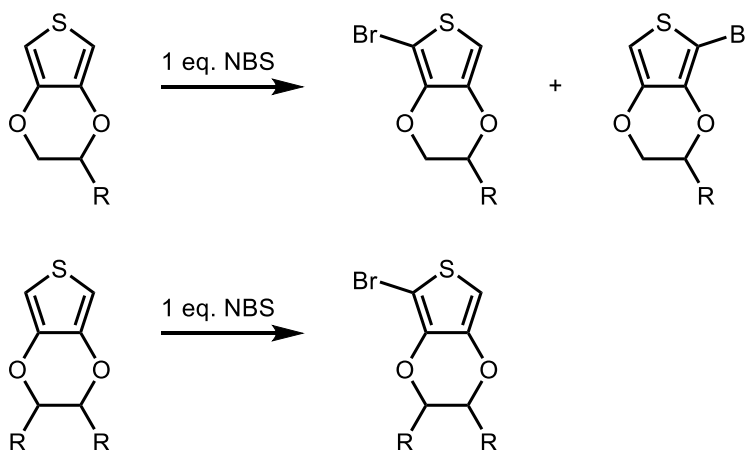


Figure 41. Derivatization of asymmetric vs. symmetric EDOT monomers.

### **5.3 Determination of Regioregularity of PEDOTs**

As discussed in section 1.5.2, the determination of the regioregularity of P3HT is well established. The method for determining regioregularity via  $^1\text{H}$  NMR spectroscopy was outlined by Barbarella *et al.*<sup>126</sup> when the authors synthesized

and characterized the different possible conformational triads (HT-HT, HH-TT, HT-HH, TT-HT) of P3HT. To the best of our knowledge, a similar study has yet to be conducted for substituted PEDOTs. Synthesis of the analogous substituted-EDOT triads (Figure 42) and characterization by  $^1\text{H}$  NMR spectroscopy would give valuable insight to how regioregularity affects the chemical shifts of the protons adjacent to the polymer backbone. The triads could be synthesized by traditional coupling methods, such as Negishi or Stille coupling. The challenge, however, is in selectively functionalizing the desired 2 or 5 positions, which are chemically very similar.

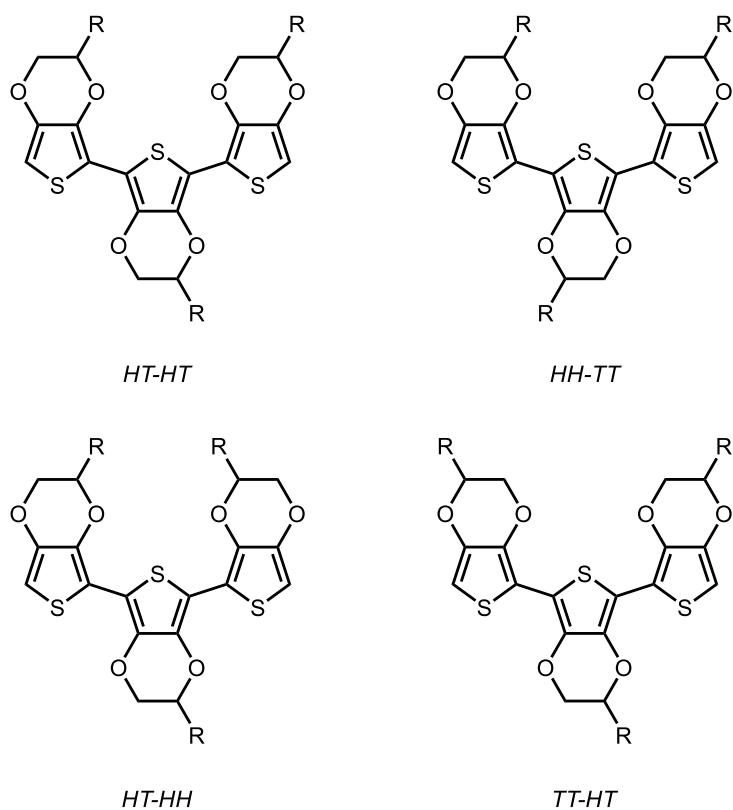
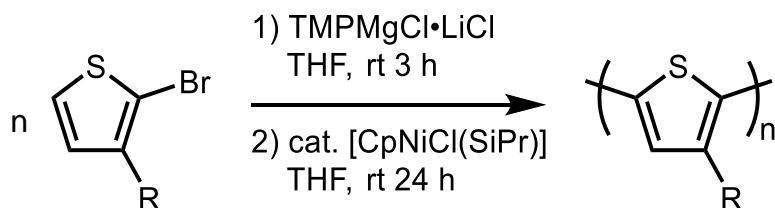


Figure 42. Four possible conformational triads in substituted PEDOTs.

## 5.4 Dehydrobrominative Polycondensation

The dehydrobrominative polycondensation (DHBP) method (Scheme 12) is a Kumada catalyst transfer polymerization capable of producing very high molecular weight P3HT (up to 828,000 g/mol).<sup>51</sup> The method can be thought of as an extension of the Kumada-type polymerizations developed by McCullough and Lowe<sup>47,48</sup> with the intention of improving practicality through enhanced atom economy and catalytic efficiency. Contrary to the GRIM method, DHBP requires only a singly brominated monomer, thereby reducing mass loss through polymerization. Additionally, the reaction requires only mild conditions and proceeds efficiently at room temperature. Although the air-stable Ni(NHC) (NHC = N-heterocyclic carbene) catalyst is currently commercially unavailable, it is easily synthesized in one step from nickelocene and the hydrochloride salt of the carbene ligand.<sup>127</sup>



Scheme 12. Dehydrobrominative polycondensation reaction.

While there are many parallels to the GRIM method, the reaction mechanism appears to operate through a pathway different from that of the GRIM method, although detailed studies to elucidate the exact mechanism remain to be performed. The differences arise from the catalyst ligand sets. Unlike the  $\text{NiCl}_2(\text{dppp})$  catalyst used in the GRIM method, which has two chloride



ligands for transmetalation,  $[\text{CpNiCl}(\text{SiPr})]$  ( $\text{Cp}$  = cyclopentadienyl,  $\text{SiPr}$  = 1,3-bis(2,6-di-*i*-propylphenyl)imidazolidin-2-ylidene) only has one (Figure 43). Therefore, the catalyst cannot directly undergo two subsequent transmetalations and begin the catalytic cycle.

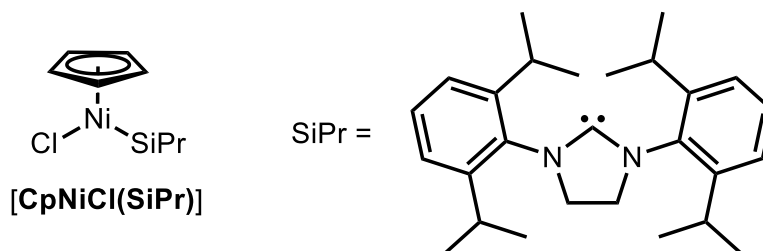


Figure 43. Structure of  $[\text{CpNiCl}(\text{SiPr})]$  catalyst and SiPr ligand.

In light of the emerging utility of Ni(I) catalysts<sup>128</sup> in cross-coupling reactions, specifically linear NHC-Ni-X (where X = amido,<sup>129</sup> cyclopentadieno<sup>130</sup>) complexes, we tentatively propose the Ni(I)/Ni(III) catalytic mechanism shown in Figure 44. The key difference from the GRIM mechanism is disproportionation of the Ni(II) catalyst in the first step to give both Ni(I) and Ni(III) species. The Ni(III) species proposed has two chloride ligands, allowing it to undergo two consecutive transmetalation steps. The catalyst can then reductively eliminate an initial TT dimer to give a linear Cp-Ni(I)-NHC complex. Additionally, the Ni(I) species generated from disproportionation of Ni(II) could undergo N-H activation of the 2,2,6,6-tetramethylpiperidine (TMP) base and reductive elimination of Cp-H to give a linear NHC-Ni(I)-amido complex. Both NHC-Ni(I)-X complexes could then enter a traditional oxidative addition, transmetalation, reductive elimination catalytic cycle akin to the GRIM method.

The next step to exploring DHBP of 3,4-alkylenedioxy monomers such as EDOT should be the synthesis of symmetrical EDOT derivatives, which simplify the synthesis and purification of singly brominated monomers by reducing the number of possible brominated stereoisomers. The prospect of new catalyst oxidation states and geometries opens new possibilities for polythiophene synthesis, the scope of which remains largely unexplored.

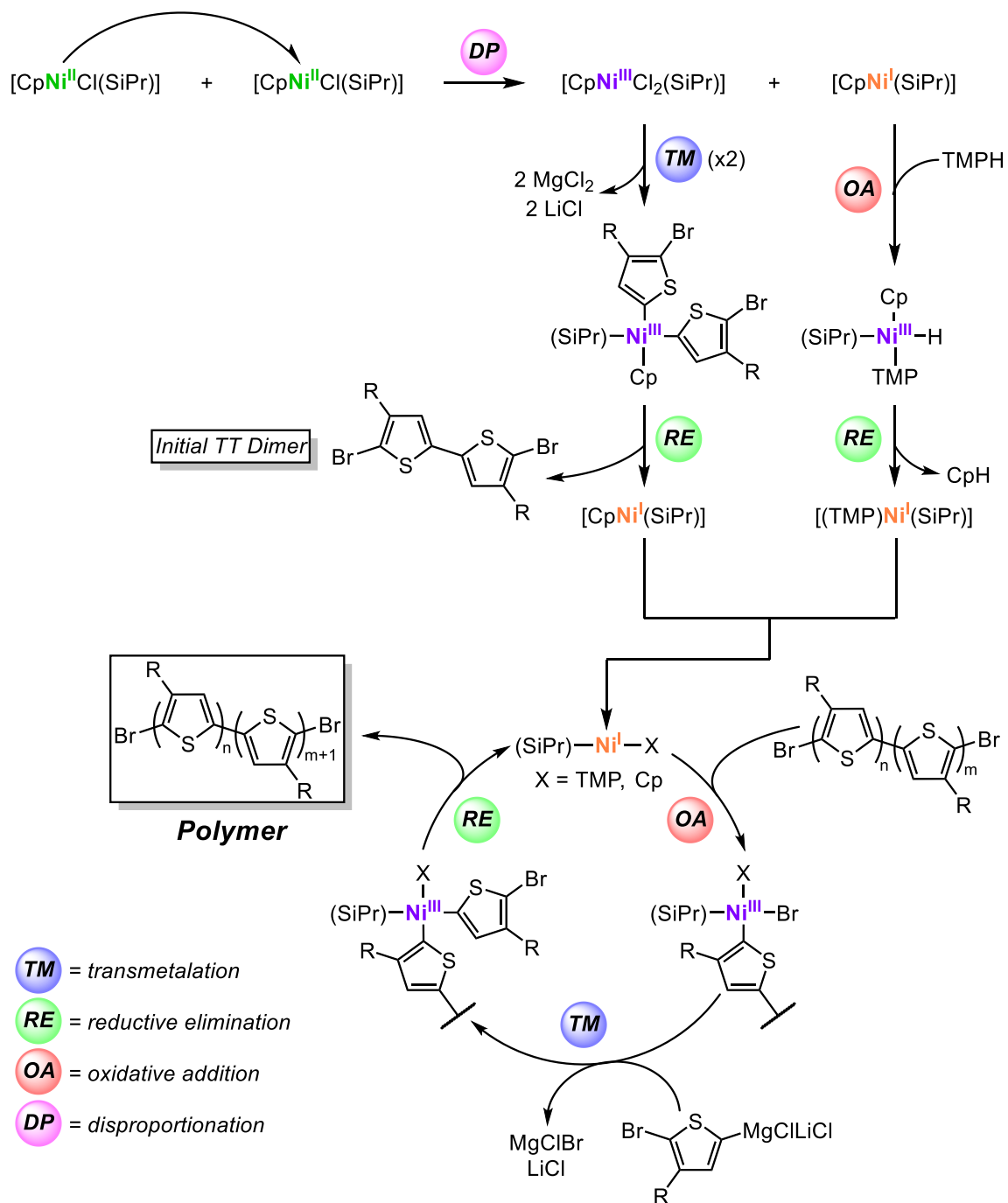
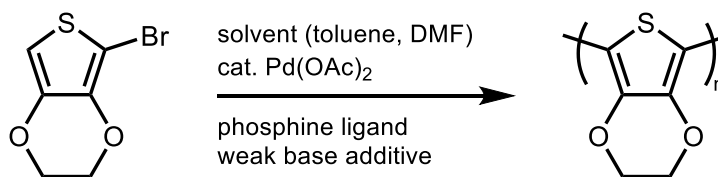


Figure 44. Tentative DHPB Mechanism.

## 5.5 Direct Arylation Polycondensation

Direct arylation polycondensation (DArP) (Scheme 13) is a palladium-catalyzed polymerization that has seen widespread<sup>71,131</sup> use in recent years thanks to its reduced environmental impact,<sup>132</sup> robustness,<sup>133,134</sup> and versatility. Notably, the reaction can be performed without the stringent anhydrous<sup>132,133</sup> and anaerobic<sup>134</sup> conditions that are necessary to other transition metal-mediated reactions like the GRIM or DHBP methods. Additionally, no pyrophoric (organomagnesium, organolithium) or toxic (organotin) metalating agents are needed. These qualities make DArP a promising approach to conjugated polymers for biochemical and other sensitive applications.



Scheme 13. Generalized direct arylation polycondensation (DArP) reaction.

While DArP has seen success in the synthesis of a wide range of conjugated homopolymers and copolymers alike, the reaction conditions and experimental procedures described in the literature are far less standardized compared to GRIM and COP, which can complicate their adaption to novel systems. Indeed, optimization of the reaction requires consideration of a number of variables, such as choice of solvent, palladium catalyst, concentrations and identities of phosphine ligands and other additives.<sup>71</sup>

An interesting feature of DArP is that polymerization can occur through either homocouplings or cross-couplings (Figure 45). This presents a level of

flexibility that few other polymerization methods possess. The cross-coupling approach has lent itself to the synthesis of a wide array of novel conjugated copolymers.<sup>135</sup>

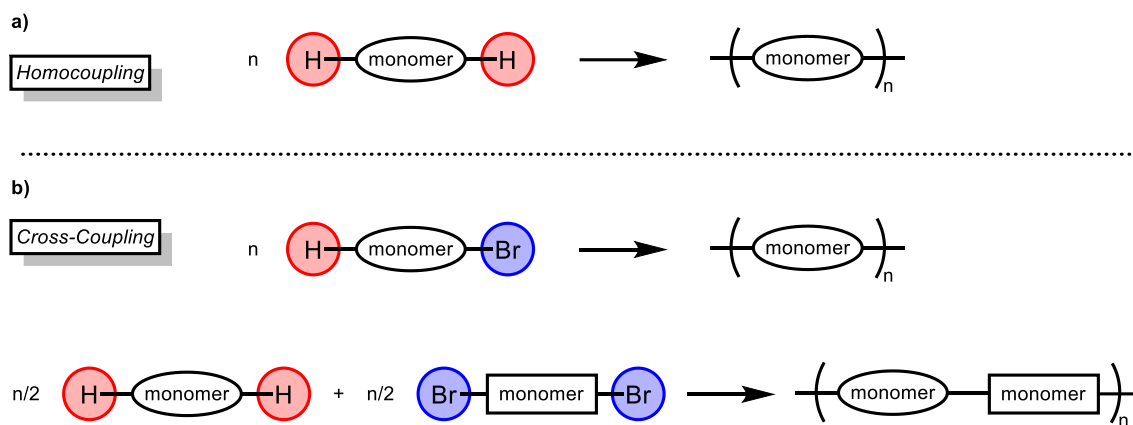


Figure 45. Examples of homocoupling and cross-coupling polymerizations possible through DArP.

While DArP presents a unique approach to polythiophenes, there is still much work to be done to explore the limits of this method, especially for the synthesis of high molecular weight homopolymers like those described in this work.

## APPENDIX SECTION

A. GPC Calibration Curves .....	89
B. GPC Chromatograms .....	90

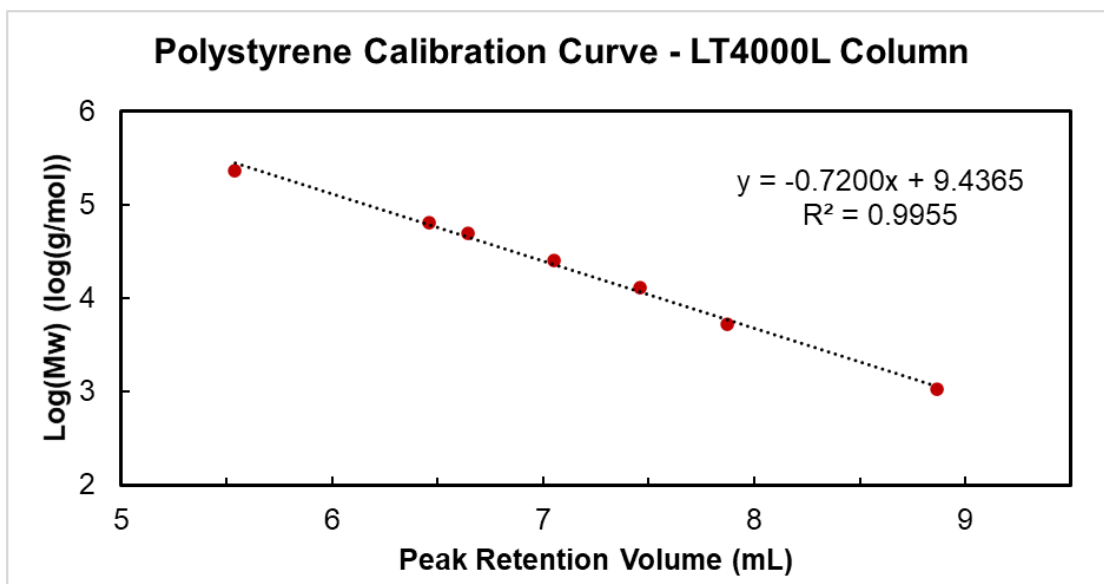


Figure A1. Polystyrene calibration curve for the LT4000L column (right-angle light scattering detector).

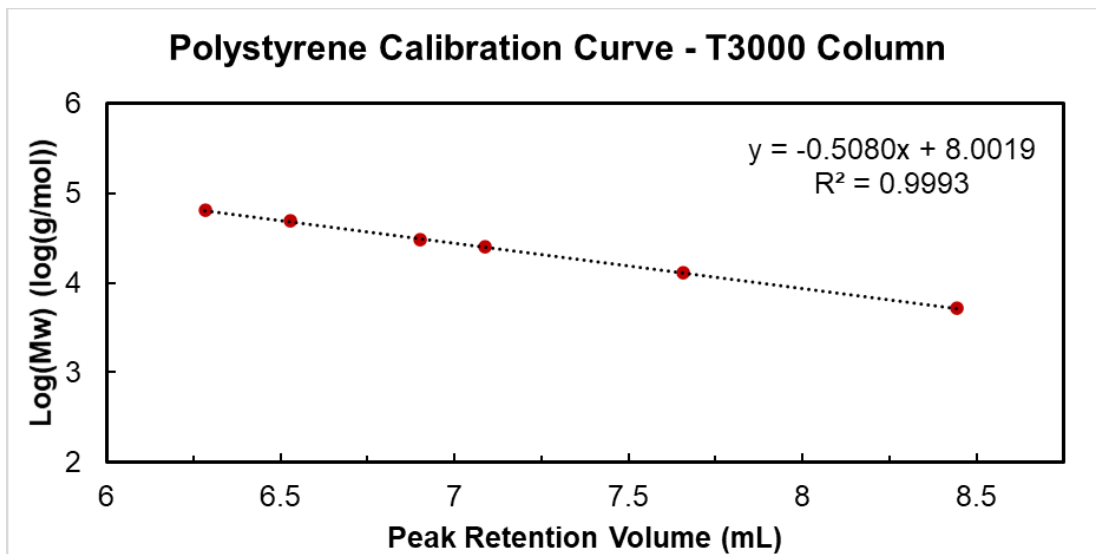


Figure A2. Polystyrene calibration curve for the T3000 column (right-angle light scattering detector).

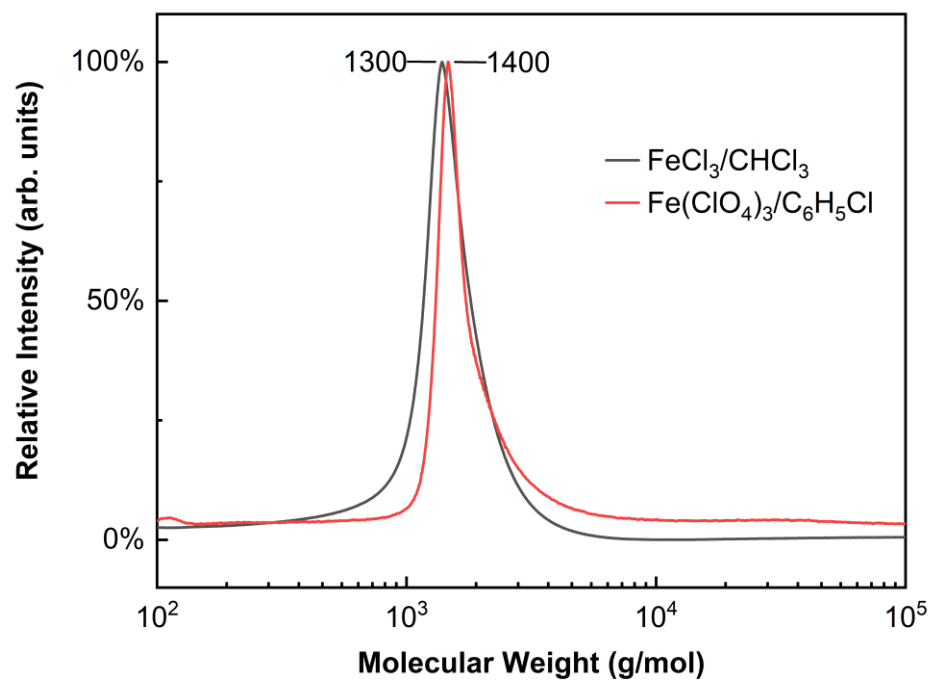


Figure B1. Other GPC chromatograms for PEDOT-C12 (right-angle light scattering detector).



## REFERENCES

- (1) Rasmussen, S. C. The Early History of Polyaniline: Discovery and Origins. *An Int. J. Hist. Chem. Subst.* **2017**, 1 (12), 99–109.
- (2) Shirakawa, H.; Ikeda, S. Infrared Spectra of Poly(Acetylene). *Polym. J.* **1971**, 2, 231.
- (3) Shirakawa, H.; Louis, E. J.; MacDiarmid, A. G.; Chiang, C. K.; Heeger, A. J. Synthesis of Electrically Conducting Organic Polymers: Halogen Derivatives of Polyacetylene, (CH)<sub>x</sub>. *J. Chem. Soc. Chem. Commun.* **1977**, No. 16, 578–580.
- (4) Roncali, J. Conjugated Poly(Thiophenes): Synthesis, Functionalization, and Applications. *Chem. Rev.* **1992**, 92 (4), 711–738.
- (5) Agbolaghi, S.; Zenoozi, S. A Comprehensive Review on Poly(3-Alkylthiophene)-Based Crystalline Structures, Protocols and Electronic Applications. *Org. Electron. physics, Mater. Appl.* **2017**, 51 (September), 362–403.
- (6) Das, T. K.; Prusty, S. Review on Conducting Polymers and Their Applications. *Polym. - Plast. Technol. Eng.* **2012**, 51 (14), 1487–1500.
- (7) Gunbas, G.; Toppare, L. Electrochromic Conjugated Polyheterocycles and Derivatives - Highlights from the Last Decade towards Realization of Long Lived Aspirations. *Chem. Commun.* **2012**, 48 (8), 1083–1101.
- (8) Mehmood, U.; Al-Ahmed, A.; Hussein, I. A. Review on Recent Advances in Polythiophene Based Photovoltaic Devices. *Renew. Sustain. Energy Rev.* **2016**, 57, 550–561.
- (9) Sun, K.; Zhang, S.; Li, P.; Xia, Y.; Zhang, X.; Du, D.; Isikgor, F. H.; Ouyang, J. Review on Application of PEDOTs and PEDOT:PSS in Energy Conversion and Storage Devices. *J. Mater. Sci. Mater. Electron.* **2015**, 26 (7), 4438–4462.
- (10) Dimitrakopoulos, C. D.; Malenfant, P. R. L. Organic Thin Film Transistors for Large Area Electronics. *Adv. Mater.* **2002**, 14 (2), 99–117.
- (11) Aasmundtveit, K. E.; Samuelsen, E. J.; Pettersson, L. A. A.; Inganäs, O.; Johansson, T.; Feidenhans'l, R. Structure of Thin Films of Poly(3,4-Ethylenedioxythiophene). *Synth. Met.* **1999**, 101 (1), 561–564.
- (12) Patil, A. O.; Heeger, A. J.; Wudl, F. Optical Properties of Conducting Polymers. *Chem. Rev.* **1988**, 88 (1), 183–200.

- (13) Kobayashi, M.; Chen, J.; Chung, T.-C.; Moraes, F.; Heeger, A. J.; Wudl, F. Synthesis and Properties of Chemically Coupled Poly(Thiophene). *Synth. Met.* **1984**, 9 (1), 77–86.
- (14) Bredas, J. L. Bipolarons in Doped Conjugated Polymers: A Critical Comparison Between Theoretical Results and Experimental Data. *Mol. Cryst. Liq. Cryst.* **1985**, 118 (1), 49–56.
- (15) Brédas, J. L. Relationship between Band Gap and Bond Length Alternation in Organic Conjugated Polymers. *J. Chem. Phys.* **1985**, 82 (8), 3808–3811.
- (16) *Conjugated Polymers: Theory, Synthesis, Properties, And Characterization (Handbook of Conducting Polymers)*, 3rd ed.; Skotheim, T. A., Reynolds, J. R., Eds.; CRC Press: Boca Raton, 2007.
- (17) Sugimoto, R.; Yoshino, K.; Inoue, S.; Tsukagoshi, K. Preparation and Property of Polytellurophene and Polyselenophene. *Jpn. J. Appl. Phys.* **1985**, 24 (6 A), L425–L427.
- (18) Sugimoto, R.; Yoshino, K.; Hayashi, S. Preparation and Properties of Conducting Heterocyclic Polymer Films by Chemical Method. *Jpn. J. Appl. Phys.* **1984**, 23 (12), L899–L900.
- (19) Sugimoto, R.; Takeda, S.; Gu, H. B.; Yoshino, K. Preparation of Soluble Polythiophene Derivatives Utilizing Transition Metal Halides As Catalysts and Their Property. *Chem. Express* **1986**, 1 (11), 635–638.
- (20) Luppi, B. T.; McDonald, R.; Ferguson, M. J.; Sang, L.; Rivard, E. Rapid Access to (Cycloalkyl)Tellurophene Oligomer Mixtures and the First Poly(3-Aryltellurophene). *Chem. Commun.* **2019**, 55 (94), 14218–14221.
- (21) Ye, S.; Steube, M.; Carrera, E. I.; Seferos, D. S. What Limits the Molecular Weight and Controlled Synthesis of Poly(3-Alkyltellurophene)S? *Macromolecules* **2016**, 49 (5), 1704–1711.
- (22) Ye, S.; Foster, S. M.; Pollit, A. A.; Cheng, S.; Seferos, D. S.; Foster, S. M.; Seferos, D. S.; Pollit, A. A. The Role of Halogens in the Catalyst Transfer Polycondensation for  $\pi$ -Conjugated Polymers. *Chem. Sci.* **2019**, 10, 2075–2080.
- (23) Ye, S.; Janasz, L.; Zajaczkowski, W.; Manion, J. G.; Mondal, A.; Marszalek, T.; Andrienko, D.; Müllen, K.; Pisula, W.; Seferos, D. S. Self-Organization and Charge Transport Properties of Selenium and Tellurium Analogues of Polythiophene. *Macromol. Rapid Commun.* **2019**, 40 (1), 1–8.

- (24) Tourillon, G.; Garnier, F. New Electrochemically Generated Organic Conducting Polymers. *J. Electroanal. Chem.* **1982**, *135* (1), 173–178.
- (25) Österholm, J.-E.; Passiniemi, P.; Isotalo, H.; Stubb, H. Synthesis and Properties of FeCl<sub>4</sub>-Doped Polythiophene. *Synth. Met.* **1987**, *18* (1–3), 213–218.
- (26) Gadiant, J.; Groch, R.; Lind, C. An in Depth Study of Solvent Effects on Yield and Average Molecular Weight in Poly(3-Hexylthiophene). *Polymer (Guildf)*. **2017**, *115*, 21–27.
- (27) Elsenbaumer, R. L.; Jen, K. Y.; Oboodi, R. Processible and Environmentally Stable Conducting Polymers. *Synth. Met.* **1986**, *15* (2–3), 169–174.
- (28) McCullough, R. D. The Chemistry of Conducting Polythiophenes. *Adv. Mater.* **1998**, *10* (2), 93–116.
- (29) Tanaka, S.; Sato, M. aki; Kaeriyama, K. Electrochemical Preparation and Properties of Poly(3-Methoxy-2,5-Thiophenediyl) and Poly(3-Methylthio-2,5-Thiophenediyl). *Synth. Met.* **1988**, *25* (3), 277–288.
- (30) Jonas, F.; Heywang, G.; Schmidtberg, W.; Heinze, J.; Dietrich, M. Neue Polythiophene, Verfahren Zu Ihrer Herstellung Und Ihre Verwendung. EP0339340A2, 1989.
- (31) Groenendaal, L.; Zotti, G.; Aubert, P. H.; Waybright, S. M.; Reynolds, J. R. Electrochemistry of Poly(3,4-Alkylenedioxythiophene) Derivatives. *Adv. Mater.* **2003**, *15* (11), 855–879.
- (32) Kumar, A.; Reynolds, J. R. Soluble Alkyl-Substituted Poly(Ethylenedioxythiophenes) as Electrochromic Materials. *Macromolecules* **1996**, *29* (23), 7629–7630.
- (33) Wolfs, M.; Darmanin, T.; Guittard, F. Versatile Superhydrophobic Surfaces from a Bioinspired Approach. *Macromolecules* **2011**, *44* (23), 9286–9294.
- (34) Lee, S.; Lee, K. K.; Lim, E.; Son, H.-Y. Synthesis and Characterization of Regioregular Alkyl-Substituted Poly(3,4-Ethylenedioxythiophenes). *J. Nanosci. Nanotechnol.* **2012**, *12* (5), 4335–4339.
- (35) Berdyczko, P.; Domagala, W.; Czardybon, A.; Lapkowski, M. Long Alkyl Chain Bearing Derivatives of Poly(3,4-Ethylenedioxythiophene) Studied by in Situ EPR Spectroelectrochemistry. *Synth. Met.* **2009**, *159* (21–22), 2240–2244.

- (36) Schottland, P.; Fichet, O.; Teyssié, D.; Chevrot, C. Langmuir-Blodgett Films of an Alkoxy Derivative of Poly(3,4-Ethylenedioxythiophene). *Synth. Met.* **1999**, *101* (1), 7–8.
- (37) Gerhard, H.; Friedrich, J. Poly(Alkylendioxythiophene)s - New, Very Stable Conducting Polymers. *Adv. Mater.* **1992**, *4* (2), 116–118.
- (38) Dey, T.; Invernale, M. A.; Ding, Y.; Buyukmumcu, Z.; Sotzing, G. A. Poly(3,4-Propylenedioxythiophene)s as a Single Platform for Full Color Realization. *Macromolecules* **2011**, *44* (8), 2415–2417.
- (39) Dong, L.; Zhang, L.; Duan, X.; Mo, D.; Xu, J.; Zhu, X. Synthesis and Characterization of Chiral PEDOT Enantiomers Bearing Chiral Moieties in Side Chains: Chiral Recognition and Its Mechanism Using Electrochemical Sensing Technology. *RSC Adv.* **2016**, *6* (14), 11536–11545.
- (40) Dufen, H.; Baoyang, L.; Xuemin, D.; Jingkun, X.; Long, Z.; Kaixin, Z.; Shimin, Z.; Shijie, Z. Synthesis of Novel Chiral L-Leucine Grafted PEDOT Derivatives with Excellent Electrochromic Performances. *RSC Adv.* **2014**, *4*, 35597–35608.
- (41) Hai, T. A. P.; Sugimoto, R. Effect of Molar Ratio of Oxidizer/3-Hexylthiophene Monomer in Chemical Oxidative Polymerization of Poly(3-Hexylthiophene). *J. Mol. Struct.* **2017**, *1146*, 660–668.
- (42) Donahue, M. J.; Sanchez-Sanchez, A.; Inal, S.; Qu, J.; Owens, R. M.; Mecerreyes, D.; Malliaras, G. G.; Martin, D. C. Tailoring PEDOT Properties for Applications in Bioelectronics. *Mater. Sci. Eng. R Reports* **2020**, *140* (January), 100546.
- (43) Freitag, D.; Groenendaal, L.; Pielartzik, H.; Jonas, F.; Reynolds, J. R.; Freitag, D.; Pielartzik, H.; Reynolds, J. R. Poly(3,4-Ethylenedioxythiophene) and Its Derivatives: Past, Present, and Future. *Adv. Mater.* **2000**, *12* (7), 481–494.
- (44) Chen, S. A.; Tsai, C. C. Structure/Properties of Conjugated Conductive Polymers. 2. 3-Ether-Substituted Polythiophenes and Poly(4-Methylthiophene)s. *Macromolecules* **1993**, *26* (9), 2234–2239.
- (45) van Hutten, P. F.; Gill, R. F.; Herrema, J. K.; Hadziioannou, G. Structure of Thiophene-Based Regioregular Polymers and Block Copolymers and Its Influence on Luminescence Spectra. *J. Phys. Chem.* **1995**, *99* (10), 3218–3224.
- (46) Thémans, B.; Salaneck, W. R.; Brédas, J. L. Theoretical Study of the Influence of Thermochemical Effects on the Electronic Structure of Poly(3-Hexylthiophene). *Synth. Met.* **1989**, *28* (1–2), 359–364.

- (47) McCullough, R. D.; Lowe, R. D. Enhanced Electrical Conductivity in Regioselectively Synthesized Poly(3-Alkylthiophenes). *J. Chem. Soc. Chem. Commun.* **1992**, No. 1, 70.
- (48) McCullough, R. D.; Lowe, R. D.; Jayaraman, M.; Anderson, D. L. Design, Synthesis, and Control of Conducting Polymer Architectures: Structurally Homogeneous Poly(3-Alkylthiophenes). *J. Org. Chem.* **1993**, 58 (4), 904–912.
- (49) Loewe, R. S.; Khersonsky, S. M.; McCullough, R. D. A Simple Method to Prepare Head-to-Tail Coupled, Regioregular Poly(3-Alkylthiophenes) Using Grignard Metathesis. *Adv. Mater.* **1999**, 11 (3), 250–253.
- (50) Guillerez, S.; Bidan, G. New Convenient Synthesis of Highly Regioregular Poly(3-Octylthiophene) Based on the Suzuki Coupling Reaction. *Synth. Met.* **1998**, 93 (2), 123–126.
- (51) Tamba, S.; Tanaka, S.; Okubo, Y.; Meguro, H.; Okamoto, S.; Mori, A. Nickel-Catalyzed Dehydrobrominative Polycondensation for the Practical Preparation of Regioregular Poly(3-Substituted Thiophene)S. *Chem. Lett.* **2011**, 40 (4), 398–399.
- (52) Tamba, S.; Shono, K.; Sugie, A.; Mori, A. C-H Functionalization Polycondensation of Chlorothiophenes in the Presence of Nickel Catalyst with Stoichiometric or Catalytically Generated Magnesium Amide. *J. Am. Chem. Soc.* **2011**, 133 (25), 9700–9703.
- (53) Daoust, G.; Leclerc, M. Structure-Property Relationships in Alkoxy-Substituted Polythiophenes. *Macromolecules* **1991**, 24 (2), 455–459.
- (54) Somanathan, N.; Wegner, G. Comparative Studies on Poly(3-Cyclohexylthiophene) with Polyalkylthiophenes. *Synth. Met.* **1995**, 75 (2), 123–126.
- (55) Amou, S.; Haba, O.; Shirato, K.; Hayakawa, T.; Ueda, M.; Takeuchi, K.; Asai, M. Head-to-Tail Regioregularity of Poly(3-Hexylthiophene) in Oxidative Coupling Polymerization with FeCl<sub>3</sub>. *J. Polym. Sci. Part A Polym. Chem.* **1999**, 37 (13), 1943–1948.
- (56) Carraher Jr., C. E. *Introduction to Polymer Chemistry*, 3rd ed.; CRC Press, 2012.
- (57) Schärftl, W. *Light Scattering from Polymer Solutions and Nanoparticle Dispersions*; Springer Laboratory; Springer Berlin Heidelberg: Berlin, Heidelberg, 2007.

- (58) Trznadel, M.; Pron, A.; Zagorska, M.; Chrzaszcz, R.; Pielichowski, J. Effect of Molecular Weight on Spectroscopic and Spectroelectrochemical Properties of Regioregular Poly(3-Hexylthiophene). *Macromolecules* **1998**, *31* (15), 5051–5058.
- (59) Zen, A.; Saphiannikova, M.; Neher, D.; Grenzer, J.; Grigorian, S.; Pietsch, U.; Asawapirom, U.; Janietz, S.; Scherf, U.; Lieberwirth, I.; Wegner, G. Effect of Molecular Weight on the Structure and Crystallinity of Poly(3-Hexylthiophene). *Macromolecules* **2006**, *39* (6), 2162–2171.
- (60) Zen, A.; Pflaum, J.; Hirschmann, S.; Zhuang, W.; Jaiser, F.; Asawapirom, U.; Rabe, J. P.; Scherf, U.; Neher, D. Effect of Molecular Weight and Annealing of Poly(3-Hexylthiophene)s on the Performance of Organic Field-Effect Transistors. *Adv. Funct. Mater.* **2004**, *14* (8), 757–764.
- (61) Matsumoto, T.; Nishi, K.; Tamba, S.; Kotera, M.; Hongo, C.; Mori, A.; Nishino, T. Molecular Weight Effect on Surface and Bulk Structure of Poly(3-Hexylthiophene) Thin Films. *Polymer (Guildf)*. **2017**, *119*, 76–82.
- (62) Kline, R. J.; McGehee, M. D.; Kadnikova, E. N.; Liu, J.; Fréchet, J. M. J. Controlling the Field-Effect Mobility of Regioregular Polythiophene by Changing the Molecular Weight. *Adv. Mater.* **2003**, *15* (18), 1519–1522.
- (63) Kline, R. J.; McGehee, M. D.; Kadnikova, E. N.; Liu, J.; Fréchet, J. M. J.; Toney, M. F. Dependence of Regioregular Poly(3-Hexylthiophene) Film Morphology and Field-Effect Mobility on Molecular Weight. *Macromolecules* **2005**, *38* (8), 3312–3319.
- (64) Qu, S.; Yao, Q.; Yu, B.; Zeng, K.; Shi, W.; Chen, Y.; Chen, L. Optimizing the Thermoelectric Performance of Poly(3-Hexylthiophene) through Molecular-Weight Engineering. *Chem. - An Asian J.* **2018**, *13* (21), 3246–3253.
- (65) Ho, P. K.-H.; Chua, L.-L.; Dipankar, M.; Gao, X. Y.; Qi, D. C.; Wee, A. T.-S.; Chang, J.-F.; Friend, R. H. Solvent Effects on Chain Orientation and Interchain  $\pi$ -Interaction in Conjugated Polymer Thin Films: Direct Measurements of the Air and Substrate Interfaces by Near-Edge X-Ray Absorption Spectroscopy. *Adv. Mater.* **2007**, *19* (2), 215–221.
- (66) Tung, L. H. Data Treatment in GPC. *Sep. Sci.* **1970**, *5* (3), 339–347.
- (67) Heffner, G. W.; Pearson, D. S. Molecular Characterization of Poly(3-Hexylthiophene). *Macromolecules* **1991**, *24* (23), 6295–6299.
- (68) Wong, M.; Hollinger, J.; Kozycz, L. M.; McCormick, T. M.; Lu, Y.; Burns, D. C.; Seferos, D. S. An Apparent Size-Exclusion Quantification Limit Reveals a Molecular Weight Limit in the Synthesis of Externally Initiated Polythiophenes. *ACS Macro Lett.* **2012**, *1* (11), 1266–1269.

- (69) Dissanayake, D. S.; Sheina, E.; Biewer, M. C.; McCullough, R. D.; Stefan, M. C. Determination of Absolute Molecular Weight of Regioregular Poly(3-Hexylthiophene) By  $^1\text{H}$ -NMR Analysis. *J. Polym. Sci. Part A Polym. Chem.* **2017**, *55* (1), 79–82.
- (70) Kuwabara, J.; Yamazaki, K.; Yamagata, T.; Tsuchida, W.; Kanbara, T. The Effect of a Solvent on Direct Arylation Polycondensation of Substituted Thiophenes. *Polym. Chem.* **2015**, *6* (6), 891–895.
- (71) Pouliot, J. R.; Grenier, F.; Blaskovits, J. T.; Beaupré, S.; Leclerc, M. Direct (Hetero)Arylation Polymerization: Simplicity for Conjugated Polymer Synthesis. *Chem. Rev.* **2016**, *116* (22), 14225–14274.
- (72) Yu, C. Y.; Ko, B. T.; Ting, C.; Chen, C. P. Two-Dimensional Regioregular Polythiophenes with Conjugated Side Chains for Use in Organic Solar Cells. *Sol. Energy Mater. Sol. Cells* **2009**, *93* (5), 613–620.
- (73) Zhai, L.; McCullough, R. D.; Loewe, R. S.; Ewbank, P.; Liu, J. Regioregular, Head-to-Tail Coupled Poly(3-Alkylthiophenes) Made Easy by the GRIM Method: Investigation of the Reaction and the Origin of Regioselectivity. *Macromolecules* **2001**, *34* (13), 4324–4333.
- (74) Rudenko, A. E.; Wiley, C. A.; Stone, S. M.; Tannaci, J. F.; Thompson, B. C. Semi-Random P3HT Analogs via Direct Arylation Polymerization. *J. Polym. Sci. Part A Polym. Chem.* **2012**, *50* (18), 3691–3697.
- (75) Andersson, M. R.; Selse, D.; Berggren, M.; Järvinen, H.; Hjertberg, T.; Inganäs, O.; Wennerström, O.; Österholm, J. E. Regioselective Polymerization of 3-(4-Octylphenyl)Thiophene with  $\text{FeCl}_3$ . *Macromolecules* **1994**, *27* (22), 6503–6506.
- (76) Winther-Jensen, B.; West, K. Vapor-Phase Polymerization of 3,4-Ethylenedioxythiophene: A Route to Highly Conducting Polymer Surface Layers. *Macromolecules* **2004**, *37* (12), 4538–4543.
- (77) Niemi, V. M.; Knuuttila, P.; Österholm, J. E.; Korvola, J. Polymerization of 3-Alkylthiophenes with  $\text{FeCl}_3$ . *Polymer (Guildf)*. **1992**, *33* (7), 1559–1562.
- (78) Fukumoto, H.; Omori, Y.; Yamamoto, T. Effects of Solvent and Temperature on Regioregularity of Poly(3-Hexylthiophene-2,5-Diyl) Prepared by Chemical Oxidative Polymerization. *Polym. J.* **2013**, *45* (4), 462–465.
- (79) Barbarella, G.; Zambianchi, M.; Di Toro, R.; Colonna, M.; Iarossi, D.; Goldoni, F.; Bongini, A. Regioselective Oligomerization of 3-(Alkylsulfanyl)Thiophenes with Ferric Chloride. *J. Org. Chem.* **1996**, *61* (23), 8285–8292.

- (80) Liu, Y.; Nishiwaki, N.; Saigo, K.; Sugimoto, R. Polymerization of 3-Hexylthiophene with FeCl<sub>3</sub> in Aromatic Solvents. *Polym. Bull.* **2015**, *72* (7), 1817–1826.
- (81) Xu, J. M.; Chan, H. S. O.; Ng, S. C.; Chung, T. S. Polymers Synthesized from (3-Alkylthio)Thiophenes by the FeCl<sub>3</sub> Oxidation Method. *Synth. Met.* **2002**, *132* (1), 63–69.
- (82) Irvin, J. Low Oxidation Potential Electroactive Polymers, 1998.
- (83) Hai, T. A. P.; Sugimoto, R. The Catalytic Oxidative Polymerization of 3-Hexylthiophene by Oxidation of Fe<sup>2+</sup> to Fe<sup>3+</sup>. *Catal. Letters* **2017**, *147* (8), 1955–1965.
- (84) Pomerantz, M.; Tseng, J. J.; Zhu, H.; Sproull, S. J.; Reynolds, J. R.; Uitz, R.; Arnott, H. J.; Haider, M. I. Processable Polymers and Copolymers of 3-Alkylthiophenes and Their Blends. *Synth. Met.* **1991**, *41* (3), 825–830.
- (85) Koeckelberghs, G.; Vangheluwe, M.; Samyn, C.; Persoons, A.; Verbiest, T. Regioregular Poly(3-Alkoxythiophene)s: Toward Soluble, Chiral Conjugated Polymers with a Stable Oxidized State. *Macromolecules* **2005**, *38* (13), 5554–5559.
- (86) Ouhib, F.; Dkhissi, A.; Iratçabal, P.; Hiorns, R. C.; Khoukh, A.; Desbrières, J.; Pouchan, C.; Dagron-Lartigau, C. Electronic Structure and Optical Properties of Poly[3-(4-Octylphenoxy)Thiophene]: Experimental and Theoretical Studies. *J. Polym. Sci. Part A Polym. Chem.* **2008**, *46*, 7505–7516.
- (87) Leclerc, M.; Diaz, F. M.; Wegner, G. Structural Analysis of Poly(3-Alkylthiophene)s. *Die Makromol. Chemie* **1989**, *190* (12), 3105–3116.
- (88) Qi, Z. J.; Wei, B.; Sun, Y. M.; Wang, X. M.; Kang, F.; Hong, M. X.; Tang, L. L. Comparative Study of Photoelectric Properties of Regiosymmetrical Poly(3,4-Dialkoxythiophene)s. *Polym. Bull.* **2011**, *66* (7), 905–915.
- (89) Abdou, M. S. A.; Lu, X.; Xie, Z. W.; Orfino, F.; Deen, M. J.; Holdcroft, S. Nature of Impurities in  $\pi$ -Conjugated Polymers Prepared by Ferric Chloride and Their Effect on the Electrical Properties of Metal-Insulator-Semiconductor Structures. *Chem. Mater.* **1995**, *7* (4), 631–641.
- (90) Koßmehl, G.; Chatzitheodorou, G. Electrical Conductivity of Poly(2,5-thiophenediyl)-AsF<sub>5</sub>-complexes. *Macromol. Rapid Commun.* **1981**, *2* (910), 551–555.
- (91) Koßmehl, G. Electrical Conductivity of Partly Oxidized Aromatic and Heteroaromatic Polymers. *Macromol. Symp.* **1986**, *4*, 45–64.



- (92) Olinga, T.; François, B. Kinetics of Polymerization of Thiophene by FeCl<sub>3</sub> in Chloroform and Acetonitrile. *Synth. Met.* **1995**, 69 (1–3), 297–298.
- (93) Jiang, C.; Chen, G.; Wang, X. High-Conversion Synthesis of Poly(3,4-Ethylenedioxythiophene) by Chemical Oxidative Polymerization. *Synth. Met.* **2012**, 162 (21–22), 1968–1971.
- (94) Cai, T.; Zhou, Y.; Wang, E.; Hellström, S.; Zhang, F.; Xu, S.; Inganäs, O.; Andersson, M. R. Low Bandgap Polymers Synthesized by FeCl<sub>3</sub> Oxidative Polymerization. *Sol. Energy Mater. Sol. Cells* **2010**, 94 (7), 1275–1281.
- (95) Andersson, M. R.; Mammo, W.; Olinga, T.; Svensson, M.; Theander, M.; Inganäs, O. Synthesis of Regioregular Phenyl Substituted Polythiophenes with FeCl<sub>3</sub>. *Synth. Met.* **1999**, 101 (1), 11–12.
- (96) Baker, M. A.; Tsai, C. H.; Noonan, K. J. T. Diversifying Cross-Coupling Strategies, Catalysts and Monomers for the Controlled Synthesis of Conjugated Polymers. *Chem. - A Eur. J.* **2018**, 24 (50), 13078–13088.
- (97) Iovu, M. C.; Sheina, E. E.; Gil, R. R.; McCullough, R. D. Experimental Evidence for the Quasi-"Living" Nature of the Grignard Metathesis Method for the Synthesis of Regioregular Poly(3-Alkylthiophenes). *Macromolecules* **2005**, 38 (21), 8649–8656.
- (98) Sheina, E. E.; Liu, J.; Iovu, M. C.; Laird, D. W.; McCullough, R. D. Chain Growth Mechanism for Regioregular Nickel-Initiated Cross-Coupling Polymerizations. *Macromolecules* **2004**, 37 (10), 3526–3528.
- (99) Pollit, A. A.; Ye, S.; Seferos, D. S. Elucidating the Role of Catalyst Steric and Electronic Effects in Controlling the Synthesis of  $\pi$ -Conjugated Polymers. *Macromolecules*. 2020, pp 138–148.
- (100) Leone, A. K.; Goldberg, P. K.; McNeil, A. J. Ring-Walking in Catalyst-Transfer Polymerization. *J. Am. Chem. Soc.* **2018**, 140 (25), 7846–7850.
- (101) Perrin, D. D.; Armarego, W. L. F. *Purification of Laboratory Chemicals*, 4th ed.; Butterworth-Heinemann, 1997.
- (102) Yiğit, D.; Aykan, M.; Güllü, M. Substituent Effect on Supercapacitive Performances of Conducting Polymer-Based Redox Electrodes: Poly(3',4'-Bis(Alkyloxy) 2,2':5',2''-Terthiophene) Derivatives. *J. Polym. Sci. Part A Polym. Chem.* **2018**, 56 (5), 480–495.
- (103) Wegener, P.; Feldhues, M.; Litterer, H. Process For the Preparation of Thiophene Ethers. 4931568, 1990.

- (104) Welsh, D. M.; Kloeppner, L. J.; Madrigal, L.; Pinto, M. R.; Thompson, B. C.; Schanze, K. S.; Abboud, K. A.; Powell, D.; Reynolds, J. R. Regiosymmetric Dibutyl-Substituted Poly(3,4-Propylenedioxythiophene)s as Highly Electron-Rich Electroactive and Luminescent Polymers. *Macromolecules* **2002**, 35 (17), 6517–6525.
- (105) Zhou, Y.; Shida, N.; Koizumi, Y.; Watanabe, T.; Nishiyama, H.; Tomita, I.; Inagi, S. Template-Free Perpendicular Growth of a Poly(3,4-Ethylenedioxythiophene) Fiber Array by Bipolar Electrolysis under an Iterative Potential Application. *J. Mater. Chem. C* **2019**, 7 (46), 14745–14751.
- (106) Breiby, D. W.; Samuelsen, E. J.; Groenendaal, L.; Struth, B. Smectic Structures in Electrochemically Prepared Poly(3,4-Ethylenedioxythiophene) Films. *J. Polym. Sci. Part B Polym. Phys.* **2003**, 41 (9), 945–952.
- (107) Mortier, C.; Darmanin, T.; Guittard, F. Major Influence of the Alkyl Chain Length of Poly(2,4-Dialkyl-3,4-Propylenedioxythiophene) on the Surface Fibrous Structures and Hydrophobicity. *Polym. Adv. Technol.* **2014**, 25 (11), 1252–1256.
- (108) Mortier, C.; Darmanin, T.; Guittard, F. The Major Influences of Substituent Size and Position of 3,4-Propylenedioxythiophene on the Formation of Highly Hydrophobic Nanofibers. *Chempluschem* **2014**, 79 (10), 1434–1439.
- (109) Guzinski, M.; Jarvis, J. M.; D’Orazio, P.; Izadyar, A.; Pendley, B. D.; Lindner, E. Solid-Contact PH Sensor without CO<sub>2</sub> Interference with a Superhydrophobic PEDOT-C14 as Solid Contact: The Ultimate “Water Layer” Test. *Anal. Chem.* **2017**, 89 (16), 8468–8475.
- (110) Zhang, S.; Zhang, W.; Zhang, G.; Bai, Y.; Chen, S.; Xu, J.; Yu, Z.; Sun, K. P-Toluenesulfonic Acid Catalytic Polymerization of EDOT without Oxidants. *Mater. Lett.* **2018**, 222, 105–108.
- (111) Snapp-Leo, M. Synthesis and Characterization of Novel Thiophene-Based Electroactive Polymers, Texas State University, 2019.
- (112) Kaupp, M. *Relativistic Effects on NMR Chemical Shifts*; Elsevier B.V., 2004; Vol. 14.
- (113) Viesser, V. R.; Ducati, L. C.; Tormena, C. F.; Autschbach, J. The Halogen Effect on the <sup>13</sup>C NMR Chemical Shift in Substituted Benzenes. *Phys. Chem. Chem. Phys.* **2018**, 20 (16), 11247–11259.

- (114) Nakatsuji, M.; Hata, Y.; Fujihara, T.; Yamamoto, K.; Sasaki, M.; Takekuma, H.; Yoshihara, M.; Minematsu, T.; Takekuma, S. I. Reactions of Azulenes with 1,2-Diaryl-1,2-Ethanediols in Methanol in the Presence of Hydrochloric Acid: Comparative Studies on Products, Crystal Structures, and Spectroscopic and Electrochemical Properties. *Tetrahedron* **2004**, 60 (28), 5983–6000.
- (115) Babudri, F.; Fiandanese, V.; Marchese, G.; Punzi, A. A Direct Access to  $\alpha$ -Diones from Oxalyl Chloride. *Tetrahedron Lett.* **1995**, 36 (40), 7305–7308.
- (116) Scheiper, B.; Bonnekessel, M.; Krause, H.; Fürstner, A. Selective Iron-Catalyzed Cross-Coupling Reactions of Grignard Reagents with Enol Triflates, Acid Chlorides, and Dichloroarenes. *J. Org. Chem.* **2004**, 69 (11), 3943–3949.
- (117) Dieter, R. K. Reaction of Acyl Chlorides with Organometallic Reagents: A Banquet Table of Metals for Ketone Synthesis. *Tetrahedron* **1999**, 55 (14), 4177–4236.
- (118) Clover, A. M. The Auto-Oxidation of Chloroform. *J. Am. Chem. Soc.* **1923**, 45 (12), 3133–3138.
- (119) Hill, D. G. Photochemical Decomposition of Chloroform. *J. Am. Chem. Soc.* **1932**, 54 (1), 32–40.
- (120) Sato, M. A.; Hiroi, M. Oxidized States of Soluble Oligothiophenes and Polythiophenes. *Polymer (Guildf.)* **1996**, 37 (9), 1685–1689.
- (121) Krische, B.; Zagorska, M. Overoxidation in Conducting Polymers. *Synth. Met.* **1989**, 28 (1–2), 257–262.
- (122) Hirao, T.; Asahara, M.; Muguruma, Y.; Ogawa, A. Highly Diastereoselective Pinacol Coupling of Secondary Aliphatic Aldehydes Induced by a Catalytic System Consisting of Vanadium Complex, Chlorosilane, and Zinc Metal. *J. Org. Chem.* **1998**, 63 (25), 2812–2813.
- (123) Wang, A.; Jiang, H. Palladium-Catalyzed Direct Oxidation of Alkenes with Molecular Oxygen: General and Practical Methods for the Preparation of 1,2-Diols, Aldehydes, and Ketones. *J. Org. Chem.* **2010**, 75 (7), 2321–2326.
- (124) Emmanuvel, L.; Shaikh, T. M. A.; Sudalai, A. NaIO<sub>4</sub>/LiBr Mediated Diastereoselective Dihydroxylation of Olefins: A Catalytic Approach to the Prevost–Woodward Reaction. *Org. Lett.* **2005**, 7 (22), 5071–5074.
- (125) Chen, X. M.; Ning, X. S.; Kang, Y. B. Aerobic Acetoxyhydroxylation of Alkenes Co-Catalyzed by Organic Nitrite and Palladium. *Org. Lett.* **2016**, 18 (20), 5368–5371.

- (126) Barbarella, G.; Bongini, A.; Zambianchi, M. Regiochemistry and Conformation of Poly(3-Hexylthiophene) via the Synthesis and the Spectroscopic Characterization of the Model Configurational Triads. *Macromolecules* **1994**, 27 (11), 3039–3045.
- (127) Kelly, R. A.; Scott, N. M.; Díez-González, S.; Stevens, E. D.; Nolan, S. P. Simple Synthesis of CpNi(NHC)Cl Complexes (Cp = Cyclopentadienyl; NHC = N-Heterocyclic Carbene). *Organometallics* **2005**, 24 (14), 3442–3447.
- (128) Lin, C. Y.; Power, P. P. Complexes of Ni(I): A “Rare” Oxidation State of Growing Importance. *Chem. Soc. Rev.* **2017**, 46 (17), 5347–5399.
- (129) Lipschutz, M. I.; Yang, X.; Chatterjee, R.; Tilley, T. D. A Structurally Rigid Bis(Amido) Ligand Framework in Low-Coordinate Ni(I), Ni(II), and Ni(III) Analogues Provides Access to a Ni(III) Methyl Complex via Oxidative Addition. *J. Am. Chem. Soc.* **2013**, 135 (41), 15298–15301.
- (130) Wu, J.; Nova, A.; Balcells, D.; Brudvig, G. W.; Dai, W.; Guard, L. M.; Hazari, N.; Lin, P. H.; Pokhrel, R.; Takase, M. K. Nickel(I) Monomers and Dimers with Cyclopentadienyl and Indenyl Ligands. *Chem. - A Eur. J.* **2014**, 20 (18), 5327–5337.
- (131) Gobalasingham, N. S.; Thompson, B. C. Direct Arylation Polymerization: A Guide to Optimal Conditions for Effective Conjugated Polymers. *Prog. Polym. Sci.* **2018**, 83, 135–201.
- (132) Ayalew, H.; Wang, T. L.; Wang, T. H.; Hsu, H. F.; Yu, H. H. Direct C-H Arylation Polymerization to Form Anionic Water-Soluble Poly(3,4-Ethylenedioxythiophenes) with Higher Yields and Molecular Weights. *Synlett* **2018**, 29 (20), 2660–2668.
- (133) Grenier, F.; Goudreau, K.; Leclerc, M. Robust Direct (Hetero)Arylation Polymerization in Biphasic Conditions. *J. Am. Chem. Soc.* **2017**, 139 (7), 2816–2824.
- (134) Ichige, A.; Saito, H.; Kuwabara, J.; Yasuda, T.; Choi, J. C.; Kanbara, T. Facile Synthesis of Thienopyrroledione-Based  $\pi$ -Conjugated Polymers via Direct Arylation Polycondensation under Aerobic Conditions. *Macromolecules* **2018**, 51 (17), 6782–6788.
- (135) Bura, T.; Blaskovits, J. T.; Leclerc, M. Direct (Hetero)Arylation Polymerization: Trends and Perspectives. *J. Am. Chem. Soc.* **2016**, 138 (32), 10056–10071.